WAVE PROPAGATION IN AN ELASTIC HALF SPACE CONTAINING A RIGID-LUBRICATED CYLINDRICAL INCLUSION

by

Edward R. Johnson

A dissertation submitted to the
Graduate Faculty in Engineering in partial
fulfillment of the requirements for the
degree of Doctor of Philosophy,
The City University of New York

1972

This manuscript has been read and accepted for the Graduate Faculty in Engineering in satisfaction of the dissertation requirement for the degree of Doctor of Philosophy.

1/26/72
date

Raymond Parnes
Chairman of Examining Committee

1/26/72
date

Jacques E. Benveniste
Executive Officer

Prof. J.E. Benveniste

Prof. D.H. Cheng

Prof. C.J. Costantino

Prof. M.K. Kassir

Prof. R. Parnes, Chairman
Supervisory Committee

The City University of New York

ABSTRACT

WAVE PROPAGATION IN AN ELASTIC HALF SPACE

CONTAINING A RIGID-LUBRICATED CYLINDRICAL INCLUSION

by

Edward R. Johnson

Advisor: Professor Raymond Parnes

The dynamic response of a linear elastic half-space containing a rigid semi-infinite cylindrical inclusion whose surface is lubricated and whose axis is perpendicular to the plane boundary is studied when an axisymmetric vertical normal line load is suddenly applied on the plane surface. Particular emphasis is given to the response at the plane boundary and the wave fronts there.

Using integral transform techniques and complex contour integration, the results are expressed in terms of finite integrals whose integrands consist of elliptic integrals and semi-infinite branch integrals.

The response at the wave fronts is studied analytically and numerical integration techniques are used to evaluate the complete solution. The results after the passage of the last wave front are shown to approach those of the corresponding static problem.

. . .

ACKNOWLEDGMENTS

I wish to express my sincere gratitude to my mentor, Professor Raymond Parnes for his guidance and effort during the research and writing of this thesis.

I am also indebted to Professor Jacques E. Benveniste for his interest and helpful discussions.

My sincere thanks to my devoted wife, Beth, who spent many hours typing the preliminary and final drafts.

The financial support of the City University of New York, and National Aeronautics and Space Administration, and the National Science Foundation is gratefully acknowledged.

. . .

TABLE OF CONTENTS

LIST OF TABLES

LIST OF FIGURES

LIST OF SYMBOLS

r, θ, z	spatial coordinates
$A(\gamma), B(\gamma)$	weighting functions
a	radius of inclusion
b	location of source
C_P, C_S, C_R	speeds of P-, S-, and R-waves
E	complete elliptic integral of the second kind
E_1	exponential integral function
e	dilatation
$\hat{F}_{q,k}$	integrands of transformed quantities
$f_{q,k}, f_e, f_u, f_w$	Laplace inversions of integrands
$f, \hat{f}$	Laplace transform pairs
H	unit step function
$H_n^{(1)}, H_n^{(2)}$	Hankel functions of order n
I_n, K_n	modified Bessel functions of order n
J_n, Y_n	Bessel functions of the first and second kinds of order n
K	complete elliptic integral of the first kind
Q	total applied force
s	Laplace transform variable
t	time
u, w	components of displacement
$\underset{\sim}{u}$	displacement vector
δ	Dirac-delta function
ε	small positive parameter
ζ	complex variable

κ	ratio of wave speeds = C_S/C_R
λ,μ	Lamé constants
ν	Poisson's ratio
Π	complete elliptic integral of the third kind
ξ	dimensionless vertical coordinate = z/a
ρ	dimensionless radial coordinate = r/a
$\sigma_{rr},\sigma_{\theta\theta},\sigma_{zz}$	normal components of stress
$\sigma_{rz},\sigma_{r\theta},\sigma_{\theta z}$	shear components of stress
τ	dimensionless time = $C_S t/a$
$\bar{\tau}$	dimensionless time = $\tau/\kappa = C_R t/a$
ϕ,ψ	displacement potential functions

CHAPTER 1

INTRODUCTION

The propagation of waves in elastic bodies has been investigated for over a century but in more recent years particular interest in this field has grown due to phenomena in such diverse areas as geophysics, seismology, and problems encountered in oil exploration.

The first studies of elastic wave propagation in an infinite elastic medium were published by Poisson [1] in 1829. This work was of particular importance in revealing the propagation of two types of waves: dilatation (P) waves and equivoluminal (S) waves.

The problem of wave propagation becomes much more complex when boundaries exist in a medium, for these permit reflections and refractions of waves. The simplest type of boundary occurs in a semi-infinite body where more complex patterns, known as Rayleigh surface waves are first encountered. These waves, which were first discovered by Rayleigh [2] in 1887, propagate parallel to the boundary of a half-space at a speed lower than that of P- or S-waves and decay rapidly in the direction normal to the boundary.

The propagation of waves due to the application of loads at the boundary of semi-infinite medium was first considered by Lamb [3] who studied the axi-symmetric propagation of a pulse created by a transient normal point load on the surface of the half-space. (Problems of this nature have subsequently been referred to in the literature as "Lamb's problem"). Using a Fourier synthesis of steady state solutions, Lamb showed that the Rayleigh surface wave was the dominant contribution

to the surface displacement at large distances from the load. Furthermore, the magnitude of the disturbance was found to vary inversely with the square root of the distance from the load.

In more recent years, Sauter [4], using an integral superposition of plane harmonic waves and contour integration, derived a closed form solution to the Lamb problem for the entire displacement field due to an impulsive line load consisting of normal and tangential components. Wave fronts in the half-space were determined and analyzed in great detail.

Using Sauter's solution, Broberg [5], numerically evaluated the vertical component of displacement at the surface and verified the presence of a Rayleigh wave which Lamb had found.

A simpler method of solution of dynamic surface load problems which utilizes the Laplace transform was first given in 1955 by Pekeris [6] and later, in 1960 by Chao [7]. The analytical expressions for the surface displacement components obtained by this method are much simpler than those obtained by either the superposition of plane harmonic waves or the Fourier synthesis of steady state solutions.

Pekeris considered the normal point load with a step in time, obtaining integral expressions for the Laplace transform of the boundary surface displacement components. The actual displacements are determined by applying the Laplace inversion to the integrands of the integral solutions. Upon integration, the vertical displacement component finally is given in terms of elementary functions and the

horizontal component is expressed in terms of elliptic integrals.

Chao considered the tangential point load with a step in time. Using both the Hankel and Laplace transforms and employing the same inversion technique as Pekeris, simple expressions for the displacement components on the surface are obtained.

Problems of wave propagation due to applied loads in a half-space containing internal boundaries are of current interest. Indeed, problems of this nature are more complex due to the reflections and refractions occuring at the internal boundaries.

In 1969, Gregory [8] considered a problem in this class, viz. a half-space containing a cylindrical cavity whose axis is parallel to and below the plane surface and subjected to a time-harmonic uniform radial pressure from within the cavity.

Using an infinite series of potential functions, each of which represents a line source, the amplitude of the dilatational component of the outgoing Rayleigh wave is obtained in the form of an asymptotic solution where the product of the forcing frequency and the cavity radius tends to zero. This method naturally provided only limited results.

From the present available literature, it is apparent that although the propagation of waves in semi-infinite media as well as in layered media has been exhaustively studied [9], the propagation due to applied boundary tractions, of elastic waves in semi-infinite media containing internal boundaries has, as yet, not thoroughly

been studied.

A first problem in this category which is the subject of this dissertation, is that of a semi-infinite body containing a rigid-lubricated cylindrical inclusion (whose axis is perpendicular to the plane surface) and which is subjected to an axi-symmetric concentric line load applied dynamically as a step function in time at the plane surface. This model may be considered to represent a bore in which a shell of considerably greater material stiffness (e.g. a thick steel shell) is embedded. Such cases may be encountered, for example, in shafts for oil exploration. The complexity of this problem is greater than that of Lamb's problem and arises from the reflection of waves at the internal boundary.

The dynamic problem considered below is formulated in terms of two potential functions which satisfy uncoupled two-dimensional wave equations along with coupled boundary conditions. Using the Laplace transform, expressions for the transform displacement and stress components throughout the body are obtained in the form of infinite superposition integrals.

A significant simplification is achieved in the method developed below for the displacement and stress expressions at the plane boundary. Extending the integration of the set of infinite integrals to the complex plane, it becomes possible to reduce the set to finite integrals having discrete points of discontinuity. Indeed this may be considered to be one of the main features of the method, for the points of discontinuity are then easily shown to correspond

to direct P- and S- wave fronts propagating along the surface of the medium as well as waves reflected from the rigid-lubricated inclusion boundary. Moreover, the derived paths of integration in the complex plane, which are based on necessary convergence criteria, establish clearly the differences of response for the field points inside and outside the source. The response due to direct incident waves are further expressed in terms of elliptic integrals. In addition, the poles of the solution are defined and are later identified with the contribution of the Rayleigh surface waves. Finally, expressions for the desired quantities are obtained by means of the Laplace inversions of the integrands of the finite integrals.

The discontinuities in the integral solutions are examined to determine the type and location of the various wave fronts. The singularities of the solution are analyzed and series expansions in the vicinity of each wave front are obtained. Additional singularities occuring under the source are similarly analyzed.

Numerical results showing both the total response and the individual contributions of different wave types are presented graphically for the displacement and stress components at the plane surface. The locations of the wave fronts as well as the arrival times of the respective wave fronts are depicted.

An interesting feature of the solution is found to be the predominant nature of the Rayleigh surface waves in relation to the total response.

CHAPTER 2

FORMULATION AND GENERAL SOLUTION

The problem considered is the time-dependent response of an isotropic linearly elastic half-space containing a rigid-lubricated cylindrical inclusion, whose axis is perpendicular to the plane surface. The half-space is loaded at the plane surface by means of an axi-symmetric concentric line load having a step function in time (Fig. 1).

The inclusion is thus considered to be imbedded in the elastic half-space in such a manner that relative displacements in the axial direction at the interface are permitted although no relative radial displacements at the interface occur. Hence, the conditions to be satisfied on the cylindrical boundary are the vanishing of the normal displacement and the shear stress components:

$$u(a,z,t) = 0 \tag{2-1}$$

$$\sigma_{rz}(a,z,t) = 0 \tag{2-2}$$

while on the plane boundary, the conditions to be satisfied are the vanishing of the shear stress component and the prescribed normal load:

$$\sigma_{zr}(r,0,t) = 0 \tag{2-3}$$

$$\sigma_{zz}(r,0,t) = -\frac{Q}{2\pi r}\delta(r-b)H(t) \tag{2-4}$$

where Q is the total force applied, and δ is the Dirac-delta function.

Using a theorem due to Helmholtz, $\underset{\sim}{u} = \nabla\phi + \nabla\times\underset{\sim}{H}$, (2-5)

the axi-symmetric problem may be formulated in terms of displacement potentials $\phi(r, z, t)$, $\psi(r, z, t)$, such that:

$$u = \phi_r + \psi_{rz} \quad , \quad w = \phi_z - \psi_{rr} - \frac{1}{r}\psi_r \tag{2-6}$$

where u(r, z, t), and w(r, z, t), are the displacement components in the r and z directions respectively. Similar potentials have been used by previous authors. [10]

Substituting eq. (2-6) into the displacement equations of motion,

$$(\lambda+2\mu)\nabla(\nabla\cdot\underset{\sim}{u}) - \mu(\nabla\times\nabla\times\underset{\sim}{u}) = \rho_m \underset{\sim}{u}_{tt} \, , \tag{2-7}$$

the potentials must satisfy the following two-dimensional wave equations:

$$\nabla_1^2\phi = \frac{1}{C_p^2}\phi_{tt} \tag{2-8}$$

$$\nabla_1^2\psi = \frac{1}{C_s^2}\psi_{tt} \tag{2-9}$$

where

$$\left.\begin{aligned} C_p^2 &= \frac{\lambda+2\mu}{\rho_m} \qquad C_s^2 = \frac{\mu}{\rho_m} \\ \nabla_1^2 &\equiv \frac{\partial^2}{\partial r^2} + \frac{1}{r}\frac{\partial}{\partial r} + \frac{\partial^2}{\partial z^2} \end{aligned}\right\} \tag{2-10}$$

λ and μ are the Lamé constants, and ρ_m is the mass density of the medium.

From the linear elastic stress-strain relations,

$$\underset{\sim}{\sigma} = \lambda\nabla\cdot\underset{\sim}{u}\,\underset{\sim}{I} + \mu(\nabla\underset{\sim}{u} + \underset{\sim}{u}\nabla) \tag{2-11}$$

where $\underset{\sim}{I}$ is the idem factor, the stress components may be expressed in terms of the potentials as follows:

$$\left.\begin{aligned}
\sigma_{rr} &= \frac{\lambda}{C_p^2}\phi_{tt} + 2\mu(\phi_{rr} + \psi_{rrz}) \\
\sigma_{\theta\theta} &= \frac{\lambda}{C_p^2}\phi_{tt} + 2\mu\left(\frac{1}{r}\phi_r + \frac{1}{r}\psi_{rz}\right) \\
\sigma_{zz} &= \frac{\lambda}{C_p^2}\phi_{tt} + 2\mu\left(\phi_{zz} + \psi_{zzz} - \frac{1}{C_s^2}\psi_{ztt}\right) \\
\sigma_{zr} &= \mu\left(2\phi_{rz} + 2\psi_{rzz} - \frac{1}{C_s^2}\psi_{rtt}\right) \\
\sigma_{r\theta} &= \sigma_{\theta z} = 0
\end{aligned}\right\} \qquad (2\text{-}12)$$

It is appropriate to change the independent variables (r,z,t) to the non-dimensional variables (ρ, ξ, τ) defined as

$$\rho = \frac{r}{a}\ , \quad \xi = \frac{z}{a}\ , \quad \tau = \frac{C_s t}{a} \qquad (2\text{-}13)$$

respectively.

The governing equations then become

$$\nabla^2\phi = \frac{1-2\nu}{2(1-\nu)}\phi_{\tau\tau} \qquad (2\text{-}14)$$

$$\nabla^2\psi = \psi_{\tau\tau} \qquad (2\text{-}15)$$

where $\nabla^2 \equiv \frac{\partial^2}{\partial\rho^2} + \frac{1}{\rho}\frac{\partial}{\partial\rho} + \frac{\partial^2}{\partial\xi^2}$, and where ν is Poisson's ratio.

Similarly, expressions for the displacement and stress components in terms of the non-dimensional variables may be readily obtained. A Laplace transform with respect to the non-dimensional time

$$\hat{f}(\rho,\xi,s) = \int_0^\infty f(\rho,\xi,\tau)\, e^{-s\tau}\, d\tau \qquad (2\text{-}16)$$

having an inversion

$$f(\rho,\xi,\tau) = \frac{1}{2\pi i}\int_{\omega-i\infty}^{\omega+i\infty} \hat{f}(\rho,\xi,s)\, e^{\tau s}\, ds \qquad (2\text{-}17)$$

is now applied to yield the following governing equations for $\hat{\phi}$ (ρ, ξ, s) and $\hat{\psi}(\rho, \xi, s)$:

$$\nabla^2\hat{\phi} - \frac{1-2\nu}{2(1-\nu)} s^2\hat{\phi} = 0 \tag{2-18}$$

$$\nabla^2\hat{\psi} - s^2\hat{\psi} = 0 \tag{2-19}$$

The expressions for the corresponding transformed displacement and stress components are then:

$$a^2\hat{u} = a\hat{\phi}_\rho + \hat{\psi}_{\rho\xi} \tag{2-20 (a)}$$

$$a^2\hat{w} = a\hat{\phi}_\xi + \hat{\psi}_{\xi\xi} - s^2\hat{\psi} \tag{b}$$

$$\frac{a^3}{\mu}\hat{\sigma}_{rr} = \frac{a\nu}{1-\nu} s^2\hat{\phi} + 2a\hat{\phi}_{\rho\rho} + 2\hat{\psi}_{\rho\rho\xi} \tag{c}$$

$$\frac{a^3}{\mu}\hat{\sigma}_{\theta\theta} = \frac{a\nu}{1-\nu} s^2\hat{\phi} + \frac{2a}{\rho}\hat{\phi}_\rho + \frac{2}{\rho}\hat{\psi}_{\rho\xi} \tag{d}$$

$$\frac{a^3}{\mu}\hat{\sigma}_{zz} = \frac{a\nu}{1-\nu} s^2\hat{\phi} + 2a\hat{\phi}_{\xi\xi} + 2\hat{\psi}_{\xi\xi\xi} - 2s^2\hat{\psi}_\xi \tag{e}$$

$$\frac{a^3}{\mu}\hat{\sigma}_{rz} = 2a\hat{\phi}_{\rho\xi} + 2\hat{\psi}_{\rho\xi\xi} - s^2\hat{\psi}_\rho \tag{f}$$

Using for example the method of separation of variables, the following integral solutions to eqs. (2-18, 2-19) are obtained:

$$\hat{\phi}(\rho,\xi,s) = \int_0^\infty A(\gamma)\, C_0(\gamma,\rho)\, e^{-s\alpha\xi}\, d\gamma \tag{2-21}$$

$$\hat{\psi}(\rho,\xi,s) = \int_0^\infty B(\gamma)\, C_0(\gamma,\rho)\, e^{-s\beta\xi}\, d\gamma \tag{2-22}$$

where

$$C_0(\gamma,\rho) = J_1(\gamma)\, Y_0(\gamma\rho) - Y_1(\gamma)\, J_0(\gamma\rho) \tag{2-23}$$

and

$$s\alpha = \sqrt{\gamma^2 + s^2\frac{1-2\nu}{2(1-\nu)}}\,, \quad s\beta = \sqrt{\gamma^2 + s^2} \tag{2-24}$$

and where γ is real.

Solutions whose dependence on ξ enters as $e^{+s\alpha\xi}$ and $e^{+s\beta\xi}$ are omitted to ensure boundedness of the solution at large ξ.

The integrals do not include the range of γ from $-\infty$ to 0 because $C_o(\gamma,\rho)$ is an odd function of γ.

Furthermore, the above solutions automatically satisfy the vanishing boundary conditions on the cylindrical surface $\rho=1$. This may be seen by noting that both $\hat{u}(\rho, \xi, s)$ and $\hat{\sigma}_{rz}(\rho, \xi, s)$ depend on the first partial derivative of $\hat{\phi}$ and $\hat{\psi}$ with respect to ρ and that the dependence enters only through $C_o(\gamma, \rho)$ whose derivative with respect to ρ vanishes at $\rho=1$. This becomes readily evident, by noting that

$$\frac{\partial}{\partial\rho} C_o(\gamma,\rho) = -\gamma C_1(\gamma,\rho) \tag{2-25a}$$

where $C_1(\gamma, \rho)$ is defined as

$$C_1(\gamma,\rho) = J_1(\gamma)Y_1(\gamma\rho) - Y_1(\gamma)J_1(\gamma\rho) \tag{2-25b}$$

where the recurrence relations of Bessel's functions have been employed.

The weighting functions $A(\gamma)$ and $B(\gamma)$ in the integral solutions can be determined from the conditions on the plane boundary, eqs.(2-3, 2-4) which in (ρ, ξ, s) space become:

$$\hat{\sigma}_{zr}(\rho,0,s) = 0 \tag{2-26}$$

$$\hat{\sigma}_{zz}(\rho,0,s) = -\frac{Q}{2\pi a^2 \rho s}\delta(\rho - b/a) \tag{2-27}$$

Using the stress-displacement potential relations, eqs. (2-20e, 2-20f) and substituting eqs. (2-21, 2-22) in the above, equations

on $A(\gamma)$ and $B(\gamma)$,

$$\int_0^\infty \left[-2a\, s\alpha\, A(\gamma) + (2\gamma^2 + s^2) B(\gamma)\right] \frac{\partial}{\partial \rho} C_0(\gamma,\rho)\, d\gamma = 0 \qquad (2\text{-}28a)$$

$$\int_0^\infty \left[(2\gamma^2+s^2)\, a\, A(\gamma) - 2\gamma^2 s\beta\, B(\gamma)\right] C_0(\gamma,\rho)\, d\gamma = -\frac{a\,Q}{2\pi\mu\rho s}\,\delta(\rho - b/a) \qquad (2\text{-}28b)$$

are established.

Eq. (2-28a) is satisfied if

$$a\, A(\gamma) = \frac{2\gamma^2 + s^2}{2\, s\alpha}\, B(\gamma) \qquad (2\text{-}29)$$

Substituting this result in eq. (2-28b) the following equation on $B(\gamma)$ is obtained:

$$\int_0^\infty M(\gamma,s)\, \frac{B(\gamma)}{2\, s\alpha}\, C_0(\gamma,\rho)\, d\gamma = -\frac{a\,Q}{2\pi\mu\rho s}\,\delta(\rho - b/a) \qquad (2\text{-}30)$$

where $$M(\gamma,s) = (2\gamma^2 + s^2)^2 - 4\gamma^2 s\alpha\, s\beta \qquad (2\text{-}31)$$

To determine the function $B(\gamma)$, use is made of the integral representation for the Dirac-delta function, eq. (A-1),

$$\delta(\rho - b/a) = \int_0^\infty \frac{C_0(\gamma,\rho)\, C_0(\gamma, b/a)}{J_1^2(\gamma) + Y_1^2(\gamma)}\, \rho\gamma\, d\gamma \qquad (2\text{-}32)$$

which is established in Appendix A.

Comparison of eqs. (2-30) and (2-32) immediately yields

$$B(\gamma) = -\frac{a\,Q}{\pi\mu s} \cdot \frac{\gamma\, s\alpha\, C_0(\gamma, b/a)}{M(\gamma,s)\left[J_1^2(\gamma) + Y_1^2(\gamma)\right]} \qquad (2\text{-}33)$$

The solution in the transform space is now formally complete

since by eqs (2-20) the following integral solutions for the displacement and stress components at all points in the body may be written.

$$\frac{a\mu}{Q}\hat{u} = -\frac{1}{2\pi s}\int_0^\infty \gamma N_1(\rho, b/a, \gamma, s)\left[P_\beta(\xi,\gamma,s) - P_\alpha(\xi,\gamma,s)\right] d\gamma \qquad (a)$$

$$\frac{a\mu}{Q}\hat{w} = -\frac{1}{2\pi s}\int_0^\infty N_0(\rho, b/a, \gamma, s)\left[\frac{\gamma^2}{s\beta}P_\beta(\xi,\gamma,s) - s\alpha P_\alpha(\xi,\gamma,s)\right] d\gamma \qquad (b)$$

$$\frac{a^2}{Q}\hat{\sigma}_{rr} = -\frac{1}{2\pi s}\int_0^\infty N_0(\rho, b/a, \gamma, s)\left[\gamma^2 P_\beta(\xi,\gamma,s) + \left(\frac{\nu}{1-\nu}s^2 - \gamma^2\right)P_\alpha(\xi,\gamma,s)\right] d\gamma$$
$$- \frac{a\mu}{Q}\frac{2}{\rho}\hat{u} \qquad (c)$$

$$\frac{a^2}{Q}\hat{\sigma}_{\theta\theta} = -\frac{1}{2\pi s}\int_0^\infty N_0(\rho, b/a, \gamma, s)\frac{\nu}{1-\nu}s^2 P_\alpha(\xi,\gamma,s)\, d\gamma$$
$$+ \frac{a\mu}{Q}\frac{2}{\rho}\hat{u} \qquad (d)$$

$$\frac{a^2}{Q}\hat{\sigma}_{zz} = \frac{1}{2\pi s}\int_0^\infty N_0(\rho, b/a, \gamma, s)\left[2\gamma^2 P_\beta(\xi,\gamma,s) - (2\gamma^2+s^2)P_\alpha(\xi,\gamma,s)\right] d\gamma \qquad (e)$$

$$\frac{a^2}{Q}\hat{\sigma}_{rz} = \frac{1}{2\pi s}\int_0^\infty N_1(\rho, b/a, \gamma, s)\, 2\gamma s\alpha (2\gamma^2+s^2)\left[e^{-s\beta\xi} - e^{-s\alpha\xi}\right] d\gamma \qquad (f)$$

(2-34)

where

$$P_\beta(\xi,\gamma,s) \equiv 2s\alpha s\beta\, e^{-s\beta\xi} \qquad (2\text{-}35a)$$

$$P_\alpha(\xi,\gamma,s) \equiv (2\gamma^2+s^2)e^{-s\alpha\xi} \qquad (2\text{-}35b)$$

and

$$N_k(\rho, b/a, \gamma, s) \equiv \frac{\gamma C_0(\gamma, b/a)\, C_k(\gamma,\rho)}{M(\gamma,s)\left[J_1^2(\gamma) + Y_1^2(\gamma)\right]}, \quad k = 0, 1 \qquad (2\text{-}36)$$

CHAPTER 3

METHOD OF INVERSION

The components of the stress and the displacement are evaluated on the plane boundary, z = 0, for Poisson's ratio $\nu = 1/4$.

In the Laplace transform space, according to eqs. (2-34a,b), the displacement quantities on the boundary $\xi = 0$ are expressed in terms of the following integrals:

$$\frac{a\mu}{Q}\,\hat{w}(\rho,0,s) = \frac{1}{2\pi}\int_0^\infty \frac{C_0(\gamma,b/a)\,C_0(\gamma,\rho)\,s\gamma\,s\alpha}{[J_1^2(\gamma)+Y_1^2(\gamma)]\,M(\gamma,s)}\,d\gamma \tag{3-1}$$

$$\frac{a\mu}{Q}\,\hat{u}(\rho,0,s) = \frac{1}{2\pi}\int_0^\infty \frac{C_0(\gamma,b/a)\,C_1(\gamma,\rho)\,\gamma^2[2\gamma^2+s^2-2s\alpha\,s\beta]}{[J_1^2(\gamma)+Y_1^2(\gamma)]\,M(\gamma,s)}\,d\gamma \tag{3-2}$$

$$\frac{a^2\mu}{Q}\,\hat{e}(\rho,0,s) = -\frac{1}{6\pi}\int_0^\infty \frac{C_0(\gamma,b/a)\,C_0(\gamma,\rho)\,s\gamma[2\gamma^2+s^2]}{[J_1^2(\gamma)+Y_1^2(\gamma)]\,M(\gamma,s)}\,d\gamma \tag{3-3}$$

where
$$e = \frac{\partial u}{\partial r} + \frac{u}{r} + \frac{\partial w}{\partial z} \tag{3-4}$$

is the dilatation, and where

$$M(\gamma,s) = (2\gamma^2+s^2)^2 - 4\gamma^2 s\alpha\, s\beta \tag{3-5}$$

The stress components, expressed in terms of the dilatation and the circumferential strain, by Hooke's Law, eq. (2-11), become:

$$\frac{a^2}{Q}\,\hat{\sigma}_{\theta\theta} = \frac{a^2\mu}{Q}\,\hat{e} + \frac{a\mu}{Q}\,\frac{2}{\rho}\,\hat{u} \tag{3-6}$$

$$\frac{a^2}{Q}\,\hat{\sigma}_{rr} = \frac{4a^2\mu}{Q}\,\hat{e} - \frac{a\mu}{Q}\,\frac{2}{\rho}\,\hat{u} + \frac{1}{2\pi\rho s}\,\delta(\rho - b/a) \tag{3-7}$$

where use has been made of the boundary condition on the normal component of stress, eq. (2-4).

Due to the nature of M(γ, s) it is convenient to introduce the change of variable

$$\gamma = s\zeta \tag{3-8}$$

into eqs. (3-1) - (3-3). Furthermore, it is expedient to express the Bessel functions appearing in these equations in terms of Hankel functions. The displacement expressions are then

$$\frac{a\mu}{Q}\hat{w}(\rho,0,s) = \frac{1}{8\pi}\int_0^\infty \zeta m_w(\zeta) W(\rho, b/a, s\zeta)\, d\zeta \tag{3-9}$$

$$\frac{a\mu}{Q}\hat{u}(\rho,0,s) = \frac{1}{8\pi}\int_0^\infty \zeta^2 m_u(\zeta) U(\rho, b/a, s\zeta)\, d\zeta \tag{3-10}$$

$$\frac{a^2\mu}{Q}\hat{e}(\rho,0,s) = -\frac{1}{24\pi}\int_0^\infty \zeta m_e(\zeta)\, s W(\rho, b/a, s\zeta)\, d\zeta \tag{3-11}$$

where

$$W(\rho, b/a, s\zeta) = H_0^{(1)}(b/a\, s\zeta)\left\{H_0^{(2)}(\rho s\zeta) - H_0^{(1)}(\rho s\zeta)\frac{H_1^{(2)}(s\zeta)}{H_1^{(1)}(s\zeta)}\right\} \cdot$$
$$+ H_0^{(2)}(b/a\, s\zeta)\left\{H_0^{(1)}(\rho s\zeta) - H_0^{(2)}(\rho s\zeta)\frac{H_1^{(1)}(s\zeta)}{H_1^{(2)}(s\zeta)}\right\} \tag{3-12}$$

$$U(\rho, b/a, s\zeta) = H_0^{(1)}(b/a\, s\zeta)\left\{H_1^{(2)}(\rho s\zeta) - H_1^{(1)}(\rho s\zeta)\frac{H_1^{(2)}(s\zeta)}{H_1^{(1)}(s\zeta)}\right\}$$
$$+ H_0^{(2)}(b/a\, s\zeta)\left\{H_1^{(1)}(\rho s\zeta) - H_1^{(2)}(\rho s\zeta)\frac{H_1^{(1)}(s\zeta)}{H_1^{(2)}(s\zeta)}\right\} \tag{3-13}$$

and where

$$m_w(\zeta) = \frac{(\zeta^2 + 1/3)^{1/2}}{D(\zeta)} \tag{3-14a}$$

$$m_u(\zeta) = \frac{2\zeta^2 + 1 - 2(\zeta^2 + 1/3)^{1/2}(\zeta^2+1)^{1/2}}{D(\zeta)} \tag{3-14b}$$

$$m_e(\zeta) = \frac{2\zeta^2 + 1}{D(\zeta)} \tag{3-14c}$$

and

$$D(\zeta) = (2\zeta^2 + 1)^2 - 4\zeta^2(\zeta^2 + 1/3)^{1/2}(\zeta^2 + 1)^{1/2} \tag{3-15}$$

Upon extending the integration to the complex ζ plane, $\zeta = u + iv$, the integrals along the real axis, which appear in eqs.(3-9) - (3-11), are reduced to an integration along the imaginary axis together with integrations along large and small circle contours.

The procedure requires choosing the proper quadrants for the paths of integration. The choice of quadrants is based on the convergence of the integral along the large quarter circle, which is determined by examining each of the terms appearing in eqs. (3-12) and (3-13) according to the following (large circle) lemma: [11]

Let $G(\zeta)$ be a function on a path C_1, given by $\zeta = Re^{i\phi}$, where R is large. If

$$\lim_{R\to\infty} |\zeta| \cdot G(\zeta) = A \text{ (constant)} \tag{3-16a}$$

then

$$\lim_{R\to\infty} \int_{C_1} G(\zeta) d\zeta = iA\theta \tag{3-16b}$$

where θ is the angle of rotation of the position vector along the curve C_1.

Consider, as an example, the following term in the integrand of eq. (3-9):

$$G(\zeta) = \zeta m_w(\zeta) H_o^{(1)}(b_a s \zeta) H_o^{(2)}(\rho s \zeta) \tag{3-17}$$

Replacing the Hankel functions by their asymptotic expansions, [12]

$$H_o^{(1)}(\zeta) = \sqrt{\frac{2}{\pi\zeta}}\, e^{i(\zeta - \pi/4)}\left\{\left(1 - \frac{9}{128\zeta^2}\cdots\right) + i\left(-\frac{1}{8\zeta}\cdots\right)\right\} \tag{3-18a}$$

$$H_o^{(2)}(\zeta) = \sqrt{\frac{2}{\pi\zeta}}\, e^{-i(\zeta - \pi/4)}\left\{\left(1 - \frac{9}{128\zeta^2}\cdots\right) - i\left(\frac{1}{8\zeta}\cdots\right)\right\} \tag{3-18b}$$

and noting that the algebraic factor becomes

$$\lim_{|\zeta|\to\infty} |\zeta| m_w(\zeta) = 3/4 \tag{3-19a}$$

the following limit is obtained:

$$\lim_{|\zeta|\to\infty} |\zeta| G(\zeta) = \frac{3}{2\pi s\sqrt{\rho\, b/a}}\, e^{is\zeta(b/a - \rho)} \tag{3-19b}$$

This limit exists or vanishes if

$$\mathrm{Re}\{i\zeta(b/a - \rho)\} \leqslant 0 \tag{3-20}$$

Hence, by the large circle lemma, eq. (3-16), for

$$(b/a - \rho)v > 0 \tag{3-21a}$$

the integral vanishes, while for

$$\rho = b/a \tag{3-21b}$$

the integral will exist.

Therefore, for the particular term of the integrand considered above, it is seen from eq. (3-21a) that for $\rho < b/a$ the contour must be taken in the first quadrant, while for $b/a < \rho$ it is taken in the fourth quadrant. On the other hand, applying the above method to the term

$$G(\zeta) = \zeta m_w(\zeta) H_o^{(2)}(b/a\, s\zeta) H_o^{(1)}(\rho s\zeta) \tag{3-22}$$

it can be shown that for $\rho < b/a$ the contour must be taken in the fourth quadrant, while for $b/a < \rho$ it is taken in the first quadrant.

Hence, for the vertical displacement component, it is necessary to separate the solution for $\rho < b/a$ (field point inside source) from the solution for $b/a < \rho$ (field point outside source). In addition, in each case, the integrand must be split into two parts, one of which yields a convergent quarter circle contour in the first quadrant, while the other yields a convergent contour in the fourth quadrant. The behavior for points under the source, i.e. for $\rho = b/a$, is investigated further in the following chapter, where singularities of the solution are examined.

Treating the radial displacement component and the dilatation in the same manner it can be shown that the same separation is required. However, in the case of the dilatation, the large quarter circle contours are not convergent when $\rho = b/a$. This singularity may be removed by adding and subracting the following term from the integrand of eq. (3-11):

$$\frac{3}{2}\zeta s W(\rho, b/a, s\zeta) \tag{3-23}$$

thus obtaining

$$\frac{a^2\mu}{Q}\hat{e}(\rho,0,s) = -\frac{1}{24\pi}\int_0^{\infty}\zeta s\left[m_e(\zeta) - \frac{3}{2}\right]W(\rho, b/a, s\zeta)d\zeta$$

$$-\frac{1}{24\pi}\int_0^{\infty}\frac{3}{2}\zeta s W(\rho, b/a, s\zeta)d\zeta \tag{3-24}$$

The former integral yields a convergent integral along the large quarter circles in the ζ-plane, while the latter may be evaluated in closed form using the integral representation for the Dirac-delta function given by eq. (A-1).

The transform of the dilatation is then given by

$$\frac{a^2\mu}{Q}\hat{e}(\rho,0,s) = -\frac{1}{24\pi}\int_0^\infty \zeta s\, m'_e(\zeta) W(\rho, b/a, s\zeta)\, d\zeta$$

$$- \frac{1}{4\pi\rho s}\delta(\rho - b/a) \qquad (3\text{-}25)$$

where

$$m'_e(\zeta) = m_e(\zeta) - \frac{3}{2} \qquad (3\text{-}26)$$

Finally then, denoting the responses for the field point inside and outside the source, by subscripts I and 0 respectively, the relevant quantities of eqs. (3-9, 10, 25) are given by the following:

$$\frac{a\mu}{Q}\hat{w}_I(\rho,0,s) = \frac{1}{8\pi}\int_0^\infty \zeta m_w(\zeta)\left[\Phi_0^{(+)}(1,2,s\zeta) + \Phi_0^{(-)}(2,1,s\zeta)\right] d\zeta \qquad (3\text{-}27a)$$

$$\frac{a\mu}{Q}\hat{w}_0(\rho,0,s) = \frac{1}{8\pi}\int_0^\infty \zeta m_w(\zeta)\left[\Phi_0^{(-)}(1,2,s\zeta) + \Phi_0^{(+)}(2,1,s\zeta)\right] d\zeta \qquad (3\text{-}27b)$$

$$\frac{a\mu}{Q}\hat{u}_I(\rho,0,s) = \frac{1}{8\pi}\int_0^\infty \zeta^2 m_u(\zeta)\left[\Phi_1^{(+)}(1,2,s\zeta) + \Phi_1^{(-)}(2,1,s\zeta)\right] d\zeta \qquad (3\text{-}27c)$$

$$\frac{a\mu}{Q}\hat{u}_0(\rho,0,s) = \frac{1}{8\pi}\int_0^\infty \zeta^2 m_u(\zeta)\left[\Phi_1^{(-)}(1,2,s\zeta) + \Phi_1^{(+)}(2,1,s\zeta)\right] d\zeta \qquad (3\text{-}27d)$$

$$\frac{a^2\mu}{Q}\hat{e}_I(\rho,0,s) = -\frac{1}{24\pi}\int_0^\infty \zeta s\, m'_e(\zeta)\left[\Phi_0^{(+)}(1,2,s\zeta) + \Phi_0^{(-)}(2,1,s\zeta)\right] d\zeta \qquad (3\text{-}27e)$$

$$\frac{a^2\mu}{Q}\hat{e}_0(\rho,0,s) = -\frac{1}{24\pi}\int_0^\infty \zeta s\, m'_e(\zeta)\left[\Phi_0^{(-)}(1,2,s\zeta) + \Phi_0^{(+)}(2,1,s\zeta)\right] d\zeta \qquad (3\text{-}27f)$$

where

$$\Phi_k^{(+)}(i,j,s\zeta) = H_0^{(i)}(b/a\, s\zeta) H_k^{(j)}(\rho s\zeta) - H_0^{(1)}(b/a\, s\zeta) H_k^{(1)}(\rho s\zeta) \frac{H_1^{(2)}(s\zeta)}{H_1^{(1)}(s\zeta)} \qquad (3\text{-}28a)$$

$k = 0, 1$
$i, j = 1, 2$

$$\Phi_k^{(-)}(i,j,s\zeta) = H_0^{(i)}(b/a\, s\zeta) H_k^{(j)}(\rho s\zeta) - H_0^{(2)}(b/a\, s\zeta) H_k^{(2)}(\rho s\zeta) \frac{H_1^{(1)}(s\zeta)}{H_1^{(2)}(s\zeta)} \qquad (3\text{-}28b)$$

and where the superscripts (+) and (-) denote that the integration in the complex plane is to be carried out in the first and fourth quadrants respectively.

Now, the integrands appearing in eq. (3-27) are multivalued due to the inherent multivaluedness of the Hankel functions and the multivaluedness of the terms m_w, m_u, and m_e'. Each must be considered separately.

The appearance of the Hankel functions requires a branch cut along the negative real axis. In addition, due to the multivaluedness of the algebraic terms m_w, m_u and m_e' which arise through the terms $(\zeta^2 + 1)^{1/2}$ and $(\zeta^2 + 1/3)^{1/2}$, appropriate branch cuts must be established with branch points at $\zeta = \pm i$, $\pm i \frac{1}{\sqrt{3}}$.

Noting further that the solutions for $\hat{\Phi}$ and $\hat{\psi}$ (eqs. (2-21) and (2-22)) depend on $e^{-(\zeta^2 + 1)^{1/2} s\xi}$ and $e^{-(\zeta^2 + 1/3)^{1/2} s\xi}$, it is observed that in order to ensure a finite response for large positive values of ξ , the branch cuts arising from these multivalued terms must be taken such that these terms have positive real parts along the paths of integration.

It can be shown (see Appendix B) that the ζ-plane sheets given in Fig. 2 satisfy this criterion. Sheets 1 and 2 are used for contour integration in the first and fourth quadrants respectively. The appropriate values of the multivalued terms in each branch are also shown in Fig. 2.

Furthermore, simple poles of the integrands, determined from the

roots of eq. (3-15) lie at

$$\zeta = \pm i\kappa \tag{3-29}$$

where $\kappa = 1.08766...$

It is recognized that this value of κ is precisely the value of the ratio C_S/C_R, where C_R is the speed of propagation of Rayleigh surface waves, and consequently the contribution of the residues at these poles to the solution may be identified with the Rayleigh surface waves.

Other poles, arising from the zeros of the Hankel functions, $H_1^{(1)}(s\zeta)$ and $H_1^{(2)}(s\zeta)$, are outside the path of integration and will not contribute to the contour integral.

The small circle contours around the poles and branch points are evaluated using the following (small circle) lemma: [11] Let $G(\zeta)$ be a function on a path C_2, given by $\zeta = \zeta_0 + \varepsilon e^{i\phi}$, where ε is small. If

$$\lim_{\zeta \to \zeta_0} (\zeta - \zeta_0) G(\zeta) = A \text{ (constant)}, \tag{3-30a}$$

then

$$\lim_{\varepsilon \to 0} \int_{C_2} G(\zeta) d\zeta = iA\theta \tag{3-30b}$$

where θ is the angle of rotation of the small position vector along C_2.

As an illustration of this procedure, consider the ζ-plane contour integration of the radial displacement, $\hat{u}_I(\rho, o, s)$, when

$\rho < b/a$

$$\frac{a\mu}{Q}\hat{u}_I(\rho,0,s) = \frac{1}{8\pi}\int_0^\infty \zeta^2 m_u(\zeta)\left[\Phi_1^{(+)}(1,2,s\zeta) + \Phi_1^{(-)}(2,1,s\zeta)\right]d\zeta \quad (3\text{-}31)$$

By contour integration, using the contours shown in Fig. 2, the displacement becomes

$$\begin{aligned}\frac{a\mu}{Q}\hat{u}_I(\rho,0,s) = &-\frac{1}{8\pi}\int_0^\infty iv^2 m_u(iv)\,\Phi_1^{(+)}(1,2,isv)\,dv \\ &+\frac{i}{8}\,\mathrm{Res.}\left\{\zeta^2 m_u(\zeta)\right\}_{\zeta=iK}\Phi_1^{(+)}(1,2,isK) \\ &+\frac{1}{8\pi}\int_0^\infty iv^2 m_u(-iv)\,\Phi_1^{(-)}(2,1,-isv)\,dv \\ &-\frac{i}{8}\,\mathrm{Res.}\left\{\zeta^2 m_u(\zeta)\right\}_{\zeta=-iK}\Phi_1^{(-)}(2,1,-isK) \end{aligned} \quad (3\text{-}32)$$

The factors $\Phi_k^{(+)}$ and $\Phi_k^{(-)}$ given by eq. (3-28) in terms of Hankel functions, and evaluated on the imaginary axis can now be expressed more conveniently in terms of modified Bessel functions. Noting that [12]

$$H_n^{(1)}(\bar{\zeta}) = \overline{H_n^{(2)}(\zeta)} \quad (3\text{-}33a)$$

$$H_n^{(2)}(\bar{\zeta}) = \overline{H_n^{(1)}(\zeta)} \quad (3\text{-}33b)$$

it is seen that

$$\Phi_1^{(-)}(2,1,-isv) = \overline{\Phi_1^{(+)}(1,2,isv)} \quad (3\text{-}34)$$

Furthermore, using the relations [12]

$$H_0^{(1)}(iv) = -\frac{i2}{\pi}K_0(v) \quad (3\text{-}35a)$$

$$H_1^{(1)}(iv) = -\frac{2}{\pi}K_1(v) \quad (3\text{-}35b)$$

$$H_1^{(2)}(iv) = \frac{2}{\pi}K_1(v) + i2I_1(v) \quad (3\text{-}35c)$$

it follows that

$$\Phi_1^{(+)}(1,2,isv) = \frac{4}{\pi}K_0(b/a\,sv)\left\{I_1(\rho sv) - K_1(\rho sv)\frac{I_1(sv)}{K_1(sv)}\right\} \quad (3\text{-}36)$$

Now the residues of the algebraic factor $\zeta^2 m_u(\zeta)$ are found as follows:

$$\operatorname{Res}_{\zeta=\pm i\kappa}\left\{\zeta^2 m_u(\zeta)\right\} = \lim_{\zeta\to\pm i\kappa}(\zeta\mp i\kappa)\zeta^2 m_u(\zeta) = \mp\frac{\kappa}{8} \tag{3-37}$$

Furthermore, the values of the factor m_u on the imaginary axis are given by

$$m_u(iv) = \begin{cases} \dfrac{1-2v^2-2\sqrt{1/3-v^2}\sqrt{1-v^2}}{(1-2v^2)^2+4v^2\sqrt{1/3-v^2}\sqrt{1-v^2}}, & v<\dfrac{1}{\sqrt{3}} \\ \dfrac{1-2v^2-i2\sqrt{v^2-1/3}\sqrt{1-v^2}}{(1-2v^2)^2+i4v^2\sqrt{v^2-1/3}\sqrt{1-v^2}}, & \dfrac{1}{\sqrt{3}}<v<1 \\ \dfrac{1-2v^2+2\sqrt{v^2-1/3}\sqrt{v^2-1}}{(1-2v^2)^2-4v^2\sqrt{v^2-1/3}\sqrt{v^2-1}}, & 1<v \end{cases} \tag{3-38a}$$

and by virtue of the complex conjugate relations

$$m_u(-iv) = \overline{m_u(iv)} \tag{3-38b}$$

Substituting eqs. (3-34, 36-38) into eq. (3-32), the following expression for the transformed radial displacement component at a field point inside the source is finally obtained.

$$\frac{a\mu}{Q}\hat{u}_I(\rho,0,s) = -\frac{1}{\pi^2}\int_0^\infty v^2 \operatorname{Im}\left\{m_u(iv)\right\}K_0(b/a\,sv)\left[K_1(\rho sv)\frac{I_1(sv)}{K_1(sv)}-I_1(\rho sv)\right]dv$$
$$-\frac{\kappa}{8\pi}K_0(b/a\,s\kappa)\left[K_1(\rho s\kappa)\frac{I_1(s\kappa)}{K_1(s\kappa)}-I_1(\rho s\kappa)\right] \tag{3-39}$$

Following a similar procedure, the ζ-plane contour integrations

on the remaining quantities of eq. (3-27) may all be expressed in the similar forms: viz.

$$\hat{T} = \frac{1}{\pi^2}\int_0^{\infty} G(v)\,\hat{F}_{q,k}(sv)\,dv + C\,\hat{F}_{q,k}(sx), \quad q = I,O \tag{3-40}$$

where

$$\hat{F}_{I,k}(sv) = K_o(b/a\,sv)\left\{(-1)^k I_k(\rho sv) + \frac{I_1(sv)}{K_1(sv)} K_k(\rho sv)\right\}, \quad k = o,1 \tag{3-41a}$$

$$\hat{F}_{O,k}(sv) = K_k(\rho sv)\left\{I_o(b/a\,sv) + \frac{I_1(sv)}{K_1(sv)} K_o(b/a\,sv)\right\}, \quad k = o,1 \tag{3-41b}$$

The terms $\hat{F}_{q,k}$, G(v), and C, appearing in the generic expression above, are given conveniently in Table 1. Furthermore, the imaginary parts of the algebraic expressions are given by

$$\mathrm{Im}\{m_w(iv)\} = \left\{\begin{array}{ll} 0, & v < 1/\sqrt{3} \\ \dfrac{3(1-2v^2)^2\sqrt{v^2-1/3}}{\Delta(v)}, & 1/\sqrt{3} < v < 1 \\ \dfrac{3(1-2v^2)^2\sqrt{v^2-1/3} + 12v^2(v^2-1/3)\sqrt{v^2-1}}{\Delta(v)}, & 1 < v \end{array}\right\} \tag{3-42a}$$

$$\mathrm{Im}\{m_u(iv)\} = \left\{\begin{array}{ll} 0, & v < 1/\sqrt{3} \\ \dfrac{6(2v^2-1)\sqrt{v^2-1/3}\sqrt{1-v^2}}{\Delta(v)}, & 1/\sqrt{3} < v < 1 \\ 0, & 1 < v \end{array}\right\} \tag{3-42b}$$

$$\mathrm{Im}\{m_e'(iv)\} = \left\{\begin{array}{ll} 0, & v < 1/\sqrt{3} \\ \dfrac{12v^2(2v^2-1)\sqrt{v^2-1/3}\sqrt{1-v^2}}{\Delta(v)}, & 1/\sqrt{3} < v < 1 \\ 0, & 1 < v \end{array}\right\} \tag{3-42c}$$

where $\Delta(v) = 3 - 24v^2 + 56v^4 - 32v^6$ (3-43)

$\hat{T}$	$G(v)$	C	q	k
$\frac{a\mu}{Q}\hat{w}_I$	$-v\,\mathrm{Im}\{m_w(iv)\}$	0	I	0
$\frac{a\mu}{Q}\hat{w}_o$	$-v\,\mathrm{Im}\{m_w(iv)\}$	0	0	0
$\frac{a\mu}{Q}\hat{u}_I$	$-v^2\,\mathrm{Im}\{m_u(iv)\}$	$-\frac{\chi}{8\pi}$	I	1
$\frac{a\mu}{Q}\hat{u}_o$	$-v^2\,\mathrm{Im}\{m_u(iv)\}$	$-\frac{\chi}{8\pi}$	0	1
$\frac{a^2\mu}{Q}\hat{e}_I$	$\frac{vs}{3}\,\mathrm{Im}\{m'_e(iv)\}$	$-\frac{s\chi}{12\pi}$	I	0
$\frac{a^2\mu}{Q}\hat{e}_o$	$\frac{vs}{3}\,\mathrm{Im}\{m'_e(iv)\}$	$-\frac{s\chi}{12\pi}$	0	0

TABLE 1. FINAL EXPRESSIONS FOR TRANSFORM SOLUTION

It is worth noting here that by means of the above analysis, all the infinite integrals have been reduced to finite integrations with the exception of the case of the vertical displacement. Furthermore, the discontinuties occuring in eqs. (3-42) at $v = 1/\sqrt{3}$ and $v = 1$ will be seen to correspond to the P and S body wave fronts respectively, and thus the immediate contribution due to each wave type may be evaluated.

The time functions of the transformed quantities, given by eq. (3-40) are now obtained by inverting the integrands in the integral terms and by direct inversion of the terms that arise from the residues at the Rayleigh poles.

As an illustration of the former case, the Laplace inversion of the integrand in the expression for the vertical displacement component, at a field point inside the source is examined.

From the Bromwich integral form of the Laplace inversion, eq. (2-17),

$$f(\tau) = \frac{1}{2\pi i}\int_{B_r} \hat{F}(s)\, e^{\tau s}\, ds$$

using eq. (3-40), the vertical displacement at the free surface may now be written as

$$\frac{a\mu}{Q} w_I(\rho,0,\tau) = -\frac{1}{\pi^2}\frac{1}{2\pi i}\int_{B_r} e^{\tau s} ds \int_0^\infty v\, \mathrm{Im}\{m_w\}\, \hat{F}_{I,0}(sv)\, dv$$

$$= -\frac{1}{\pi^2}\int_0^\infty \mathrm{Im}\{m_w\}\, dv \frac{1}{2\pi i}\int_{B_r} e^{\tau s} \hat{F}_{I,0}(sv)\, v\, ds \qquad (3\text{-}44)$$

Introducing the change of variables

$$p = sv \tag{3-45}$$

$$x = \frac{\tau}{v} \tag{3-46}$$

the displacement becomes

$$\frac{a\mu}{Q} W_I(\rho,0,\tau) = -\frac{1}{\pi^2}\int_0^\infty \mathrm{Im}\{m_w(iv)\} f_{wI}(x)\, dv \tag{3-47}$$

where

$$f_{wI}(x) \equiv \mathcal{L}^{-1}\left\{\hat{F}_{I,o}(p)\right\} = \frac{1}{2\pi i}\int_{Br} \hat{F}_{I,o}(p)\, e^{xp}\, dp \tag{3-48}$$

and where the subscripts w and I refer to the vertical displacement component and the field point inside the source, respectively.

Now, considering the inversion of the residue terms, it is obvious from eq. (3-40), that the resulting expressions are of the same form as eq. (3-48) with v replaced by κ , i.e.,

$$f_{q,\kappa}\left(\frac{\tau}{x}\right) = f_{q,\kappa}(x) = \frac{1}{2\pi i}\int_{Br} \hat{F}_{q,\kappa}(p)\, e^{xp}\, dp, \quad q = I, 0, \quad \kappa = 0, 1 \tag{3-49}$$

Since all of the required inversions are of the same form as the inversion for the integrand of the vertical displacement component, eq. (3-48), this case will be used to illustrate the method of Laplace inversion.

Before proceeding with the actual inversion of this integrand, it is profitable and indeed necessary to examine first the general nature of $f_{wI}(\bar{x})$, for, as will be seen subsequently, the inverse vanishes and possesses discontinuities for certain values of x.

These properties of $f_{wI}(x)$ for finite values of x, may be

investigated by considering the Bromwich integral contour closed to the right with a large semi-circle as shown in Fig. 3.

The function $F_{I\rho}(p)$ requires a branch cut along the negative real axis. Moreover, it possesses no poles and is analytic for all Re $\{p\} > 0$. [12]

By Cauchy's Theorem, therefore,

$$\int_{ABCA} \hat{F}_{I,o}(p)\, e^{xp}\, dp = 0 \tag{3-50}$$

and hence

$$f_{wI}(x) = -\frac{1}{2\pi i} \lim_{|p|\to\infty} \int_{BCA} \hat{F}_{I,o}(p) e^{xp} dp \tag{3-51a}$$

or, more explicity,

$$f_{wI}(x) = -\frac{1}{2\pi i} \lim_{|p|\to\infty} \int_{BCA} \left[K_o(b/a\, p) I_o(\rho p) + \frac{I_1(p)}{K_1(p)} K_o(b/a\, p) K_o(\rho p) \right] e^{xp} dp \tag{3-51b}$$

The above integral along the infinite arc BCA is now examined for various ranges of x. Using the asymptotic expansions for the Bessel functions [12],

$$I_n(p) \sim \frac{e^p}{\sqrt{2\pi p}} \left(1 - \frac{4n^2-1}{8p} \ldots\right), \quad K_n(p) \sim \frac{\sqrt{\pi} e^{-p}}{\sqrt{2p}} \left(1 + \frac{4n^2-1}{8p} \ldots\right) \tag{3-52a,b}$$

and letting $|p| \to \infty$, the following limits, corresponding to the two terms of the integrand of eq. (3-51b), are obtained

$$\lim_{|p|\to\infty} p e^{xp} K_o(b/a\, p) I_o(\rho p) \sim \frac{1}{2\sqrt{\rho\, b/a}} e^{[x - (b/a - \rho)]p} \tag{3-53a}$$

$$\lim_{|p|\to\infty} p e^{xp} K_o(b/a\, p) K_o(\rho p) \frac{I_1(p)}{K_1(p)} \sim \frac{1}{2\sqrt{\rho\, b/a}} e^{[x - (\rho + b/a - 2)]p} \tag{3-53b}$$

Using the large circle lemma, eq. (3-16), it follows that the integral of the first term vanishes for $0 < x < b/a - \rho$, while that of the second term vanishes for $0 < x < \rho + b/a - 2$.

Hence, the inversion is as follows:

$$f_{wI}(x) = \begin{cases} 0 , & 0 < x < b/a - \rho \quad (3\text{-}54a) \\ \mathcal{I}^{-1}\{K_o(b/a\,p) I_o(\rho p)\} \equiv f^D_{wI}(x) , & b/a - \rho < x < \rho + b/a - 2 \quad (3\text{-}54b) \\ \mathcal{I}^{-1}\left\{K_o(b/a\,p)\left[K_o(\rho p)\frac{I_1(p)}{K_1(p)} + I_o(\rho p)\right]\right\} \equiv f^R_{wI}(x) , & \rho + b/a - 2 < x \quad (3\text{-}54c) \end{cases}$$

It may be noted that the values of x at which the above discontinuities occur correspond to arrival time parameters of direct and reflected wave fronts; therefore the corresponding quantities are denoted as above by superscripts D and R respectively.

Following a similar procedure, the inversion of the integrands of the remaining quantities of eq. (3-40) are found to exhibit discontinuities at the same values of x.

Having established and located the discontinuities of the integrand it is now possible to proceed with the actual inversions for the two separate nonvanishing cases.

Consider first the case where $b/a - \rho < x < \rho + b/a - 2$. Then, by eq. (3-54),

$$f^D_{wI}(x) = \frac{1}{2\pi i}\int_{Br} K_o(b/a\,p) I_o(\rho p) e^{xp}\, dp \qquad (3\text{-}55)$$

Letting $x = b/a - \rho + y$, (3-56)

the above may be rewritten as

$$f^{D}_{wI}(x) = \frac{1}{2\pi i}\int_{Br}\left[K_o(b/a\,p)e^{b/a\,p}\right]\left[I_o(\rho p)e^{-\rho p}\right]e^{yp}\,dp \tag{3-57}$$

Now the Laplace inversion of each factor above is readily known [13]: viz.

$$\mathcal{I}^{-1}\left\{K_o(b/a\,p)e^{b/a\,p}\right\} = \frac{H(y)}{\sqrt{y(y+2b/a)}} \tag{3-58a}$$

$$\mathcal{I}^{-1}\left\{I_o(\rho p)e^{-\rho p}\right\} = \frac{H(y)-H(y-2\rho)}{\pi\sqrt{y(2\rho-y)}} \tag{3-58b}$$

where H(y) is the unit step function.

Application of the convolution theorem yields immediately

$$f^{D}_{wI}(x) = \int_0^y \frac{[H(\eta)-H(\eta-2\rho)]\cdot H(y-\eta)}{\pi\sqrt{\eta(2\rho-\eta)(y-\eta)(y-\eta+2b/a)}}\,d\eta \tag{3-59a}$$

or, for $y < 2\rho$, i.e., $x < \rho + b/a$,

$$f^{D}_{wI}(x) = \int_0^y \frac{d\eta}{\pi\sqrt{\eta(2\rho-\eta)(y-\eta)(y-\eta+2b/a)}} \tag{3-59b}$$

This integral reduces to an elliptic integral by the change of variable suggested by Cayley [14],

$$\eta = \frac{2\rho y(1-q^2)}{2\rho - yq^2} \tag{3-60}$$

yielding

$$f^{D}_{wI}(x) = \frac{1}{\pi\sqrt{\rho\, b/a}}\,K(m) \tag{3-61}$$

where

$$K(m) = \int_0^1 \frac{dq}{\sqrt{(1-q^2)(1-mq^2)}} \tag{3-62a}$$

is the complete elliptic integral of the first kind and

$$m = \frac{x^2 - (b/a - \rho)^2}{4\rho\, b/a} \tag{3-62b}$$

is the modulus. [13]

For the case $\rho + b/a - 2 < x$, the required inversion, according to eq. (3-54) is

$$f_{wI}^{R}(x) = \frac{1}{2\pi i}\int_{Br}\left[K_o(b/a\,p)I_o(\rho p) + K_o(b/a\,p)K_o(\rho p)\frac{I_1(p)}{K_1(p)}\right]e^{xp}\,dp \tag{3-63}$$

Due to the multivalued character of the function $K_n(p)$, a branch cut is required and is taken along the negative real axis (Fig. 4.). From Cauchy's theorem along the closed contour,

$$\oint \hat{F}_{I,o}(p)e^{xp}\,dp = 0, \tag{3-64}$$

it follows that

$$f_{wI}^{R}(x) = -\frac{1}{2\pi i}\left\{\left(\int_{BC} + \int_{FA}\right) + \left(\int_{CD} + \int_{EF}\right) + \int_{DE}\right\} \tag{3-65}$$

Using asymptotic expansions and series representations of the modified Bessel functions, and applying the large and small circle lemmas above, the integrals along the arcs BC, FA, and DE are found to vanish.

The remaining integrals along the branch cut are readily evaluated using the following relations: [12]:

$$I_k(\eta e^{\pm i\pi}) = e^{\pm ik\pi} I_k(\eta), \qquad k = 0,1 \tag{3-66a}$$

$$K_k(\eta e^{\pm i\pi}) = e^{\mp ik\pi} K_k(\eta) \mp i\pi I_k(\eta), \qquad k = 0,1 \tag{3-66b}$$

where $p = \eta e^{+i\pi}$ along CD, and $p = \eta e^{-i\pi}$ along EF. Thus, upon the correct substitutions,

$$f^{R}_{wI}(x) = \int_0^\infty \frac{e^{-x\eta} G_w(\rho, b/a, \eta)}{K_1^2(\eta) + \pi^2 I_1^2(\eta)} d\eta \ , \tag{3-67}$$

where

$$G_w(\rho, b/a, \eta) = [I_1(\eta)K_0(\rho\eta) + K_1(\eta)I_0(\rho\eta)][I_1(\eta)K_0(b/a\,\eta) + K_1(\eta)I_0(b/a\,\eta)] \tag{3-68}$$

In a similar manner, the integrands of the expression for the vertical displacement at a field point outside the source maybe inverted. In addition, the required inversions for the radial displacement component are all obtained similarly.

A different approach however is appropriate for the dilatation due to the presence of Dirac-delta functions.

Noting that the integrands as well as the residue terms are simply those of the vertical displacement multiplied by p, the inversion may be obtained by use of the following theorem in Laplace transform theory. [15]

Let f(x) be a piecewise continuous function of exponential order, with finite discontinuities of magnitudes B_k at $x = x_k$, $k = 0, 1, \ldots$

Then, if $\hat{F}(p) = \mathcal{L}\{f(x)\}$, (3-69a)

$$\mathcal{L}^{-1}\{p\hat{F}(p)\} = \frac{df(x)}{dx} + \sum_{k=0}^{\infty} B_k \delta(x - x_k) \tag{3-69b}$$

Consider now the integrand for the dilatation at a field point inside the source.

Then
$$f_{eI}(x) = \mathcal{I}^{-1}\left\{p\hat{F}_{I,o}(p)\right\} \tag{3-70}$$

and, by the above theorem,

$$f_{eI}(x) = \frac{i}{dx} f_{wI}(x) + \left[f_{wI}\right]_{x = b/a - \rho} \delta(x - (b/a - \rho)) + \left[f_{wI}\right]_{x = \rho + b/a - 2} \delta(x - (\rho + b/a - 2)) \tag{3-71}$$

where the bracketed quantities indicate the discontinuities.

The discontinuities in $f_{wI}(x)$ at $x = b/a - \rho$ and $x = \rho + b/a - 2$ may now be evaluated by means of the initial value theorem.

To illustrate this procedure, for the discontinuity at $x = b/a - \rho$, application of the initial value theorem to eq. (3-57) yields

$$\begin{aligned} \lim_{x \to b/a - \rho} f^{D}_{wI}(x) &= \lim_{y \to 0} f^{D}_{wI}(y) \\ &= \lim_{|p| \to \infty} p K_o(b/a\, p) e^{b/a\, p} I_o(\rho p) e^{-\rho p} \\ &= \frac{1}{2\sqrt{\rho\, b/a}} \end{aligned} \tag{3-72}$$

where, again, use has been made of the asymptotic expansions of the modified Bessel Functions. [12]

In a similar manner, the discontinuity at $x = \rho + b/a - 2$ may be obtained. Thus, subtracting eq. (3-54b) from (3-54c)

$$\left(f^{R}_{wI} - f^{D}_{wI}\right)_{x = \rho + b/a - 2} = \mathcal{I}^{-1}\left\{K_o(b/a\, p) K_o(\rho p) \frac{I_1(p)}{K_1(p)}\right\} \tag{3-73}$$

A change of variable, $x = \rho + b/a - 2 + y$ and application of the initial value theorem yields,

$$\left[f_{wI}(x)\right]_{x=\rho+b/a-2} = \frac{1}{2\sqrt{\rho\, b/a}} \tag{3-74}$$

The derivative term in eq. (3-71) is readily evaluated from eqs. (3-54, 61, or 67), where in the range $b/a - \rho < x < \rho + b/a - 2$ the following relationships are used: [16]

$$\frac{dK(m)}{dm} = \frac{E(m) - (1-m)K(m)}{2m(1-m)} \tag{3-75a}$$

where

$$E(m) = \int_0^1 \frac{\sqrt{1-mq^2}}{\sqrt{1-q^2}}\, dq \tag{3-75b}$$

is the complete elliptic integral of the second kind.

Thus, eq. (3-71) finally becomes

$$f_{eI}(x) = \frac{1}{2\sqrt{\rho\, b/a}}\left[\delta(x-(b/a-\rho)) + \delta(x-(\rho+b/a-2))\right] + \begin{cases} 0 & x < b/a - \rho \\ f_{eI}^{D}(x) & b/a-\rho < x < \rho+b/a-2 \\ f_{eI}^{R}(x) & \rho+b/a-2 < x \end{cases} \tag{3-76}$$

where

$$f_{eI}^{D}(x) = \frac{x}{4\pi(\rho\, b/a)^{3/2}}\left[\frac{E(m)-(1-m)K(m)}{m(1-m)}\right] \tag{3-77a}$$

and

$$f_{eI}^{R}(x) = -\int_0^{\infty} \frac{G_w(\rho, b/a, \eta)\, e^{-x\eta}\, \eta}{K_1^2(\eta) + \pi^2 I_1^2(\eta)}\, d\eta \tag{3-77b}$$

The inversion for the field point outside the source is similarly obtained.

Finally then, the inversions for all of the quantities given by eq. (3-40) may be expressed as follows, with the aid of the change of variable $v = \frac{I}{x}$ given by eq. (3-46),

$$\frac{a\mu}{Q} w(\rho,0,\tau) = -\frac{1}{\pi^2}\int_{\frac{1}{\sqrt{3}}}^{\tau/|\rho-b/a|} \mathrm{Im}\{m_w\} f_w(\rho, b/a, \tau/v)\, dv \tag{3-78a}$$

$$\frac{a\mu}{Q} u_{(I,0)}(\rho,0,\tau) = -\frac{1}{\pi^2}\int_{\frac{1}{\sqrt{3}}}^{1} v\,\mathrm{Im}\{m_u\} f_{u(I,0)}(\rho, b/a, \tau/v)\, dv - \frac{1}{8\pi} f_{u(I,0)}(\rho, b/a, \tau/x) \tag{3-78b}$$

$$\frac{a^2\mu}{Q} e(\rho,0,\tau) = -\frac{1}{4\pi\rho}\delta(\rho-b/a)H(\tau) + \frac{1}{3\pi^2}\int_{\frac{1}{\sqrt{3}}}^{1} \frac{1}{v}\mathrm{Im}\{m'_e\} \cdot$$

$$\cdot\left[f_e(\rho, b/a, \tau/v) + \frac{v\,\delta(v-\tau/|\rho-b/a|)}{2\sqrt{\rho\, b/a}\,|\rho-b/a|} + \frac{v\,\delta(v-\tau/(\rho+b/a-2))}{2\sqrt{\rho\, b/a}\,(\rho+b/a-2)}\right] dv$$

$$-\frac{1}{12\pi}\left\{f_e(\rho, b/a, \tau/x) - \frac{S(\tau/x-|\rho-b/a|)}{2\sqrt{\rho\, b/a}} - \frac{S(\tau/x-(\rho+b/a-2))}{2\sqrt{\rho\, b/a}}\right\} \tag{3-78c}$$

where the functions $f_{(\ )}(\rho, b/a, \tau/v)$, are defined in their respective domains as follows:

$$f_{(\ )}(\rho, b/a, \tau/v) = \begin{cases} 0, & \frac{\tau}{|\rho-b/a|} < v \\ f^D_{(\ )}(\rho, b/a, \tau/v), & \frac{\tau}{\rho+b/a-2} < v < \frac{\tau}{|\rho-b/a|} \\ f^R_{(\ )}(\rho, b/a, \tau/v), & v < \frac{\tau}{\rho+b/a-2} \end{cases} \tag{3-79}$$

The direct wave responses are given by

$$f^D_w = f^D_{wI} = f^D_{w0} = \frac{1}{\pi\sqrt{\rho\, b/a}} K(m) \tag{3-80a}$$

$$f^D_{uI} = \frac{1}{\pi\sqrt{\rho\, b/a}}\left\{K(m) - \frac{(\rho+b/a-\tau/v)}{\rho}\Pi(n_1,m)\right\} \tag{3-80b}$$

$$f^D_{u0} = \frac{1}{\pi\sqrt{\rho\, b/a}}\left\{\frac{(\tau/v-b/a)}{\rho}K(m) + \frac{(\rho+b/a-\tau/v)}{\rho}\Pi(n_2,m)\right\} \tag{3-80c}$$

$$f_e^D = f_{eI}^D = f_{eO}^D = \frac{\tau/v}{4\pi(\rho\, b/a)^{3/2}} \left\{ \frac{E(m) - (1-m)K(m)}{m(1-m)} \right\} \tag{3-80d}$$

where

$$\Pi(n,m) = \int_0^1 (1-nq^2)^{-1}(1-q^2)^{-1/2}(1-mq^2)^{-1/2}\, dq \tag{3-81}$$

is the complete elliptic integral of the third kind, with modulus, m, and characteristic n, and where

$$m = \frac{(\tau/v)^2 - (b/a - \rho)^2}{4\rho\, b/a} \tag{3-82a}$$

$$n_1 = \frac{\tau/v - (b/a - \rho)}{2\rho} \tag{3-82b}$$

$$n_2 = \frac{\tau/v - (\rho - b/a)}{2\, b/a} \tag{3-82c}$$

In addition, the response functions after reflections have occured are given by

$$f_w^R = f_{wI}^R = f_{wO}^R = \int_0^\infty \frac{G_w(\rho, b/a, \eta)\, e^{-\tau/v\,\eta}}{K_1^2(\eta) + \pi^2 I_1^2(\eta)}\, d\eta \tag{3-83a}$$

$$f_{uI}^R = \int_0^\infty \frac{G_{uI}(\rho, b/a, \eta) e^{-\tau/v\,\eta}}{K_1^2(\eta) + \pi^2 I_1^2(\eta)}\, d\eta \tag{3-83b}$$

$$f_{uO}^R = \frac{1}{\rho} + \int_0^\infty \frac{G_{uO}(\rho, b/a, \eta)\, e^{-\tau/v\,\eta}}{K_1^2(\eta) + \pi^2 I_1^2(\eta)}\, d\eta \tag{3-83c}$$

$$f_e^R = f_{eI}^R = f_{eO}^R = -\int_0^\infty \frac{G_w(\rho, b/a, \eta)\, \eta\, e^{-\tau/v\,\eta}}{K_1^2(\eta) + \pi^2 I_1^2(\eta)}\, d\eta \tag{3-83d}$$

where

$$G_w = \left[I_1(\eta)K_0(\rho\eta) + K_1(\eta)I_0(\rho\eta)\right] \cdot \left[I_1(\eta)K_0(b/a\,\eta) + K_1(\eta)I_0(b/a\,\eta)\right] \tag{3-84a}$$

$$G_{uI} = \left[K_1(\eta)I_1(\rho\eta) - I_1(\eta)K_1(\rho\eta)\right] \cdot \left[I_1(\eta)K_0(b/a\,\eta) + K_1(\eta)I_0(b/a\,\eta)\right] \tag{3-84b}$$

$$G_{uO} = \left[K_1(\eta)I_1(\rho\eta) + I_1(\eta)K_1(\rho\eta)\right] \cdot \left[I_1(\eta)K_0(b/a\,\eta) + K_1(\eta)I_0(b/a\,\eta)\right] \tag{3-84c}$$

It should be noted that, for finite τ , and $\rho \neq b/a$, the integrals with respect to v in all of the above quantities are finite and contain integrands consisting of the algebraic quantites of eq. (3-42), and either the elliptic integrals of eq. (3-80), or the semi-infinite branch integrals of eq. (3-83). The singularites occuring at $\rho = b/a$ are treated subsequently.

The stress components on the free surface are expressed immediately in terms of the dilatation and the radial displacement component, by eqs.(3-6,7) as follows:

$$\frac{a^2}{Q}\sigma_{\theta\theta(I,0)}(\rho,0,\tau) = \frac{a^2\mu}{Q}e(\rho,0,\tau) + \frac{a\mu}{Q}\frac{2}{\rho}u_{(I,0)}(\rho,0,\tau) \qquad (3\text{-}85a)$$

$$\frac{a^2}{Q}\sigma_{rr(I,0)}(\rho,0,\tau) = \frac{4a^2\mu}{Q}e(\rho,0,\tau) - \frac{a\mu}{Q}\frac{2}{\rho}u_{(I,0)}(\rho,0,\tau) \qquad (3\text{-}85b)$$

$$+ \frac{1}{2\pi\rho}\delta(\rho - b/a)H(\tau)$$

CHAPTER 4

ANALYSIS OF SINGULARITIES OF THE SOLUTION AND BEHAVIOR AT WAVE FRONTS

The response on the plane boundary is seen to be a combination of the three fundamental wave types: dilatation (P), equivoluminal (S), and Rayleigh (R) surface waves.

An analysis of the discontinuties in the expressions of eqs. (3-78) leads to the type and location of the wave fronts. Consider for example, the radial component of displacement, i.e.

$$\frac{a\mu}{Q} u_{(I,0)}(\rho, 0, \tau) = -\frac{1}{\pi^2}\int_{\frac{1}{\sqrt{3}}}^{1} v \cdot \mathrm{Im}\{m_u\} f_{u_{(I,0)}}(\rho, b/a, \tau/v)\, dv - \frac{1}{8\pi} f_{u_{(I,0)}}(\rho, b/a, \tau/\chi) \tag{4-1}$$

The second term on the right hand side, which arises from the Rayleigh poles has, in view of eq. (3-79), discontinuities at

$$\frac{\tau}{|\rho - b/a|} = \chi, \qquad \frac{\tau}{\rho + b/a - 2} = \chi \tag{4-2a,b}$$

or, in terms of the original variables, at

$$t_R^D = \frac{|r-b|}{C_R} \tag{4-3a}$$

and

$$t_R^R = \frac{(r-a) + (b-a)}{C_R} \tag{4-3b}$$

It is noted that t_R^D and t_R^R are the arrival times of a Rayleigh wave traveling the direct (D) and reflected (R) route from the source to the field point respectively.

Similarly, the integrand appearing in the integral of eq. (4-1)

has discontinuities at

$$v = \frac{\tau}{|\rho - b/a|} \quad , \quad v = \frac{\tau}{\rho + b/a - 2} \tag{4-4a,b}$$

At a particular field point, ρ, as time, τ, elapses, these discontinuities interact with the limits of the integration. There are therefore, critical times at which the discontinuities in the integrand coincide with the end points of the domain of integration, viz.

$$\frac{\tau}{|\rho - b/a|} = \frac{1}{\sqrt{3}} \quad , \quad \frac{\tau}{|\rho - b/a|} = 1 \tag{4-5a,b}$$

$$\frac{\tau}{\rho + b/a - 2} = \frac{1}{\sqrt{3}} \quad , \quad \frac{\tau}{\rho + b/a - 2} = 1 \tag{4-6a,b}$$

or, again in terms of the original variables,

$$t_P^D = \frac{|r - b|}{C_P} \quad , \quad t_S^D = \frac{|r - b|}{C_S} \tag{4-7a,b}$$

$$t_P^R = \frac{(r-a)+(b-a)}{C_P} \quad , \quad t_S^R = \frac{(r-a)+(b-a)}{C_S} \tag{4-8a,b}$$

As above, t_P^D and t_P^R are the arrival times of the direct (D) and reflected (R) P-waves, while t_S^D and t_S^R are the arrival times of the corresponding S-waves.

Summarizing the above results, it is seen that a total of six wave fronts exist on the plane boundary: three direct outgoing waves of the P, S, and R types, and three direct ingoing waves which reflect as three reflected outgoing waves of the same type.

The contribution of each wave in the region of the wave front can be analyzed by considering the wave profile, i.e. the variation of magnitude with position.

To illustrate the procedure in the vicinity of a P-wave front, consider the profile for the radial displacement immediately behind the direct outgoing P-wave. Let

$$\rho_P = b/a + \sqrt{3}\,\tau \;, \quad \rho_P^- = \rho_P - \epsilon\, b/a \tag{4-9a,b}$$

where ρ_P and ρ_P^- denote points at and immediately behind the P-wave front, respectively, and where ϵ is a small (positive) parameter.

Then
$$\frac{\tau}{\rho_P - b/a} = \frac{1}{\sqrt{3}} \tag{4-10a}$$

and
$$\frac{\tau}{\rho_P^- - b/a} = \frac{1}{\sqrt{3}}\left(1 + \frac{\epsilon\, b/a}{\sqrt{3}\,\tau}\right) \tag{4-10b}$$

Substituting eqs. (3-42b) and (3-79) into eq. (4-1), it follows from the above, that for any τ ,

$$\frac{a\mu}{Q} u_0(\rho_P, 0, \tau) = 0 \tag{4-11a}$$

$$\frac{a\mu}{Q} u_0(\rho_P^-, 0, \tau) = -\frac{6}{\pi^2}\int_{1/\sqrt{3}}^{1/\sqrt{3}\left(1 + \frac{\epsilon\, b/a}{\sqrt{3}\,\tau}\right)} \sqrt{v - \frac{1}{\sqrt{3}}}\cdot$$

$$\left\{\frac{v^2(2v^2-1)\sqrt{v + 1/\sqrt{3}}\sqrt{1-v^2}}{\Delta(v)} \cdot f_{u0}^{D}(\rho_P^-, b/a, \tau/v)\right\} dv \tag{4-11b}$$

Now, eq. (4-11b) may be evaluated for small values of ϵ by expanding the analytic portions of the integrand in a Taylor series, combining and integrating term by term.

It is noted that the factor $\sqrt{v - \frac{1}{\sqrt{3}}}$ is not analytic at $v = \frac{1}{\sqrt{3}}$ and therefore cannot be expanded in a Taylor series in any region

containing that point. However, it can be shown that the term $f^D_{u0}(\bar{\rho_p}, b/a, \tau/v)$ is analytic. To this end, consider the original expression, analogous to eq. (3-54), that led to $f^D_{u0}(x)$, eq. (3-80c):

$$f^D_{u0}(x) = \frac{1}{2\pi i}\int_{Br} I_o(b/a\, p) K_1(\bar{\rho_p} p)\, e^{xp}\, dp \qquad (4\text{-}12a)$$

where

$$\bar{\rho_p} - b/a < x < \bar{\rho_p} + b/a - 2 \qquad (4\text{-}12b)$$

From eq. (4-10b) and according to the relation $x = \tau/v$, the range of integration of v in eq. (4-11b) corresponds to an integration in the range

$$\bar{\rho_p} - b/a < x < \bar{\rho_p} - b/a + \epsilon\, b/a \qquad (4\text{-}13)$$

Hence it follows that if it can be shown that $f^D_{u0}(\bar{\rho_p}, b/a, x)$ is analytic at $x = \bar{\rho_p} - b/a$ the analyticity in the range of integration is established.

Introducing a change of variables

$$x = \bar{\rho_p} - b/a + y\,, \quad p = \frac{\bar{p}}{y} \qquad (4\text{-}14a,b)$$

eq. (4-12a) becomes:

$$f^D_{u0}(x) = \frac{1}{2\pi i}\int_{B'_r} I_o\left(b/a\, \frac{\bar{p}}{y}\right) K_1\left(\bar{\rho_p}\, \frac{\bar{p}}{y}\right) e^{\bar{\rho_p}\frac{\bar{p}}{y}}\, e^{-b/a\,\frac{\bar{p}}{y}}\, e^{\bar{p}}\, \frac{d\bar{p}}{y} \qquad (4\text{-}15)$$

Replacing the modified Bessel functions by their asymptotic expansions eq. (3-52), for small y, $(x \to \bar{\rho_p} - b/a)$ and using eq. (4-14b), eq. (4-15) becomes:

$$f_{u0}^{D}(x) = \frac{1}{2\pi i}\int_{Br} \frac{1}{2\sqrt{\rho_p^- - b/a}}\left\{\frac{1}{p} + \frac{1}{p^2}\left(\frac{1}{8b/a} + \frac{3}{8\rho_p^-}\right) + O\left(\frac{1}{p^3}\right)\right\} e^{yp}\,dp \qquad (4\text{-}16)$$

from which, by means of the known Laplace inversions

$$f_{u0}^{D}(y) = \frac{1}{2\sqrt{\rho_p^- - b/a}}\left\{1 + \left(\frac{1}{8b/a} + \frac{3}{8\rho_p^-}\right)y + O(y^2)\right\} \qquad (4\text{-}17)$$

Since $f_{u0}^{D}(y)$ is analytic at y=0, it follows that $f_{u0}^{D}(x)$ is analytic at $x=\rho_p^- - b/a$, and hence from the above also in the range of integration of eq. (4-11b).

Moreover, since the algebraic term within the brackets of eq. (4-11b) is readily seen to be analytic, it follows that this equation may finally be written as

$$\frac{a\mu}{Q} u_0(\rho_p^-, 0, \tau) = \int_{\frac{1}{\sqrt{3}}}^{\frac{1}{\sqrt{3}}\left(1 + \frac{\epsilon\, b/a}{\sqrt{3}\tau}\right)} F(v)\sqrt{v - 1/\sqrt{3}}\; dv \qquad (4\text{-}18)$$

where F(v), the analytic portion of the integrand, has the expansion

$$F(v) = F\left(\frac{1}{\sqrt{3}}\right) + \frac{dF}{dv}\left(\frac{1}{\sqrt{3}}\right)\cdot\left(v - \frac{1}{\sqrt{3}}\right) + \cdots \qquad (4\text{-}19)$$

The dominant term of eq. (4-18) is readily found upon integration to be

$$\frac{a\mu}{Q} u_0(\rho_p^-, 0, \tau) = A\,\epsilon^{3/2} \qquad (4\text{-}20)$$

where A is constant.

It therefore follows that the radial displacement component is continuous, i.e. there are no jumps in displacement across the direct

P-wave front. Furthermore, it is noted that the slope $\left\{\frac{\partial u_o}{\partial \rho}\right\}_{\rho=\rho_P}$ of the displacement profile is also continuous across the direct P-wave front.

In a similar manner, it can be shown that both the radial and vertical displacement components exhibit the same behavior behind the P-wave fronts and immediately in front of all the S-wave fronts, while behind the S-wave fronts, no discontinuity exists.

A similar procedure may be used for the dilatation, and to further illustrate the details of the method, the dilatation in the vicinity of the direct outgoing S-wave front is now considered.

The P- and S-wave contribution of the dilatation given by eq. (3-78c) becomes, upon substituting eq. (3-42c), the following.

$$\frac{a^2\mu}{Q} e_o(\rho,o,\tau) = \frac{4}{\pi^2}\int_{1/\sqrt{3}}^{1} \frac{v(2v^2-1)\sqrt{1-v^2}\sqrt{v^2-1/3}}{\Delta(v)} \cdot$$

$$\left\{ f_{-}(\rho, b/a, \tau/v) + \frac{v\,\delta\left(v - \frac{\tau}{\rho - b/a}\right)}{} + \frac{v\,\delta\left(v - \frac{\tau}{\rho + b/a - 2}\right)}{} \right\} dv$$

Let $\rho_s = b/a + \tau$ (4-

Let and $\rho_s^{\pm} = \rho_s \pm \epsilon\, b/a$ (4-)

and where ρ_s^+, ρ_s, ρ_s^- denote points immediately ahead, at, and behind)

where ρ_s^+, ρ_s, ρ_s^- denote points immediately ahead, at, and behind the S front respectively.

Then $$\frac{\tau}{\rho_s - b/a} = 1 \qquad (4\text{-}23a)$$

and $$\frac{\tau}{\rho_s^{\pm} - b/a} = 1 \mp \frac{\epsilon\, b/a}{\tau} \qquad (4\text{-}23b)$$

Furthermore, let τ be within the range

$$\frac{\tau}{\rho_s + b/a - 2} < \frac{1}{\sqrt{3}} \tag{4-24}$$

thus restricting the analysis here to the case where the reflected P-wave has not yet reached the field point ρ_s.

Following a procedure similar to that above, the dominant terms of eq. (4-21) yield the following:

$$\frac{a^2\mu}{Q}\left[e_o\right]_{S^+} \equiv \frac{a^2\mu}{Q}\left\{e_o(\rho_s) - e_o(\rho_s^+)\right\} \approx A\epsilon^{1/2} + B\epsilon \tag{4-25a}$$

$$\frac{a^2\mu}{Q}\left[e_o\right]_{S^-} \equiv \frac{a^2\mu}{Q}\left\{e_o(\rho_s^-) - e_o(\rho_s)\right\} \approx B\epsilon \tag{4-25b}$$

where A and B are constants, and the bracketed quantities S^+ and S^- indicate the variation immediately preceding and behind the S wave front.

Although there is no discontinuity in the dilatation in the vicinity of the S front, it is noted that due to the term with coefficient A, the slope of the dilatation profile approaches infinity just in front of the direct outgoing S-wave.

In a similar manner, it is found that such a cusp is present just in front of the direct ingoing as well as the reflected S-wave and immediately behind all direct and reflected P-waves.

Furthermore, it follows from eqs. (3-85) and the above, that the profiles of the stresses, σ_{rr} and $\sigma_{\theta\theta}$, exhibit the same cusps as the profile of the dilatation near the P-and S-wave fronts.

The behavior of the vertical displacement in the region of the

R-wave front may be considered in a similar manner.

For the case of an outgoing wave, let

$$\rho_R = b/a + \tau/\kappa \quad , \quad \rho_R^{\pm} = \rho_R \pm \epsilon\, b/a \tag{4-26a,b}$$

where ρ_R indicates the position of the R-wave front and where the (+) and (-) signs indicate positions immediately preceding and behind the front.

Then

$$\frac{\tau}{\rho_R^{\pm} - b/a} = \kappa\left(1 \mp \frac{\epsilon\, b/a}{\tau/\kappa}\right) . \tag{4-27}$$

Furthermore, let τ be within the range

$$\frac{\tau}{\rho_R + b/a - 2} < \frac{1}{\sqrt{3}} \tag{4-28}$$

thus restricting the analysis for the purposes of illustration to the case where the reflected P-wave has not reached the point ρ_R.

Then, from eq. (3-78a),

$$\frac{a\mu}{Q} W_0(\rho_R^{\pm}, 0, \tau) = -\frac{1}{\pi^2}\int_{1/\sqrt{3}}^{1} \frac{3(1-2v^2)^2\sqrt{v^2-1/3}}{\Delta(v)} f_{w0}^{D}(\rho_R^{\pm}, b/a, \tau/v)\, dv$$

$$-\frac{1}{\pi^2}\int_{1}^{\kappa\left(1 \mp \frac{\epsilon\, b/a}{\tau/\kappa}\right)} \left(3(1-2v^2)^2\sqrt{v^2-1/3} + 12v^2(v^2-1/3)\sqrt{v^2-1}\right) \cdot$$

$$f_{w0}^{D}(\rho_R^{\pm}, b/a, \tau/v) \cdot \left\{\frac{1/2}{1/4 - v^2} + \frac{1/12(2\sqrt{3}-3)}{\kappa^2 - v^2} - \frac{1/12(2\sqrt{3}+3)}{3/4 - \sqrt{3}/4 - v^2}\right\} dv \tag{4-29}$$

where the term $\frac{1}{\Delta(v)}$, appearing in the second integral has been

expressed in terms of partial fractions.

For small ϵ , the above becomes

$$\frac{a\mu}{Q} W_0(\rho_R^{\pm}, 0, \tau) \approx -\frac{1}{\pi^2}\int_1^{\kappa\left(1 \mp \frac{\epsilon\, b/a}{\tau/\kappa}\right)} \frac{1/24\kappa\,(2\sqrt{3}-3)}{\kappa - v} \cdot$$

$$\left\{\left(3(1-2v^2)^2\sqrt{v^2-1/3} + 12v^2(v^2-1/3)\sqrt{v^2-1}\right) f^D_{w0}(\rho_R^{\pm}, b/a, \tau/v)\right\} dv \qquad (4\text{-}30)$$

Upon expanding the bracketed term in a Taylor series about $v = \kappa$ (in a similar manner to the above) and performing the integration, the dominant term is found to be

$$\frac{a\mu}{Q} W_0(\rho_R^{\pm}, 0, \tau) \approx \frac{A}{\sqrt{\rho_R\, b/a}} \ln \epsilon \qquad (4\text{-}31)$$

where A is constant.

Thus a logarithmic singularity exists immediately in front of and behind the direct outgoing R-wave. Similarly, upon examination of the vertical displacements at the other R-wave fronts, it is found that the same singularity is present immediately preceding and behind both the direct and reflected R-wave fronts.

A different method is required for examination of the radial displacement and dilatation in the region of the R-wave fronts since, as noted above, these quantities occur in uncoupled form, viz. as the residues of eqs. (3-78b) and (3-78c) respectively:

$$\frac{a\mu}{Q} u_{(I,0)}(\rho, 0, \tau) = -\frac{1}{8\pi} f_{u(I,0)}(\rho, b/a, \tau/\kappa) \qquad (4\text{-}32a)$$

$$\frac{a^2\mu}{Q} e(\rho, 0, \tau) = -\frac{1}{12\pi}\left\{f_e(\rho, b/a, \tau/\kappa) + \frac{S(\tau/\kappa - |\rho - b/a|)}{2\sqrt{\rho\, b/a}} + \frac{S(\tau/\kappa - (\rho + b/a - 2))}{2\sqrt{\rho\, b/a}}\right\} \qquad (4\text{-}32b)$$

The discontinuities across the R-wave fronts of the terms $f(\zeta, \rho, b/a, \tau/\kappa)$ appearing above are readily evaluated by the method used in obtaining eqs. (3-72) and (3-74). In the case of the dilatation, the Dirac-delta terms above define the additional singularities existing at the fronts.

Thus, combining the results, the following behavior is found to occur at the R-wave fronts:

$$\frac{a\mu}{Q}\{u_I\}^D = \frac{a\mu}{Q}[u_I]^D \tag{4-33a}$$

$$\frac{a\mu}{Q}\{u_O\}^D = \frac{a\mu}{Q}[u_O]^D \tag{4-33b}$$

$$\frac{a\mu}{Q}\{u\}^R = \frac{a\mu}{Q}[u]^R \tag{4-33c}$$

$$\frac{a^2\mu}{Q}\{e_I\}^D = \frac{a^2\mu}{Q}[e_I]^D - \frac{1}{24\pi\sqrt{\rho\, b/a}}\delta(\rho - \rho_I^D) \tag{4-33d}$$

$$\frac{a^2\mu}{Q}\{e_O\}^D = \frac{a^2\mu}{Q}[e_O]^D + \frac{1}{24\pi\sqrt{\rho\, b/a}}\delta(\rho - \rho_O^D) \tag{4-33e}$$

$$\frac{a^2\mu}{Q}\{e\}^R = \frac{a^2\mu}{Q}[e]^R + \frac{1}{24\pi\sqrt{\rho\, b/a}}\delta(\rho - \rho^R) \tag{4-33f}$$

where the superscripts D and R denote the direct and reflected wave fronts respectively, and where

$$\rho_I^D = b/a - \tau/\kappa \tag{4-34a}$$

$$\rho_O^D = b/a + \tau/\kappa \tag{4-34b}$$

and

$$\rho^R = 2 - b/a + \tau/\kappa \tag{4-34c}$$

indicate the locations of the various wave fronts.

The square brackets in eqs. (4-33) indicate the following finite

jump discontinuities across the corresponding wave fronts.

$$\frac{a\mu}{Q}\left[u_I\right]^D = \frac{1}{16\pi\sqrt{\rho\, b/a}} \tag{4-35a}$$

$$\frac{a\mu}{Q}\left[u_0\right]^D = -\frac{1}{16\pi\sqrt{\rho\, b/a}} \tag{4-35b}$$

$$\frac{a\mu}{Q}\left[u\right]^R = -\frac{1}{16\pi\sqrt{\rho\, b/a}} \tag{4-35c}$$

$$\frac{a^2\mu}{Q}\left[e_I\right]^D = -\frac{b/a - \rho}{192\pi(\rho\, b/a)^{3/2}} \tag{4-35d}$$

$$\frac{a^2\mu}{Q}\left[e_0\right]^D = -\frac{\rho - b/a}{192\pi(\rho\, b/a)^{3/2}} \tag{4-35e}$$

$$\frac{a^2\mu}{Q}\left[e\right]^R = \frac{\rho + b/a + 6\rho\, b/a}{192\pi(\rho\, b/a)^{3/2}} \tag{4-35f}$$

In addition, from eqs. (3-85a) and (3-85b), and the above the behavior of the stresses σ_{rr} and $\sigma_{\theta\theta}$ at the R-wave fronts is found to be as follows:

$$\frac{a^2}{Q}\left\{\sigma_{rrI}\right\}^D = \frac{a^2}{Q}\left[\sigma_{rrI}\right]^D - \frac{1}{6\pi\sqrt{\rho\, b/a}}\,\delta(\rho - \rho_I^D) \tag{4-36a}$$

$$\frac{a^2}{Q}\left\{\sigma_{rr0}\right\}^D = \frac{a^2}{Q}\left[\sigma_{rr0}\right]^D + \frac{1}{6\pi\sqrt{\rho\, b/a}}\,\delta(\rho - \rho_0^D) \tag{4-36b}$$

$$\frac{a^2}{Q}\left\{\sigma_{rr}\right\}^R = \frac{a^2}{Q}\left[\sigma_{rr}\right]^R + \frac{1}{6\pi\sqrt{\rho\, b/a}}\,\delta(\rho - \rho^R) \tag{4-36c}$$

$$\frac{a^2}{Q}\left\{\sigma_{\theta\theta I}\right\}^D = \frac{a^2}{Q}\left[\sigma_{\theta\theta I}\right]^D - \frac{1}{24\pi\sqrt{\rho\, b/a}}\,\delta(\rho - \rho_I^D) \tag{4-36d}$$

$$\frac{a^2}{Q}\left\{\sigma_{\theta\theta 0}\right\}^D = \frac{a^2}{Q}\left[\sigma_{\theta\theta 0}\right]^D + \frac{1}{24\pi\sqrt{\rho\, b/a}}\,\delta(\rho - \rho_0^D) \tag{4-36e}$$

$$\frac{a^2}{Q}\left\{\sigma_{\theta\theta}\right\}^R = \frac{a^2}{Q}\left[\sigma_{\theta\theta}\right]^R + \frac{1}{24\pi\sqrt{\rho\, b/a}}\,\delta(\rho - \rho^R) \tag{4-36f}$$

where the square brackets indicate the following finite jump discontinuities at the corresponding wave fronts:

$$\frac{a^2}{Q}\left[\sigma_{rrI}\right]^D = \frac{\rho - 7\,b/a}{48\pi(\rho\, b/a)^{3/2}} \tag{4-37a}$$

$$\frac{a^2}{Q}\left[\sigma_{rr0}\right]^D = -\frac{\rho - 7\,b/a}{48\pi(\rho\, b/a)^{3/2}} \tag{4-37b}$$

$$\frac{a^2}{Q}\left[\sigma_{rr}\right]^R = \frac{\rho + 7\,b/a + 6\rho\, b/a}{48\pi(\rho\, b/a)^{3/2}} \tag{4-37c}$$

$$\frac{a^2}{Q}\left[\sigma_{\theta\theta I}\right]^D = \frac{\rho + 23\,b/a}{192\pi(\rho\, b/a)^{3/2}} \tag{4-37d}$$

$$\frac{a^2}{Q}\left[\sigma_{\theta\theta 0}\right]^D = -\frac{\rho + 23\,b/a}{192\pi(\rho\, b/a)^{3/2}} \tag{4-37e}$$

$$\frac{a^2}{Q}\left[\sigma_{\theta\theta}\right]^R = \frac{\rho + 6\rho\, b/a - 23\,b/a}{192\pi(\rho\, b/a)^{3/2}} \tag{4-37f}$$

A significant aspect of the response which merits investigation is the behavior under the load at $\rho = b/a$, where it is recognized that two kinds of irregularities in the response may occur at this point: finite discontinuities and singularities.

In investigating the displacement quantities, it is necessary to recall that the relevant integral representation, eqs. (3-40), which were derived from eqs. (3-27), are valid for points $\rho \neq b/a$ and were obtained by considering the contour integrations in the ζ-plane. Specifically, criteria for the convergence of the integrals of eqs. (3-27) were based on the behavior of the complex integrals along the large quarter circle arcs of the closed contours.

In the particular case of the dilatation, this investigation led

to the determination of the Dirac-delta strength, as shown in eq. (3-78c).

It is now necessary to reexamine the integrals along the large quarter circles for $\rho = b/a$ for the cases of the vertical and radial displacement components. Using the identical procedures of Chapter 3, it is then found from the large circle lemma, eq. (3-16), that the combined sum of the integrals along the large arcs in sheets 1 and 2 of the ζ-plane vanish for the vertical displacement, while for the radial displacement the sum becomes finite.

Upon taking the limit $\rho \to b/a^-$ the large quarter circle contribution for the radial transform displacement then becomes

$$\frac{a\mu}{Q}\hat{u}_I(\rho,0,s) = -\frac{1}{16\pi\rho s} \tag{4-38a}$$

while for $\rho \to b/a^+$

$$\frac{a\mu}{Q}\hat{u}_O(\rho,0,s) = \frac{1}{16\pi\rho s} \tag{4-38b}$$

It is these quantites that are to be added to the expressions for the radial displacement, eqs. (3-40) and (3-78b), when $\rho = b/a$.

Points of finite discontinuity in the response may now be determined from examination of the behavior of the Laplace transforms, eq.(3-40). As an example, consider the jump in the transformed radial displacement at $\rho = b/a$. Eq. (3-40) yields:

$$\frac{a\mu}{Q}\left[\hat{u}(\rho,0,s)\right]_{\rho=b/a} = \frac{a\mu}{Q}\left\{\hat{u}_O - \hat{u}_I\right\}$$
$$= -\frac{1}{\pi^2}\int_{1/\sqrt{3}}^{1} v^2 \mathrm{Im}\{m_u\}\left(\frac{1}{\frac{b}{a}vs}\right)dv - \frac{\chi}{8\pi}\left(\frac{1}{\frac{b}{a}\chi s}\right) \tag{4-39}$$

where use has been made of the Wronskian relation of the modified Bessel functions:

$$I_0(v)K_1(v) + I_1(v)K_0(v) = \frac{1}{v} \tag{4-40}$$

The Laplace inversion of eq. (4-39) is then readily obtained. The v-integral, which may be evaluated in closed form, is found to vanish, and consequently

$$\frac{a\mu}{Q}\left[u(\rho,0,t)\right]_{\rho=b/a} = -\frac{1}{8\pi\, b/a}\, H(t) \tag{4-41}$$

where the square bracket denotes the jump (discontinuity) at the point.

Thus, it is seen that a time-independent finite discontinuity exists in the radial displacement under the source.

In a similar manner, it is found that the vertical displacement and the dilatation have no discontinuity under the source.

The significance of the expressions in eqs. (4-38) can now be assessed in view of eq. (4-41). It is observed that the value obtained for the radial displacement at ρ = b/a is halfway between the values just inside and outside the source. This is a common feature in integral transform techniques, viz. the value at a point of discontinuity is the average of the values immediately to the left and to the right of the point.

The singularities of the response at ρ = b/a may be determined

from an investigation of the final displacement quantities, given by the expressions of eqs. (3-78) as $\rho \to b/a$.$^{(\pm)}$

Consider for example, the vertical displacement at a field point outside the source, as given by eq. (3-78a).

$$\frac{a\mu}{Q} W_0(\rho,0,\tau) = -\frac{1}{\pi^2}\int_{1/\sqrt{3}}^{\tau/(\rho-b/a)} \mathrm{Im}\{m_w\} f_w(\rho, b/a, \tau/v)\, dv \qquad (4\text{-}42)$$

where $f_w(\rho, b/a, \tau/v)$ is given by eqs. (3-79, 80a, 83a) and $\mathrm{Im}\{m_w\}$ by eq. (3-42). As $\rho \to b/a$, the upper limit of integration approaches positive infinity. Furthermore, as $v \to \frac{\tau}{\rho-b/a} \to \infty$, the integrand terms behave as follows:

$$\mathrm{Im}\{m_w\} \longrightarrow -3/4v \qquad (4\text{-}43a)$$

$$f_w(\rho, b/a, \tau/v) \longrightarrow \frac{1}{2\sqrt{\rho\, b/a}} \qquad (4\text{-}43b)$$

where in eq. (4-43b) use has been made of the series representation of the complete elliptic integral of the first kind

$$K(m) \approx \frac{\pi}{2}\left\{1 + \frac{m}{4} + \frac{9m^2}{64} + \cdots\right\} \qquad (4\text{-}44)$$

with $m \to 0$ as $v \to \frac{\tau}{\rho-b/a}$.

Thus, eq. (4-42) can be written as the sum of two integrals

$$\lim_{\rho \to b/a^+} \frac{a\mu}{Q} W_0(\rho,0,\tau) = -\frac{1}{\pi^2}\int_{1/\sqrt{3}}^{N} \mathrm{Im}\{m_w\} f_w(\rho, b/a, \tau/v)\, dv$$

$$+\frac{1}{\pi^2}\int_{N}^{\tau/(\rho-b/a)\to\infty} \frac{3}{8\sqrt{\rho\, b/a}\, v}\, dv \qquad (4\text{-}45)$$

where N is large.

The second integral is seen to contribute a logarithmic singularity to the vertical component of displacement under the source. Similarly, it can be shown, that as $\rho \to b/a^-$ the same type of singularity is present.

Following a similar procedure, the radial displacement is found to exhibit no singularity under the source. Moreover, no additional singularities are found to occur in the dilatation, aside from the Dirac-delta function previously established in eq. (3-78c), viz.

$$\frac{a^2\mu}{Q}\left\{e(\rho,0,\tau)\right\} = -\frac{1}{4\pi\rho}\,\delta(\rho - b/a)\,H(\tau) \tag{4-46}$$

Using eqs. (3-85) the discontinuities and singularities of the stress components at the source ($\rho = b/a$) are immediately established from the corresponding displacement quantities, and are summarized as follows:

$$\frac{a^2}{Q}\left\{\sigma_{rr}\right\} = \frac{a^2}{Q}\left[\sigma_{rr}\right] - \frac{1}{2\pi\rho}\,\delta(\rho - b/a)\,H(\tau) \tag{4-47a}$$

$$\frac{a^2}{Q}\left\{\sigma_{\theta\theta}\right\} = \frac{a^2}{Q}\left[\sigma_{\theta\theta}\right] - \frac{1}{4\pi\rho}\,\delta(\rho - b/a)\,H(\tau) \tag{4-47b}$$

where the square brackets denote the following time-independent finite jumps:

$$\frac{a^2}{Q}\left[\sigma_{rr}\right] = \frac{1}{4\pi(b/a)^2}\,H(\tau) \tag{4-48a}$$

$$\frac{a^2}{Q}\left[\sigma_{\theta\theta}\right] = -\frac{1}{4\pi(b/a)^2}\,H(\tau) \tag{4-48b}$$

CHAPTER 5

NUMERICAL RESULTS AND CONCLUSIONS

a). Results for a given typical source location b/a = 3.0.

In the first part of this chapter, numerical results, evaluated from the relevant expressions of Chapter 3, are presented for the response at the plane surface boundary. Typical results are first given for a source at b/a = 3.0. (The numerical techniques and methods used in the calculations are discussed in some detail in Appendix C).

Typical profiles of the vertical displacement are shown in Fig. 5 for various non-dimensional times, τ . Locations of the direct and reflected wave fronts are indicated. The logarithmic singularities at the R wave front (as given in eq. (4-31)), and at the source (eq. (4-45)) are seen to be the dominant features of the response. Indeed the effects at the P and S wave fronts appear to be relatively insignificant in the profile. It is also of interest to note that the singularity of the R- wave does not change sign upon reflection at the inclusion boundary.

The vertical displacement at a fixed field point $\rho = 5.0$, is presented as a function of time τ in Fig. 6. The arrival times of the various direct and reflected wave fronts are given with the observed singularities occuring at the R- wave fronts. In particular, the response is seen to approach asymptotically the static response for large values of time.

As noted in Chapter 4, the contributions of the body waves (i.e. the P- and S- waves) and the Rayleigh surface waves to the radial displacement and dilatation are uncoupled and it is therefore possible to present the effects of these waves separately. Furthermore, from eqs. (3-85), the body wave and surface wave contributions to the stresses may also be presented separately.

Profiles of the radial displacement due to the body waves as well as positions of the wave fronts at various times τ are shown in Figs. 7 and 8 for field points inside and outside the source respectively.

Direct ingoing waves and the corresponding reflected waves are shown in Figs. 7a and 7b respectively. From the former figure it is seen that the response between the P and S wave fronts consist of a single sine shaped pulse with a peak roughly equidistant from the end points of the pulse, while behind the S wave front the response is small in comparison to this peak. The peak increases as the waves approach the inclusion.

From Fig. 7b it is observed that the reflected pulse is opposite in sign to the incident pulse and the peak decreases as the waves diverge from the inclusion.

The interaction of the direct outgoing and the reflected waves at two typical times, $\tau = 5.0$ and $\tau = 10.0$, are shown in Fig. 8 where a reinforcement of the peak is observed. The apparent discontinuities in the slopes at the P and S wave fronts in the above figures are spurious due to the relatively small scales along the abscissas.

Profiles of the radial displacement due to the Rayleigh surface waves for various times τ are shown in Fig. 9 for outgoing waves. The finite jump discontinuities at the direct and reflected R wave fronts are seen to decay with distance from the origin (eqs. (4-35)). Moreover, the discontinuity under the source, at $\rho = 3.0$ given by eq. (4-41) is noted to remain constant for all times. The profile of the static radial displacement is also shown and it is noticed that at points inside the source the displacement vanishes.

A clear representation of the variations of the jump discontinuities in the radial displacement at the R-wave fronts is presented in Fig. 10a where according to eqs. (4-34, 35) the discontinuity is plotted against a nondimensional time $\bar{\tau} = \frac{c_R t}{a} = \frac{\tau}{\kappa}$. In Fig. 10b the positions of these R-wave fronts are given as a function of time $\bar{\tau}$ (eqs. (4-34)). The jump at the direct outgoing wave front is seen to decay with time and hence with distance from the source while the direct ingoing discontinuity increases until the inclusion is reached ($\bar{\tau} = b/a - 1$). The reflected discontinuity is of opposite sign and decays in the same manner as the direct outgoing wave.

A typical total radial displacement profile (representating the combined effects of all the waves) is shown in Fig. 11 for time $\tau = 5.0$. The locations of the wave fronts are indicated and it is observed that for this value of time all the ingoing waves have been reflected at the inclusion. The figure therefore represents the case for sufficiently large times in which all waves are radiating outward. It is again noted that the Rayleigh surface waves dominate the

the contribution of the body waves.

The radial displacement at field points inside and outside the source is presented as a function of time τ in Figs. 12 and 13, respectively. The arrival times of the various wave fronts are given with the observed discontinuities occurring at the R-wave fronts. The response is seen to approach asymptotically the static response for large values of time.

For the case of the stress components at the surface, it is again possible to separate the effects of the body waves from those of the Rayleigh surface waves.

Typical profiles of the stresses $\sigma_{\theta\theta}$ and σ_{rr} due to the body waves as well as the positions of the various wave fronts are shown in Figs. 14a and 14b, respectively, for the field points inside the source at various times. The response between the P- and S-wave fronts is seen to be approximately an N-shaped pulse with the peak near the P-wave front being slightly larger than that near the S-wave front. There are cusps in the profiles immediately behind and in front of the P- and S-waves respectively (eq. (4-25a)). As in the radial displacement, the response behind the direct ingoing S-wave front is small in comparison to the above mentioned peaks. It is also noticed that the profiles of $\sigma_{\theta\theta}$ and σ_{rr} are similar in shape with the peaks in σ_{rr} being approximately four times as great as those in $\sigma_{\theta\theta}$. In addition, the reflected pulse is opposite in sign to the incident pulse.

Due to the similarity of the profiles, the behavior of $\sigma_{\theta\theta}$ and σ_{rr}

due to the body waves, for points outside the source may be illustrated for various times by means of typical profiles of the radial stress appearing in Fig. 15. Again, the positions of the various wave fronts are indicated. The interaction of the reflected and direct outgoing N-shaped pulses results in a decrease in the peaks near the reflected P-wave and direct S-wave fronts. The peaks are seen to decay as the waves diverge from the inclusion.

Profiles of $\sigma_{\theta\theta}$ and σ_{rr} due to the Rayleigh surface waves are shown in Figs. 16 and 17 respectively, for outgoing waves. The Dirac-delta functions are illustrated by means of heavy solid lines and their respective strengths indicated. The finite jump discontinuities (eqs. (4-37)) and the Dirac-delta functions (eqs. (4-36)) at the R-wave fronts, as well as the time independent finite discontinuities under the source (eqs. (4-48)) are the dominant features. Decay with distance from the inclusion is again observed. The results are seen to approach the static profiles where it is noticed that both $\sigma_{\theta\theta}$ and σ_{rr} vanish for field points inside the source (eq. (D-26)).

As in the case of the radial displacement it is possible to represent more clearly the jumps in the stress components at the various R-wave fronts by considering the variation of the jumps with time $\bar{\tau}$, (Eqs. (4-37)). Figs. 18a and 18b present these variations for $\sigma_{\theta\theta}$ and σ_{rr} respectively. The direct ingoing discontinuities increase until the inclusion is reached ($\bar{\tau} = b/a - 1$). The reflected discontinuities are opposite in sign to the incident discontinuities, where $\frac{a^2}{Q}[\sigma_{\theta\theta}]$ is observed to decrease while $\frac{a^2}{Q}[\sigma_{rr}]$

increases immediately after reflection. For the circumferential stress, the direct outgoing discontinuity decays with time, $\bar{\tau}$, while the reflected discontinuity decreases, changes sign, and finally decays for large values of time. The reverse is true for the radial stress; the reflected discontinuity decays with time $\bar{\tau}$, while the direct outgoing discontinuity decreases, changes sign, and finally decays for large values of time.

As above, the behavior of $\sigma_{\theta\theta}$ and σ_{rr} may be illustrated by means of a profile of the radial stress only. A profile of the total radial stress as well as the location of the various wave fronts is shown in Fig. 19 for outgoing waves. It is of interest to note that the N-shaped pulses arising from the body waves are larger than the direct R-wave discontinuity but much smaller than the reflected R-wave discontinuity. Moreover, the Dirac-delta strengths at the R-wave fronts (eqs. (4-36)) and under the source eqs. (4-47)) dominate the response.

b). Discussion of geometric changes of source location.

As noted previously, the numerical results presented above were calculated for a typical load located at b/a = 3.0. Consideration is now given to the effect of a variation in the location of the source, b/a, on the response. From the derived analytical expressions of the preceding chapter, it is evident that the qualitative aspects of the response cannot depend upon the position of the source, although the quantitative results will naturally be a function of this parameter.

It was observed above, for b/a = 3.0, that the dominant aspects of the response occur at the R-wave fronts. Furthermore, it may be recalled that the singularities at the R-wave fronts are expressed in terms of elementary functions (eqs. (4-31, 4-35, 4-37)); it therefore follows that the relationship between the geometry of the source location and the behavior at these wave fronts is readily obtained.

At this point it is no longer advantageous to consider the dimensionless form of the results. This is so because the magnitude of the applied vertical stress depends upon the applied force Q and the location of the source b, and consequently, when considering a variation in the geometry of the problem it is necessary to decide whether to maintain the applied stress or the applied force constant.

Consider for example the effect of changing the location of the source b, while the applied force Q, the location of the field point r, and the radius of the inclusion a, are held constant. The behavior at the R-wave fronts is as follows: the jump discontinuity in the

radial displacement [u], the magnitude of the vertical displacement w, and the Dirac-delta strengths in the stresses $\sigma_{\theta\theta}$ and σ_{rr}, vary inversely as the square root of b; and for the field points at large distances from the source, the jump discontinuities in the stresses $\sigma_{\theta\theta}$ and σ_{rr} vary inversely as $b^{3/2}$.

On the other hand, consider the effect of changing the position of the source b, while the applied stress $\frac{Q}{2\pi b}$, the position of the field point r, and the radius of the inclusion a, are held constant. In this case the following behavior at the R-wave front is observed: the jump discontinuity in the radial displacement [u], the magnitude of the vertical displacement w, and the Dirac-delta strengths in the stresses $\sigma_{\theta\theta}$ and σ_{rr}, vary directly as the square root of b; and, for $r >> b$, the jump discontinuties in the stresses $\sigma_{\theta\theta}$ and σ_{rr} vary inversely as the square root of b.

c). General conclusions.

The complete response at the plane boundary has been evaluated and analyzed. The results obtained may serve as influence functions for arbitrary axi-symmetric normal loadings.

It was found that, at any given time, there are six wave fronts present, thus indicating that each wave (P, S, or R) reflects as a wave of the same type from the rigid-lubricated inclusion. The vertical displacement reflects positively, while the radial displacement and the radial and circumferential stress components reflect negatively. In addition, upon reflection of the R-wave, there is a loss in the magnitude of the jump $[\ \sigma_{\theta\theta}\ ]_{\rho=1}$ and a gain in the magnitude of $[\ \sigma_{rr}\ ]_{\rho=1}$.

The displacement and stress components are directly proportional to the total applied force, Q, as must be the case for a linear system. Furthermore, the stresses are seen to be independent of the material constants, whereas, the displacements are found to vary inversely with μ .

At large distances from the source, the stress and displacement components near the R-wave fronts decay as $\frac{1}{\sqrt{r}}$ and are thus in agreement with the Rayleigh wave stud of Lamb [3].

For large values of time the dynamic response approaches the corresponding static response (Appendix E). In addition, for the radial displacement and the stress components on the plane boundary, the time independent finite discontinuities and Dirac-delta strengths

under the source are identical to the singularities in the static problem.

The major dynamic effects which are found to occur at the Rayleigh surface wave fronts may be summarized briefly as follows: the vertical displacement contains a logarithmic singularity; the radial displacement contains a finite jump discontinuity; and the stresses contain Dirac-delta singularities as well as finite jump discontinuities.

APPENDIX A

INTEGRAL REPRESENTATION OF THE DIRAC-DELTA FUNCTION

The following integral representation for the Dirac-delta function, required in the general solution, is established.

$$\delta(\rho - b/a) = \int_0^\infty \frac{C_0(\gamma, b/a)\, C_0(\gamma, \rho)\, \gamma\rho}{J_1^2(\gamma) + Y_1^2(\gamma)}\, d\gamma, \quad 0 < \rho\ , \ 0 < b/a \tag{A-1}$$

The derivation proceeds as follows. Consider

$$\Psi(\rho, b/a) = \int_0^\infty \frac{C_0(\gamma, b/a)\, C_1(\gamma, \rho)}{J_1^2(\gamma) + Y_1^2(\gamma)}\, d\gamma \tag{A-2}$$

where

$$C_0(\gamma, \rho) = J_1(\gamma) Y_0(\gamma\rho) - Y_1(\gamma) J_0(\gamma\rho) \tag{A-3}$$

$$C_1(\gamma, \rho) = J_1(\gamma) Y_1(\gamma\rho) - Y_1(\gamma) J_1(\gamma\rho) \tag{A-4}$$

Expressing the integrand in terms of Hankel functions, eq. (A-2) may be written as

$$\Psi(\rho, b/a) = \frac{1}{4} \int_0^\infty \left\{ H_0^{(1)}(b/a\,\gamma) \left[H_1^{(2)}(\rho\gamma) - H_1^{(1)}(\rho\gamma) \frac{H_1^{(2)}(\gamma)}{H_1^{(1)}(\gamma)} \right] + H_0^{(2)}(b/a\,\gamma) \left[H_1^{(1)}(\rho\gamma) - H_1^{(2)}(\rho\gamma) \frac{H_1^{(1)}(\gamma)}{H_1^{(2)}(\gamma)} \right] \right\} d\gamma \tag{A-5}$$

The above integral may be evaluated by extending the integration to the complex plane $\gamma = u + iv$. The integration along the real axis is then replaced by integrals along the imaginary axis together with integrals along large and small arcs by Cauchy's theorem.

This procedure required choosing the proper quadrants for the path of integration for each term in the integrand of eq. (A-5). The appropriate choice is based on the convergence of the integral along the large quarter circle, which is determined by using the

following (large circle) lemma: [11]

Let C_1 be the path $\gamma = |\gamma| e^{i\phi}$ and let $G(\gamma)$ be a function along this path. If

$$\lim_{|\gamma| \to \infty} |\gamma| \cdot G(\gamma) = A \quad \text{(constant)} \tag{A-6a}$$

then

$$\lim_{|\gamma| \to \infty} \int_{C_1} G(\gamma) d\gamma = iA\theta \tag{A-6b}$$

where θ is the angle of rotation of the position vector along the curve C_1.

Consider as an example, the term

$$G(\gamma) = H_0^{(1)}(b/a\,\gamma) H_1^{(2)}(\rho\gamma) \tag{A-7}$$

Using the asymptotic expansions of the Hankel functions [12]

$$H_n^{(1)}(\gamma) \sim \sqrt{\frac{2}{\pi\gamma}}\, e^{i\left(\gamma - \frac{n\pi}{2} - \frac{\pi}{4}\right)} \tag{A-8a}$$

$$H_n^{(2)}(\gamma) \sim \sqrt{\frac{2}{\pi\gamma}}\, e^{-i\left(\gamma - \frac{n\pi}{2} - \frac{\pi}{4}\right)} \tag{A-8b}$$

the following limit is obtained

$$\lim_{|\gamma| \to \infty} |\gamma| \cdot G(\gamma) = \frac{i2}{\pi\sqrt{\rho\, b/a}}\, e^{i\gamma(b/a - \rho)} \tag{A-9}$$

This limit exists or vanishes if

$$\mathrm{Re}\left\{i\gamma(b/a - \rho)\right\} \leq 0 \tag{A-10}$$

Hence, by the large circle lemma, the integral of this term vanishes for $(b/a - \rho)v > 0$, and exists for $\rho = b/a$.

It is seen that for $\rho < b/a$ the contour for this term must be taken in the first quadrant, while for $b/a < \rho$ it is taken in the fourth quadrant. The remaining three terms in the integrand of eq. (A-5) are treated similarly, and it is found, contrary to the above, that for two of these terms, the contour for $\rho < b/a$ must be taken in the fourth quadrant, while for $b/a < \rho$ it is taken in the first quadrant.

Thus it is observed that the convergence of the integral depends on the relative magnitudes of ρ and b/a, and therefore, it is necessary to separate the expression for Ψ when $\rho < b/a$, from the expression when $b/a < \rho$. In addition, in each case, the integrand is split into two parts; one of which yields a convergent quarter circle contour in the first quadrant, while the other converges in the fourth quadrant.

Let

$$\Psi_1(\rho, b/a) = \frac{1}{4}\int_0^\infty \left\{ \Phi^{(+)}(1,2,\gamma) + \Phi^{(-)}(2,1,\gamma) \right\} d\gamma, \quad \rho < b/a \tag{A-11a}$$

and

$$\Psi_2(\rho, b/a) = \frac{1}{4}\int_0^\infty \left\{ \Phi^{(-)}(1,2,\gamma) + \Phi^{(+)}(2,1,\gamma) \right\} d\gamma, \quad b/a < \rho \tag{A-11b}$$

where

$$\Phi^{(+)}(i,j,\gamma) = H_0^{(i)}(b/a\,\gamma) H_1^{(j)}(\rho\gamma) - H_0^{(1)}(b/a\,\gamma) H_1^{(1)}(\rho\gamma) \frac{H_1^{(2)}(\gamma)}{H_1^{(1)}(\gamma)} \tag{A-12a}$$

$$\Phi^{(-)}(i,j,\gamma) = H_0^{(i)}(b/a\,\gamma) H_1^{(j)}(\rho\gamma) - H_0^{(2)}(b/a\,\gamma) H_1^{(2)}(\rho\gamma) \frac{H_1^{(1)}(\gamma)}{H_1^{(2)}(\gamma)} \qquad i,j = 1,2 \tag{A-12b}$$

and where the superscripts (+) and (-) denote that the integration in the γ-plane is to be carried out in the first and fourth quadrants,

respectively.

Now the integrands above require a branch cut along the negative real axis due to the multivaluedness of the Hankel functions. Furthermore, it is noted that the poles corresponding to the zeros of $H_1^{(1)}(\gamma)$ and $H_1^{(2)}(\gamma)$ lie outside the path of integration and therefore do not contribute to the contour integral; the integrands within the closed contour are then analytic.

Using the integration paths shown in Fig. 20, and applying Cauchy's theorem, contour integration yields,

$$\int_{AB} \Phi^{(+)} d\gamma = -\left\{ \int_{BC} \Phi^{(+)} + \int_{CD} \Phi^{(+)} + \int_{DA} \Phi^{(+)} \right\} d\gamma \qquad \text{(A-13a)}$$

$$\int_{AB} \Phi^{(-)} d\gamma = -\left\{ \int_{BC'} \Phi^{(-)} + \int_{C'D'} \Phi^{(-)} + \int_{D'A} \Phi^{(-)} \right\} d\gamma \qquad \text{(A-13b)}$$

Hence,

$$\int_{AB} [\Phi^{(+)} + \Phi^{(-)}] d\gamma = -\left\{ \left(\int_{BC} \Phi^{(+)} + \int_{BC'} \Phi^{(-)} \right) + \left(\int_{CD} \Phi^{(+)} + \int_{C'D'} \Phi^{(-)} \right) + \left(\int_{DA} \Phi^{(+)} + \int_{D'A} \Phi^{(-)} \right) \right\} d\gamma \qquad \text{(A-14)}$$

The integrals along BC and BC' are evaluated by the large circle lemma, eq. (A-6) given above, and are found to vanish when $\rho \neq b/a$. From the following known relations [12],

$$H_n^{(1)}(\bar{\gamma}) = \overline{H_n^{(2)}(\gamma)} \qquad \text{(A-15a)}$$

$$H_n^{(2)}(\bar{\gamma}) = \overline{H_n^{(1)}(\gamma)} \qquad \text{(A-15b)}$$

and,

$$H_0^{(1)}(i\gamma) = -\frac{i2}{\pi} K_0(\gamma), \quad H_1^{(1)}(i\gamma) = -\frac{2}{\pi} K_1(\gamma) \qquad \text{(A-16a,b)}$$

$$H_0^{(2)}(i\gamma) = 2I_0(\gamma) + \frac{i2}{\pi}K_0(\gamma) \tag{A-16c}$$

$$H_1^{(2)}(i\gamma) = \frac{2}{\pi}K_1(\gamma) + 2iI_1(\gamma) \tag{A-16d}$$

it follows that

$$\Phi^{(-)}(2,1,-iv) = \overline{\Phi^{(+)}(1,2,iv)} \tag{A-17a}$$

$$\Phi^{(-)}(1,2,-iv) = \overline{\Phi^{(+)}(2,1,iv)} \tag{A-17b}$$

and

$$\Phi^{(+)}(1,2;iv) = \frac{4}{\pi}K_0(b/a\,v)\left[I_1(\rho v) - K_1(\rho v)\frac{I_1(v)}{K_1(v)}\right] \tag{A-17c}$$

$$\Phi^{(+)}(2,1,iv) = -\frac{4}{\pi}K_1(\rho v)\left[I_0(b/a\,v) + K_0(b/a\,v)\frac{I_1(v)}{K_1(v)}\right] \tag{A-17d}$$

Upon direct substitution in eq. (A-14) it is seen that the integrals along the paths CD and C'D' cancel for both of eqs. (A-11).

The integrals along DA and D'A are evaluated by means of the following (small circle) lemma [11].

Let $G(\gamma)$ be a function on a path C_2, given by $\gamma=\gamma_0 + \varepsilon e^{i\phi}$, where ε is small. If

$$\lim_{\gamma\to\gamma_c}(\gamma-\gamma_c)G(\gamma) = A \quad \text{(constant)} \tag{A-18a}$$

then

$$\lim_{\epsilon\to 0}\int_{C_2} G(\gamma)d\gamma = iA\Theta \tag{A-18b}$$

where Θ is the angle of rotation of the small position vector along C_2.

Using the series representation of the Hankel functions [12],

$$H_0^{(1)}(\gamma) \approx 1 + \frac{i2}{\pi} \ln \frac{\gamma}{2} \tag{A-19a}$$

$$H_0^{(2)}(\gamma) \approx 1 - \frac{i2}{\pi} \ln \frac{\gamma}{2} \tag{A-19b}$$

$$H_1^{(1)}(\gamma) \approx \frac{\gamma}{2} - \frac{i2}{\pi\gamma} \tag{A-19c}$$

$$H_1^{(2)}(\gamma) \approx \frac{\gamma}{2} + \frac{i2}{\pi\gamma} \tag{A-19d}$$

it is seen from eq. (A-18) that these integrals combine to yield

$$\int_{DA} \Phi^{(+)}(1,2,\gamma)\,d\gamma + \int_{D'A} \Phi^{(-)}(2,1,\gamma)\,d\gamma = 0 \qquad \rho < b/a \tag{A-20a}$$

and

$$\int_{DA} \Phi^{(+)}(2,1,\gamma)\,d\gamma + \int_{D'A} \Phi^{(-)}(1,2,\gamma)\,d\gamma = -\frac{4}{\rho} \qquad b/a < \rho \tag{A-20b}$$

Hence, from eq (A-11) and (A-14) the following result is obtained:

$$\Psi_1(\rho, b/a) = 0 \qquad \rho < b/a \tag{A-21a}$$

$$\Psi_2(\rho, b/a) = \frac{1}{\rho}, \qquad b/a < \rho \tag{A-21b}$$

from which, according to eq. (A-2), it follows that

$$\int_0^\infty \frac{C_0(\gamma, b/a)\, C_1(\gamma, e)\, \rho}{J_1^2(\gamma) + Y_1^2(\gamma)}\, d\gamma = H(\rho - b/a) \tag{A-22}$$

Differentiating both sides with respect to ρ, and noting that

$$\frac{\partial}{\partial \rho} C_1(\gamma, \rho) = \gamma\, C_0(\gamma, \rho) - \frac{1}{\rho} C_1(\gamma, \rho) \tag{A-23}$$

yields the identity sought, viz.

$$\int_0^\infty \frac{C_0(\gamma, b/a)\, C_0(\gamma, e)\, \rho\gamma}{J_1^2(\gamma) + Y_1^2(\gamma)}\, d\gamma = \delta(\rho - b/a) \tag{A-24}$$

APPENDIX B

BRANCH CUTS FOR THE MULTIVALUED FUNCTIONS

It was observed in Chapter 3 that the branch cuts for the multivalued functions $(\zeta^2 + 1)^{1/2}$ and $(\zeta^2 + 1/3)^{1/2}$ must be chosen so that their real parts along the path of integration are positive. It remains to be shown that the sheets given in Fig. 21 satisfy this criterion.

Since the two functions are of the same form, it is sufficient to consider only one of them, e.g. $(\zeta^2 + 1)^{1/2}$. Define the function $w(\zeta)$ by the expression

$$w^2 = (\zeta^2+1) = (\zeta+i)(\zeta-i) \tag{B-1}$$

and let r_1, r_2 and θ_1, and θ_2, denote respectively the magnitudes and angles of the position vectors from the branch points $\zeta = +i$, $-i$, to an arbitrary point in the ζ-plane, as shown below.

According to the branch cuts for the sheet 1 (Fig. 21), the ranges of θ_1 and θ_2 must be

$$\begin{aligned} -\pi &< \theta_1 \leq \pi \\ 0 &< \theta_2 \leq 2\pi \end{aligned} \tag{B-2}$$

From the expression

$$w^2 = r_1 r_2 e^{i(\theta_1+\theta_2)} \tag{B-3}$$

the function w can be assigned either of the following values:

$$w_1 = \sqrt{r_1 r_2}\, e^{i\frac{\theta_1+\theta_2}{2}} \tag{B-4a}$$

$$w_2 = \sqrt{r_1 r_2}\, e^{i\frac{\theta_1+\theta_2+2\pi}{2}} \tag{B-4b}$$

the first of which corresponds to choosing $(-1)^{1/2} = +i$, while for the second value $(-1)^{1/2} = -i$.

Considering w_1, it is seen that its argument is in the range

$$0 < \frac{\theta_1 + \theta_2}{2} < \frac{\pi}{2} \tag{B-5}$$

for all ζ in the first quadrant.

Therefore, the condition $\mathrm{Re}\{w_1(\zeta)\} > 0$ is satisfied in the first quadrant of sheet 1.

The analysis for sheet 2 is similar. In this case the ranges of θ_1 and θ_2 must be:

$$\begin{aligned} 0 &< \theta_1 \leq 2\pi \\ -\pi &< \theta_2 \leq \pi \end{aligned} \tag{B-6}$$

Then, considering w_2, it is seen that its argument is in the range

$$\frac{3\pi}{2} < \frac{\theta_1 + \theta_2 + 2\pi}{2} < 2\pi \tag{B-7}$$

for all ζ in the fourth quadrant.

Therefore, the condition $\mathrm{Re}\{w_2(\zeta)\} > 0$ is satisfied in the fourth quadrant of sheet 2.

APPENDIX C

NUMERICAL METHODS OF EVALUATION AND ERROR ANALYSIS

Quantitative results behind the wave fronts are obtained from the numerical evaluation of the expressions in eqs. (3-78). The discussion below is concerned with the general method of evaluation and provides an indication of the accuracy and errors arising in the calculations.

As is noted in Chapter 3, the direct waves requires integrations in the range

$$\frac{\tau}{\rho + b/a - 2} < v < \frac{\tau}{|\rho - b/a|} \qquad \text{(C-1a)}$$

while the combined response to direct and reflected waves require integrations in the range

$$v < \frac{\tau}{\rho + b/a - 2} \qquad \text{(C-1b)}$$

Within each of these ranges, the integrands are the products of algebraic terms given by eq. (3-42) and functions of $f^{D}_{(\ )}$ or $f^{R}_{(\ )}$, eqs. (3-80), (3-83), which must be evaluated numerically.

The errors in evaluation of the displacement quantities arise from two sources: numerical evaluation of the integrand and numerical integration of the calculated integrands.

Consideration is first given to the evaluation of the integrands.

For the direct waves, as seen from eq. (3-80), it is necessary

to evaluate complete elliptic integrals of the first and third kinds. These quantities are expressible in terms of complete and incomplete elliptic integrals of the first and second kinds [13] which may be evaluated numerically to six significant figures from available IBM subprograms in FORTRAN IVG programming language.

For the combination of direct and reflected waves, the relevant integrands eq. (3-83), contain semi-infinite branch integrals. These are readily evaluated by means of Gauss-Laguerre quadrature formulas [17]. The results, which were used to calculate the displacement quantities presented in Chapter 5 part a, were computed by means of a thirty-two term formula. The relative accuracy of the values, obtained by comparing the results using a twenty-four term formula, showed a relative difference of less than 0.2 percent.

Consideration is now given to the final numerical integration of the integral expressions of eqs. (3-78). However, it should first be noted, that in the case of the radial displacement and the dilatation, the Rayleigh wave and body wave effects are uncoupled, while in the case of the vertical displacement, the effects of the Rayleigh waves and body waves are not separable but are expressed simultaneously in terms of a single integral. This coupled representation thus gives rise to some difficulty: more specifically, the term $\mathrm{Im}\{m_w\}$ in the range $1 < v$, is singular due to the simple Rayleigh pole at $v = \varkappa$. Hence, the evaluation of the vertical displacement requires a separate treatment which will be considered subsequently.

Therefore, consider first the dilatation and the radial displacement.

In view of the above, it is immediately established that the uncoupled effect of the direct R-wave is determined to an accuracy of six significant figures, while the error in the calculated reflected R wave effect is less than 0.2 percent.

The body wave contribution which require a final numerical integration over v, are evaluated by means of trapezoidal integration formulae.

Since, as previously noted, the integrands are discontinuous, the range of integration is subdivided into regions where the trapezoidal formula is applied to sub-integrals having continuous integrands. Furthermore, due to the factor $(2v^2-1)$, appearing in eqs. (3-42b) and (3-42c) the integrands change sign only at $v = \frac{1}{\sqrt{2}}$; by choosing this value as the end point of sub-interval, the integrand will not change sign in any sub-interval.

Hence, the manner and number of sub-integrals required is seen to depend on the values of $\frac{1}{|\rho - b/a|}$ and $\frac{1}{\rho + b/a - 2}$ in relation to the critical points $v = \frac{1}{\sqrt{3}}$, $v = \frac{1}{\sqrt{2}}$, and $v = 1$, (C-2)
and thus there are as many as three sub-integrals.

The trapezoidal formula is then applied successively to each sub-integral, where at each successive iteration, the spacing is bisected. Thus a series of iterated integrations is performed with spacing h, $\frac{h}{2}$, $\frac{h}{4}$ ... respectively. In order to maintain a reasonable computational time it was found necessary to limit the iteration to a maximum of seven successive bisections, i.e. a spacing of order

$\frac{h}{2^6} = \frac{h}{64}$. The difference in value obtained from the last two successive iterations may be assumed to be the maximum error of each subintegral. Using this criterion, it was found that the sum of each of these errors over all of the sub-integrals was less than 3.2 percent of the body wave contribution to the dilatation or radial displacement in front of the direct Rayleigh wave, while behind the direct Rayleigh wave the maximum error was found to be less than 8.0 percent of the body wave contribution. However, it is important to note that in this latter region, the body wave effect is small compared with the Rayleigh wave effect (as shown in Chapter 5), and therefore the seemingly large relative error indicated above is effectively of a significantly smaller magnitude when compared to the total response.

Irrespective of the numerical integration scheme used, another possible source of error in evaluating these integrals arises from the relative error in the integrands. Since as established above, the integrands do not change sign in each sub-integral, the maximum relative error of this type in the sub-integral, is equal to that of the integrand, i.e. 0.2 percent for the response behind the reflected waves. This source of error is thus seen to be small compared with the errors from the trapezoidal formulae above.

Consider now the vertical displacement, where as noted above, it is not possible to evaluate separately the body and Rayleigh wave contributions.

First, it is observed that the singularity in the expression for the vertical displacement, corresponding to the Rayleigh pole, exists

due to the vanishing of $\Delta(v)$ (given by eq. (3-43)) at $v = \kappa$. Since this value lies within the range of integration of eq. (3-78a), a means of performing the required integration must be devised.

The integration of this singularity is accomplished essentially, by subtracting out a singular portion of the integrand which can be integrated in closed form. To illustrate this process, consider as an example, the vertical displacement behind the direct R-wave, i.e. for values

$$\frac{\tau}{|\rho - b/a|} > \kappa \tag{C-3}$$

and in front of the reflected P-wave, i.e.

$$\frac{\tau}{\rho + b/a - 2} < \frac{1}{\sqrt{3}} \tag{C-4}$$

From eq. (3-78a) the vertical displacement is then given by

$$\frac{a\mu}{Q} W(\rho,0,\tau) = -\frac{1}{\pi^2}\int_{1/\sqrt{3}}^{\tau/|\rho-b/a|} \frac{3(1-2v^2)^2\sqrt{v^2-1/3}}{\Delta(v)} f_w^D(\rho, b/a, \tau/v)\,dv$$
$$-\frac{1}{\pi^2}\int_{1}^{\tau/|\rho-b/a|} \frac{12v^2(v^2-1/3)\sqrt{v^2-1}}{\Delta(v)} f_w^D(\rho, b/a, \tau/v)\,dv \tag{C-5}$$

The nature of the singularity becomes evident by noting that the term $\frac{1}{\Delta(v)}$ may be rewritten in terms of partial fractions as

$$\frac{1}{\Delta(v)} = \frac{1/2}{1/4 - v^2} + \frac{1/12(2\sqrt{3}-3)}{\kappa^2 - v^2} - \frac{1/12(2\sqrt{3}+3)}{3/4 - \sqrt{3}/4 - v^2} \tag{C-6}$$

Consider, as an illustration, the singular portion of the

integrand appearing in the first integral of eq. (C-5), viz.

$$N = \frac{(2\sqrt{3}-3)(1-2v^2)^2\sqrt{v^2-1/3}}{4(\kappa^2-v^2)} f_w^D(\rho, b/a, \tau/v) \qquad \text{(C-7a)}$$

The order of this singularity, may be reduced by adding and subtracting the term

$$M = \frac{(2\sqrt{3}-3)(1-2v^2)^2\sqrt{v^2-1/3}}{4(\kappa^2-v^2)} f_w^D(\rho, b/a, \tau/\kappa) \qquad \text{(C-7b)}$$

The first integral of eq. (C-5) is then written as the sum of two integrals:

$$I_1 = -\frac{1}{\pi^2}\int_{1/\sqrt{3}}^{\tau/|\rho-b/a|} 3(1-2v^2)^2\sqrt{v^2-1/3}\cdot$$
$$\left\{\left(\frac{1/2}{1/4-v^2} - \frac{1/12(2\sqrt{3}+3)}{3/4-\sqrt{3}/4-v^2}\right) f_w^D(\tau/v) + \frac{1/12(2\sqrt{3}-3)}{\kappa^2-v^2}\left\{f_w^D(\tau/v) - f_w^D(\tau/\kappa)\right\}\right\} dv \qquad \text{(C-8a)}$$

and $$I_2 = -\frac{(2\sqrt{3}-3)}{4\pi^2} f_w^D(\tau/\kappa)\int_{1/\sqrt{3}}^{\tau/|\rho-b/a|} \frac{(1-2v^2)^2\sqrt{v^2-1/3}}{\kappa^2-v^2}\, dv \qquad \text{(C-8b)}$$

The latter integral, I_2, may readily be evaluated in terms of elementary functions

$$I_2 = -\frac{2\sqrt{3}-3}{4\pi^2} f_w^D(\tau/\kappa)\cdot\left\{-\sqrt{v^2-1/3}\left(v^3 + \frac{3\sqrt{3}-4}{6}v\right)\right. \qquad \text{(C-9)}$$
$$\left. -\frac{1}{3}\left(\frac{10}{3}+\sqrt{3}\right)\ln\left(\sqrt{3}\left(v+\sqrt{v^2-1/3}\right)\right) + \frac{27+11\sqrt{3}}{48\kappa\sqrt{\kappa^2-1/3}}\ln\left|\frac{v\sqrt{\kappa^2-1/3}+\kappa\sqrt{v^2-1/3}}{v\sqrt{\kappa^2-1/3}-\kappa\sqrt{v^2-1/3}}\right|\right\}$$
$$v = \tau/|\rho-b/a|$$

Moreover, since the former integral, I_1, contains a weaker singularity (in the form of $\frac{0}{0}$, at $v = \kappa$) than the original integral of eq. (C-5) a numerical integration becomes possible. However, in order to avoid

divison by zero numerically, it is necessary to divide this integral into two parts as follows:

$$I_1 = -\frac{1}{\pi^2}\int_{\frac{1}{\sqrt{3}}}^{K-\epsilon} \{\ \}dv - \frac{1}{\pi^2}\int_{K+\epsilon}^{\tau/|e-b/a|} \{\ \}dv \qquad \text{(C-10)}$$

where the small positive parameter ϵ has been introduced.

The integral I_1, may then be considered to be a function of ϵ, i.e. $I_1 = I_1(\epsilon)$, which ideally converges to a definite value as $\epsilon \to 0$. However, due to the indeterminate nature of the integrand at $\epsilon = 0$, the integral is evaluated for various values of ϵ approaching zero, i.e. $I_1 = I_1(\epsilon \to 0)$.

Before defining the criterion for choosing the most appropriate value of the parameter ϵ, it is worth emphasizing that the total vertical displacement is given by the contribution of I_1 and I_2 as well as the second integral appearing in eq. (C-5). Therefore in determining the value of ϵ, it must be realized that its effect on the value of I_1 is not of concern in itself but rather it is necessary to consider the effect of ϵ on the value of the total vertical displacement.

Moreover, it should be noted that by changing the value of ϵ the inherent error in the numerical integration by the trapezoidal rule is also affected since the region of integration is itself altered.

Consequently, the criteria for choosing the optimum value of ϵ was determined by an empirical numerical analysis of the total vertical displacement and the corresponding errors arising from the trapezoidal

rule, Typical results are shown in Table 2 for various values of $\mathcal{E}$. The parameters ρ, b/a, and τ have been chosen to represent various positions with respect to the different wave fronts.

From this table, it is seen that as ε decreases the sum of the errors arising from the trapezoidal integration formula tends to increase while the change in the value of the total displacement decreases. There is thus a value w_{k+1}, using ε_{k+1}, which gives an estimate of the total that is no better than the value w_k obtained from the previous ε_k. Moreover, further difficulty is encountered since the results do not converge uniformly with ε, i.e. the appropriate value of ε changes with the variables ρ, b/a, and τ.

However, it may also be noticed from the table, that for $\varepsilon = 0.001$ the error term is the same order of magnitude as the change in the total quantity sought.

Consequently, the value $\varepsilon = 0.001$ appears to be the most appropriate value of ε for a wide range of parameters.

DATA	ϵ	$\frac{a\mu}{Q}w \cdot (10)$	$\left\|\Delta\left(\frac{a\mu}{Q}w\right)\right| \cdot (10)$	Σ ERRORS $\cdot (10)$
ρ = 1.8	0.002	0.0723	---	0.00015
b/a = 3.0	0.001	0.0719	0.0004	0.00011
τ = 1.7	0.0005	0.0716	0.0003	0.00020
	0.00025	0.0714	0.0002	0.00024
ρ = 1.8	0.002	0.217	---	0.00037
b/a = 3.0	0.001	0.216	0.001	0.00035
τ = 3.2	0.0005	0.217	0.001	0.00108
	0.00025	0.215	0.002	0.00079
ρ = 5.0	0.01	0.00562	---	0.00005
b/a = 3.0	0.001	0.00349	0.00213	0.00005
τ = 2.4	0.0001	0.00266	0.00083	0.00057
ρ = 5.0	0.01	-0.0602	---	0.00005
b/a = 3.0	0.001	-0.0623	0.0021	0.00005
τ = 2.2	0.0001	-0.0631	0.0008	0.00053

TABLE 2. EMPIRICAL NUMERICAL ANALYSIS FOR THE PARAMETER ϵ

APPENDIX D

SOLUTION TO THE CORRESPONDING STATIC PROBLEM

Formulation and general solution.

The response for large values of times after the arrival of the reflected Rayleigh wave corresponds to the response due to a statically applied load.

The solution to the corresponding static problem, therefore, is not only of interest per se, but will serve to confirm the accuracy of the solution to the main problem for large times, and also provide an indication of the order of the singularities in the solution.

Love [18] and Timoshenko [19] have shown that a single stress potential may be used to solve a two-dimensional, axisymmetric static problem.

Defining the problem in terms of the non-dimensional variables

$$\rho = r/a \quad , \quad \xi = z/a \tag{D-1}$$

the non-dimensional displacement and stress components are defined in terms of the potential function $\chi(\rho, \xi)$ as follows:

$$\frac{a\mu}{Q} u = -\frac{1}{2aQ}\chi_{\rho\xi} \tag{D-2a}$$

$$\frac{a\mu}{Q} w = \frac{1}{2aQ}\left[(1-2\nu)\nabla^2\chi + \chi_{\rho\rho} + \frac{1}{\rho}\chi_{\rho}\right] \tag{D-2b}$$

$$\frac{a^2}{Q}\sigma_{rr} = \frac{1}{aQ}\left[\nu\frac{\partial}{\partial\xi}\nabla^2\chi - \chi_{\rho\rho\xi}\right] \tag{D-2c}$$

$$\frac{a^2}{Q}\sigma_{\theta\theta} = \frac{1}{aQ}\left[\nu\frac{\partial}{\partial\xi}\nabla^2\chi - \frac{1}{\rho}\chi_{\rho\xi}\right] \tag{D-2d}$$

$$\frac{a^2}{Q}\sigma_{zz} = \frac{1}{aQ}\left[(2-\nu)\frac{\partial}{\partial\xi}\nabla^2\chi - \chi_{\xi\xi\xi}\right] \qquad \text{(D-2e)}$$

$$\frac{a^2}{Q}\sigma_{zr} = \frac{1}{aQ}\left[(1-\nu)\frac{\partial}{\partial\rho}\nabla^2\chi - \chi_{\rho\xi\xi}\right] \qquad \text{(D-2f)}$$

where

$$\nabla^2 = \frac{\partial^2}{\partial\rho^2} + \frac{1}{\rho}\frac{\partial}{\partial\rho} + \frac{\partial^2}{\partial\xi^2} \qquad \text{(D-3)}$$

The stress equations of equilibrium and the compatibility equations are then satisfied if

$$\nabla^4\chi = 0 \qquad \text{(D-4)}$$

The boundary conditions to be satisfied are

$$u(1,\xi) = 0 \qquad \sigma_{rz}(1,\xi) = 0 \qquad \text{(D-5a,b)}$$

$$\sigma_{zr}(\rho,0) = 0 \qquad \frac{a^2}{Q}\sigma_{zz}(\rho,0) = -\frac{1}{2\pi\rho}\delta(\rho - b/a) \qquad \text{(D-5c,d)}$$

Using e.g., the method of separation of variables, the following integral solution to eq. (D-4) is obtained:

$$\chi(\rho,\xi) = \int_0^\infty \left[\xi A(\gamma) + B(\gamma)\right] e^{-\gamma\xi} C_0(\gamma,\rho)\, d\gamma \qquad \text{(D-6)}$$

where

$$C_0(\gamma,\rho) = J_1(\gamma)Y_0(\gamma\rho) - Y_1(\gamma)J_0(\gamma\rho) \qquad \text{(D-7)}$$

It can be shown that this solution automatically satisfies the homogeneous boundary conditions on the cylindrical boundary, eqs. (D-5a,b). The weighting functions $A(\gamma)$ and $B(\gamma)$ are determined from the conditions on the plane boundary.

From eq. (D-2f), the boundary condition of eq. (D-5c) is satisfied provided

$$A(\gamma) = \frac{\gamma}{2\nu} B(\gamma) \tag{D-8}$$

The remaining boundary condition, eq. (D-5d), then leads to the following integral equation on $B(\gamma)$:

$$\frac{1}{aQ} \int_0^\infty \frac{\gamma^3 B(\gamma)}{2\nu} C_0(\gamma,\rho)\, d\gamma = -\frac{1}{2\pi\rho} \delta(\rho - b/a) \tag{D-9}$$

Using the relation, eq. (A-1),

$$\delta(\rho - b/a) = \rho \int_0^\infty \frac{C_0(\gamma,\rho)\, C_0(\gamma, b/a)\gamma}{J_1^2(\gamma) + Y_1^2(\gamma)}\, d\gamma \tag{D-10}$$

which was established in Appendix A, the weighting function $B(\gamma)$ is found by inspection as

$$B(\gamma) = -\frac{aQ\nu}{\pi\gamma^2} \cdot \frac{C_0(\gamma, b/a)}{J_1^2(\gamma) + Y_1^2(\gamma)} \tag{D-11}$$

Hence the potential solution is

$$\chi(\rho,\xi) = -\frac{Qa}{\pi} \int_0^\infty \left[\nu + \frac{\gamma}{2}\xi\right] \frac{e^{-\gamma\xi}}{\gamma^2} \cdot \frac{C_0(\gamma,\rho)\, C_0(\gamma, b/a)}{J_1^2(\gamma) + Y_1^2(\gamma)}\, d\gamma \tag{D-12}$$

Substituting in eqs. (D-2), the stresses and displacements throughout the body are expressed explicity in terms of the following integrals:

$$\frac{a\mu}{Q} u(\rho,\xi) = -\frac{1}{4\pi} \int_0^\infty \frac{[(1-2\nu) - \gamma\xi] e^{-\gamma\xi} C_0(\gamma, b/a)\, C_1(\gamma,\rho)}{J_1^2(\gamma) + Y_1^2(\gamma)}\, d\gamma \tag{D-13a}$$

$$\frac{a\mu}{Q} w(\rho,\xi) = \frac{1}{2\pi} \int_0^\infty \frac{[(1-\nu) + \frac{\gamma}{2}\xi] e^{-\gamma\xi} C_0(\gamma, b/a)\, C_0(\gamma,\rho)}{J_1^2(\gamma) + Y_1^2(\gamma)}\, d\gamma \tag{D-13b}$$

$$\frac{a^2}{Q}\sigma_{rr}(\rho,\xi) = -\frac{\nu}{\pi}\int_0^\infty \frac{\gamma e^{-\gamma\xi} C_0(\gamma,b/a) C_0(\gamma,\rho)}{J_1^2(\gamma)+Y_1^2(\gamma)}\,d\gamma + \frac{2a\mu}{Q}\frac{\partial u(\rho,\xi)}{\partial \rho} \tag{D-13c}$$

$$\frac{a^2}{Q}\sigma_{\theta\theta}(\rho,\xi) = -\frac{\nu}{\pi}\int_0^\infty \frac{\gamma e^{-\gamma\xi} C_0(\gamma,b/a) C_0(\gamma,\rho)}{J_1^2(\gamma)+Y_1^2(\gamma)}\,d\gamma + \frac{2a\mu}{Q}\frac{1}{\rho}u(\rho,\xi) \tag{D-13d}$$

$$\frac{a^2}{Q}\sigma_{zz}(\rho,\xi) = -\frac{1}{2\pi}\int_0^\infty \frac{\gamma[1+\gamma\xi] e^{-\gamma\xi} C_0(\gamma,b/a) C_0(\gamma,\rho)}{J_1^2(\gamma)+Y_1^2(\gamma)}\,d\gamma \tag{D-13e}$$

$$\frac{a^2}{Q}\sigma_{zr}(\rho,\xi) = \frac{1}{2\pi}\int_0^\infty \frac{\gamma\xi\, e^{-\gamma\xi} C_0(\gamma,b/a) C_1(\gamma,\rho)}{J_1^2(\gamma)+Y_1^2(\gamma)}\,d\gamma \tag{D-13f}$$

where

$$C_1(\gamma,\rho) = J_1(\gamma)Y_1(\gamma\rho) - Y_1(\gamma)J_1(\gamma\rho) \tag{D-14}$$

Evaluation of components on the plane boundary.

The displacement and unknown stress components on the plane bo

$$\frac{a\mu}{Q} u(\rho,0) = -\frac{1-2\nu}{4\pi}\int_0^\infty \frac{C_0(\gamma,b/a)C_1(\gamma,\rho)}{J_1^2(\gamma)+Y_1^2(\gamma)}\,d\gamma \tag{D-15a}$$

$$\frac{a\mu}{Q} w(\rho,0) = \frac{1-\nu}{2\pi}\int_0^\infty \frac{C_0(\gamma,b/a)C_0(\gamma,\rho)}{J_1^2(\gamma)+Y_1^2(\gamma)}\,d\gamma \tag{D-15b}$$

$$\frac{a^2}{Q}\sigma_{rr}(\rho,0) = -\frac{\nu}{\pi}\int_0^\infty \frac{\gamma C_0(\gamma,b/a)C_0(\gamma,\rho)}{J_1^2(\gamma)+Y_1^2(\gamma)}\,d\gamma + \frac{2a\mu}{Q}\frac{\partial u(\rho,0)}{\partial\rho} \tag{D-15c}$$

$$\frac{a^2}{Q}\sigma_{\theta\theta}(\rho,0) = -\frac{\nu}{\pi}\int_0^\infty \frac{\gamma C_0(\gamma,b/a)C_0(\gamma,\rho)}{J_1^2(\gamma)+Y_1^2(\gamma)}\,d\gamma + \frac{2a\mu}{Q}\frac{1}{\rho}u(\rho,0) \tag{D-15d}$$

$$\frac{a^2}{Q}\sigma_{\theta\theta}(\rho,0) = -\frac{\nu}{\pi}\int_0^\infty \frac{\gamma C_0(\gamma,b/a)C_0(\gamma,\rho)}{J_1^2(\gamma)+Y_1^2(\gamma)}\,d\gamma + \frac{2a\mu}{Q}\frac{1}{\rho}u(\rho,0) \tag{D-15d}$$

Now the radial displacement component, eq. (D-15a), is immediately evaluated by making use of the following relation which was obtained in Appendix A, eq. (A-22),

$$H(\rho-b/a) = \rho\int_0^\infty \frac{C_0(\gamma,b/a)C_1(\gamma,\rho)}{J_1^2(\gamma)+Y_1^2(\gamma)}\,d\gamma \tag{D-16}$$

Hence

$$\frac{a\mu}{Q} u(\rho,0) = -\frac{1-2\nu}{4\pi\rho} H(\rho-b/a) \tag{D-17}$$

Consider now the vertical displacement component, eq. (D-15b). It is noticed that this integral is similar to the integral expression appearing in the dynamic problem, eq. (3-1). The present integral may be evaluated by contour integration in the complex plane $\gamma = u + iv$ in the same manner as eq. (3-9) was reduced to eq. (3-40) by integration in the complex ζ-plane. As in Chapter 3, the results are found to depend on the relative position of the field and source points.

Following this procedure, the results are given as:

$$\frac{a\mu}{Q} w_I(\rho,0) = \frac{1-\nu}{\pi^2}\int_0^\infty K_0(b/a\,v)I_0(\rho v)\,dv + \frac{1-\nu}{\pi^2}\int_0^\infty K_0(b/a\,v)K_0(\rho v)\frac{I_1(v)}{K_1(v)}\,dv \tag{D-18a}$$

$$\frac{a\mu}{Q} w_0(\rho,0) = \frac{1-\nu}{\pi^2}\int_0^\infty K_0(\rho v) I_0(\tfrac{b}{a}v)dv + \frac{1-\nu}{\pi^2}\int_0^\infty K_0(\rho v) K_0(\tfrac{b}{a}v)\frac{I_1(v)}{K_1(v)}dv \qquad \text{(D-18b)}$$

where the subscripts I and 0 refer to the field point inside and outside the source respectively.

The first integrals of eqs. (D-18a,b) consisting of products of the modified Bessel functions can be simplified further by means of the relation [20],

$$\int_0^\infty I_0(\kappa v) K_0(lv)dv = \frac{1}{l} K(m) , \quad \kappa < l \qquad \text{(D-19)}$$

where

$$m = \frac{\kappa^2}{l^2} \qquad \text{(D-20)}$$

is the modulus of the complete elliptic integral of the first kind

$$K(m) = \int_0^1 (1-mq^2)^{-1/2}(1-q^2)^{-1/2}dq \qquad \text{(D-21)}$$

Thus the displacement components w_I and w_0 may finally be written as

$$\frac{a\mu}{Q} w_I(\rho,0) = \frac{1-\nu}{\pi^2 b/a} K\left(\frac{\rho^2}{b^2/a^2}\right) + \frac{1-\nu}{\pi^2}\int_0^\infty K_0(\rho v) K_0(\tfrac{b}{a}v)\frac{I_1(v)}{K_1(v)}dv \qquad \text{(D-22a)}$$

$$\frac{a\mu}{Q} w_0(\rho,0) = \frac{1-\nu}{\pi^2 \rho} K\left(\frac{b^2/a^2}{\rho^2}\right) + \frac{1-\nu}{\pi^2}\int_0^\infty K_0(\rho v) K_0(\tfrac{b}{a}v)\frac{I_1(v)}{K_1(v)}dv \qquad \text{(D-22b)}$$

Returning now to eq. (D-15), the expressions for the stress components are readily evaluated since the integrals are immediately expressed in terms of the Dirac-delta function, by eq. (D-10).

Making the proper substitutions from eq. (D-17) the stress components are written as:

$$\frac{a^2}{Q}\,\sigma_{rr}(\rho,0) = -\frac{1}{2\pi\rho}\,\delta\left(\rho-\frac{b}{a}\right) + \frac{1-2\nu}{2\pi\rho^2}\,H\left(\rho-\frac{b}{a}\right) \qquad \text{(D-23)}$$

$$\frac{a^2}{Q}\,\sigma_{\theta\theta}(\rho,0) = -\frac{\nu}{\pi\rho}\,\delta\left(\rho-\frac{b}{a}\right) - \frac{1-2\nu}{2\pi\rho^2}\,H\left(\rho-\frac{b}{a}\right) \qquad \text{(D-24)}$$

Singularities of the solution.

Although the radial displacement, $u(\rho,o)$, exhibits a finite jump under the load $\rho = b/a$, it contains no singularity. Therefore, the only possible displacement singularities occur in the vertical displacement, $w(\rho,o)$, eq. (D-22a,b).

From the known properties of elliptic integrals, it is seen that the first term is singular for K(1), i.e. at $\rho = b/a$, and for no other values. The order of this singularity may be established from the approximation to the elliptic integral with argument near unity, viz. [13]

$$K(m) \approx \frac{1}{2} \ln\left(\frac{16}{1-m}\right) \approx -\frac{1}{2} \ln(1-m) \qquad \text{(D-25)}$$

Hence, this term contributes a logarithmic singularity, $\ln(|b/a-\rho|)$, under the load.

The possible singularities arising from the integrals of eq. (D-22) must now be considered. Using the series representations of the modified Bessel functions, the value of the integrand for small values of the argument v, can be written as follows:

$$K_o\left(\frac{b}{a}v\right)K_o(\rho v)\frac{I_1(v)}{K_1(v)} \approx \frac{v^2}{2} \ln\frac{\rho v}{2} \ln\frac{\frac{b}{a}v}{2} \qquad \text{(D-26)}$$

and thus it is seen that the integrand is finite as v approaches zero. For large values of v, the asymptotic expansions of the modified Bessel functions yield the following:

$$K_o\left(\frac{b}{a}v\right)K_o(\rho v)\frac{I_1(v)}{K_1(v)} \approx \frac{1}{2v\sqrt{\rho\frac{b}{a}}} e^{-v\left(\rho+\frac{b}{a}-2\right)} \qquad \text{(D-27)}$$

Since, it has been shown that the integrand is finite for all values of v, it follows that the only singularity that can arise is from the infinite range of integration.

Now, the following inequalities can be established for large arguments by considering the asymptotic expansions of the modified Bessel functions:

$$I_1(v) < \frac{1}{\sqrt{2\pi v}} e^{v} \tag{D-28a}$$

$$K_0(v) < \sqrt{\frac{\pi}{2v}}\, e^{-v} \tag{D-28b}$$

$$K_1(v) > \sqrt{\frac{\pi}{2v}}\, e^{-v} \tag{D-28c}$$

Therefore

$$\int_N^\infty K_0(\rho v) K_0\left(\frac{b}{a} v\right) \frac{I_1(v)}{K_1(v)} dv < \int_N^\infty \frac{1}{2\sqrt{\rho\, b/a}\, v} e^{-(\rho + b/a - 2)v} dv$$

$$= \frac{1}{2\sqrt{\rho\, b/a}} E_1(N(\rho + b/a - 2)) \tag{D-29}$$

where

$$E_1(x) = \int_x^\infty \frac{1}{\eta} e^{-\eta} d\eta \tag{D-30}$$

the exponential integral function, is known to be finite except when its argument is zero. Thus, a singularity in the integral can only occur if $\rho = b/a = 1$. Since the assumed loading circle is $b/a > 1$, such a singularity must be excluded from consideration.

It is therefore finally established that the only displacement singularity existing is a logarithmic singularity in the vertical

displacement directly under the source. It should be noted that other cases of logarithmic singularities associated with a circular line load have been reported in the literature. [21]

Stress singularities in the radial and circumferential components in the form of Dirac-delta functions also exist under the load.

Finally, it is worth noting that the radial displacement and the above stress components vanish for all points on the plane boundary within the interior of the circle of load application.

APPENDIX E

RELATION BETWEEN STATIC AND DYNAMIC SOLUTIONS

The solution to the corresponding static problem, which is given independently in Appendix D, may be readily obtained from the dynamic solution by application of the Laplace final value theorem to the integrands of the integral expression of eqs. (2-34).

As an illustration, consider the transform of the vertical displacement, eq. (2-34b).

$$\frac{a\mu}{Q}\,\hat{w}(\rho,\xi,s) = -\frac{1}{2\pi}\int_0^\infty \frac{C_0(\gamma,b/a)\,C_0(\gamma,\rho)}{J_1^2(\gamma)+Y_1^2(\gamma)} \left\{2\gamma^2 e^{-s\beta\xi} - (2\gamma^2+s^2)e^{-s\alpha\xi}\right\} \frac{\gamma\, s\alpha}{s\,M(\gamma,s)}\,d\gamma \tag{E-1}$$

From the definitions of $s\alpha$ and $s\beta$ given by eq. (2-24) the following limits are established:

$$\lim_{s\to 0} s\alpha \approx \gamma + \frac{(1-2\nu)s^2}{4(1-\nu)\gamma} \tag{E-2a}$$

$$\lim_{s\to 0} s\beta \approx \gamma + \frac{s^2}{2\gamma} \tag{E-2b}$$

thus yielding

$$\lim_{s\to 0} s\cdot\left\{2\gamma^2 e^{-s\beta\xi} - (2\gamma^2+s^2)e^{-s\alpha\xi}\right\}\frac{\gamma\, s\alpha}{s\,M(\gamma,s)} \approx -\left\{(1-\nu)+\frac{\gamma}{2}\xi\right\}e^{-\gamma\xi} \tag{E-3}$$

Hence, by means of the final value theorem, the long time vertical displacement becomes:

$$\lim_{\tau\to\infty}\frac{a\mu}{Q}w(\rho,\xi,\tau)=\frac{1}{2\pi}\int_0^\infty\frac{C_0(\gamma,b/a)\,C_0(\gamma,\rho)\left[(1-\nu)+\frac{\gamma}{2}\xi\right]e^{-\gamma\xi}}{J_1^2(\gamma)+Y_1^2(\gamma)}d\gamma \tag{E-4}$$

It is noted that this expression is identical to eq. (D-13b) which was independently established.

Upon application of the final value theorem to the remaining dynamic displacement and stress components of eqs. (2-34), the resulting expressions are found to be identical to the corresponding quantities of the static solution given in Appendix D.

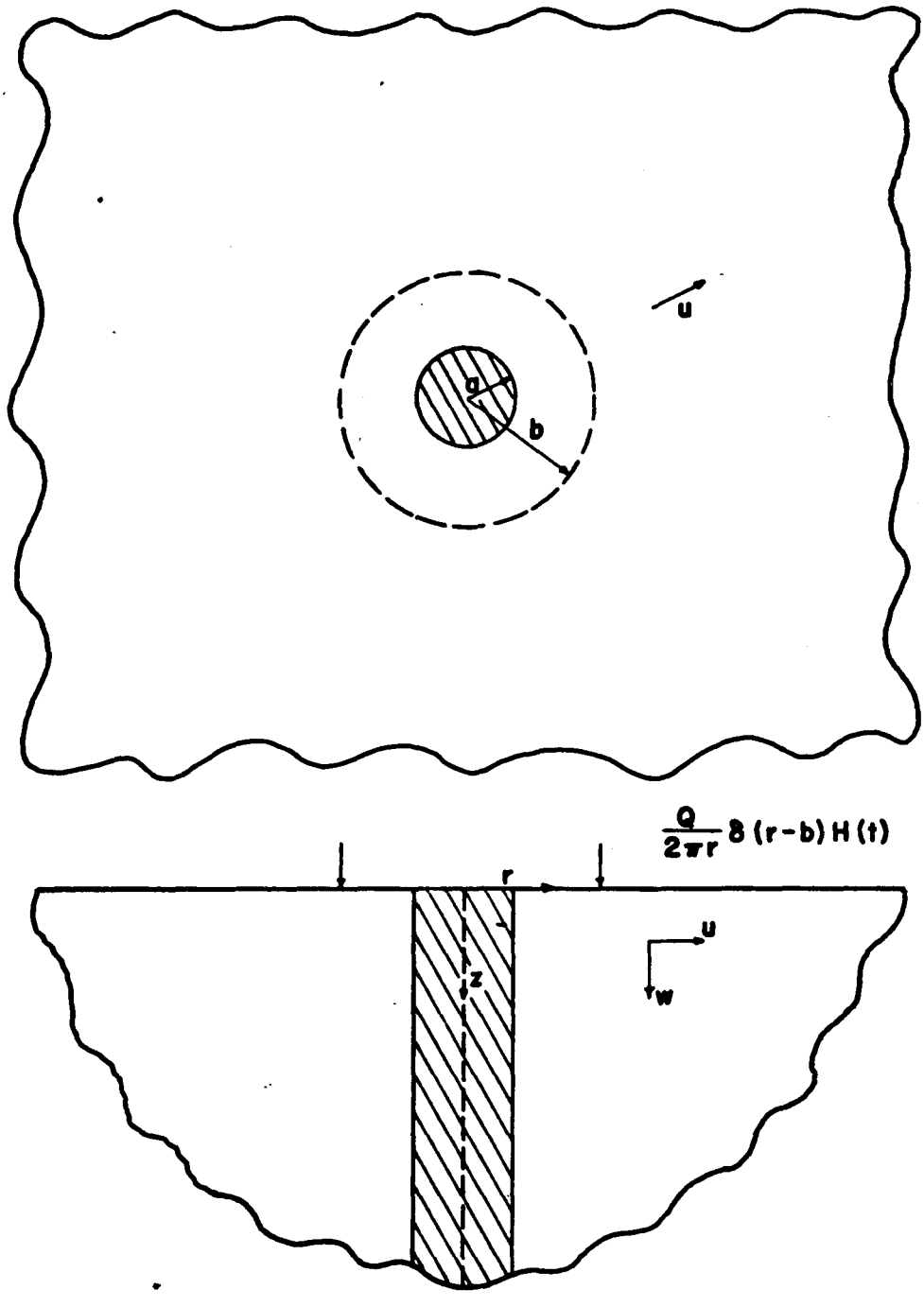

FIGURE 1. GEOMETRY OF PROBLEM

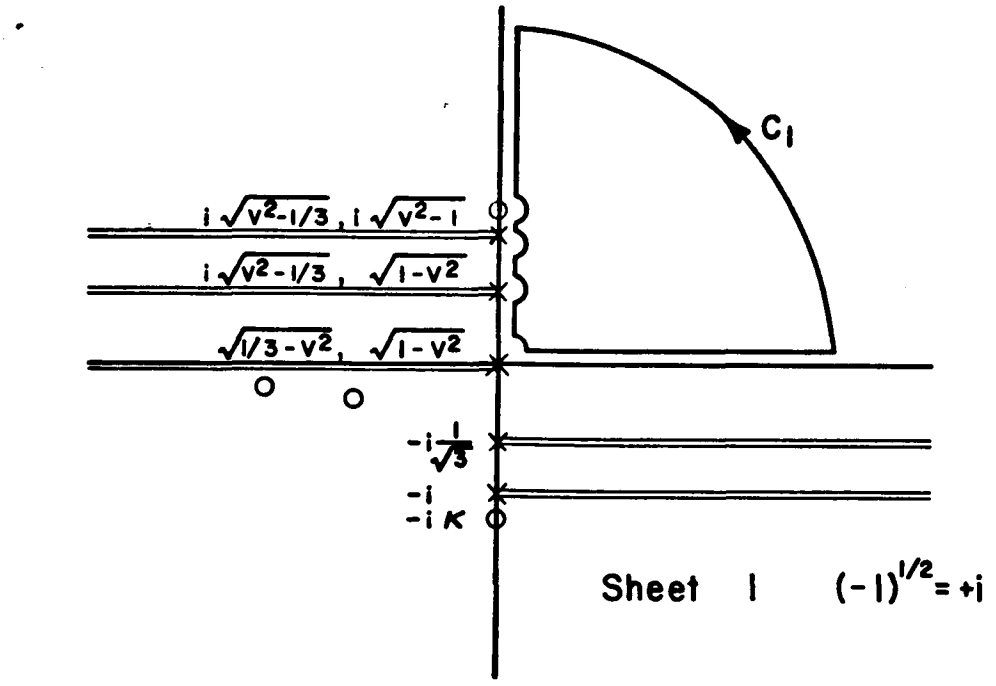

Branch points ×
Branch cuts ═══
Poles ○

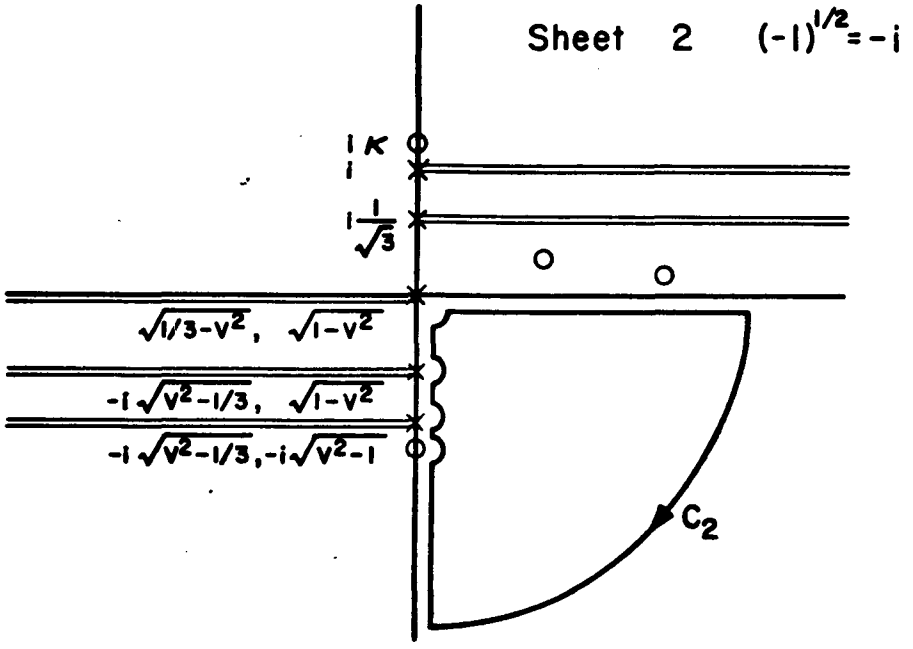

FIGURE 2. INTEGRATION PATHS IN COMPLEX ζ-PLANE

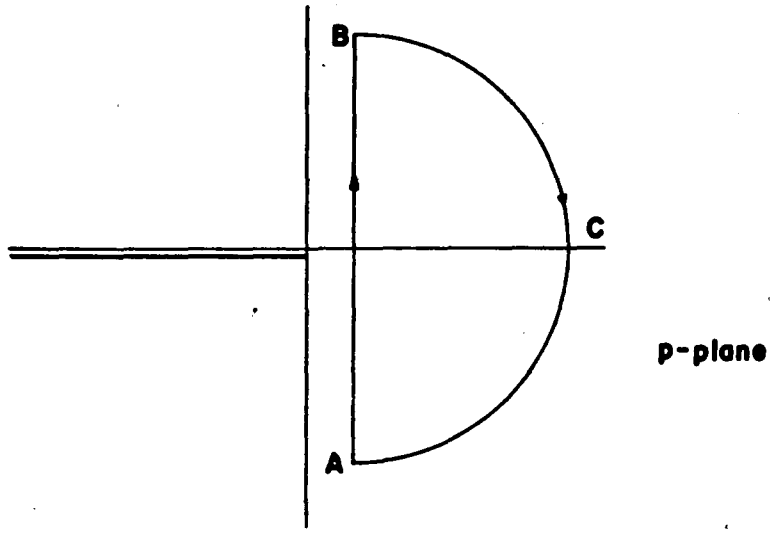

FIGURE 3. INTEGRATION PATH IN COMPLEX p-PLANE

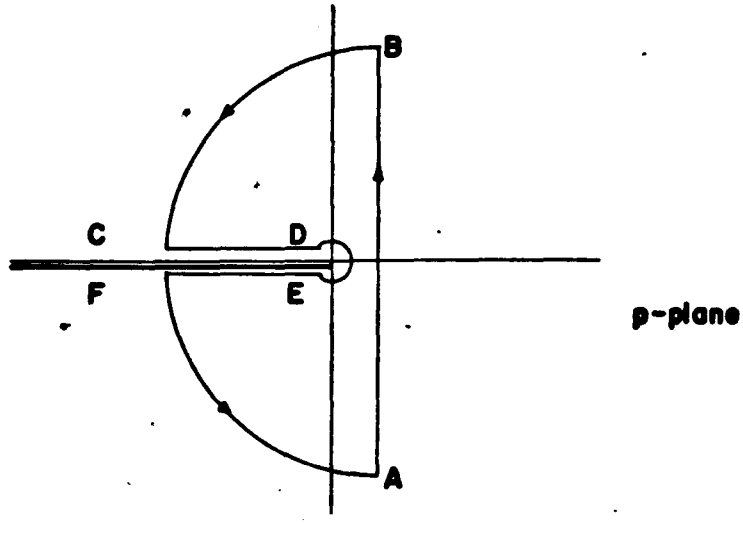

FIGURE 4. LAPLACE INVERSION CONTOUR

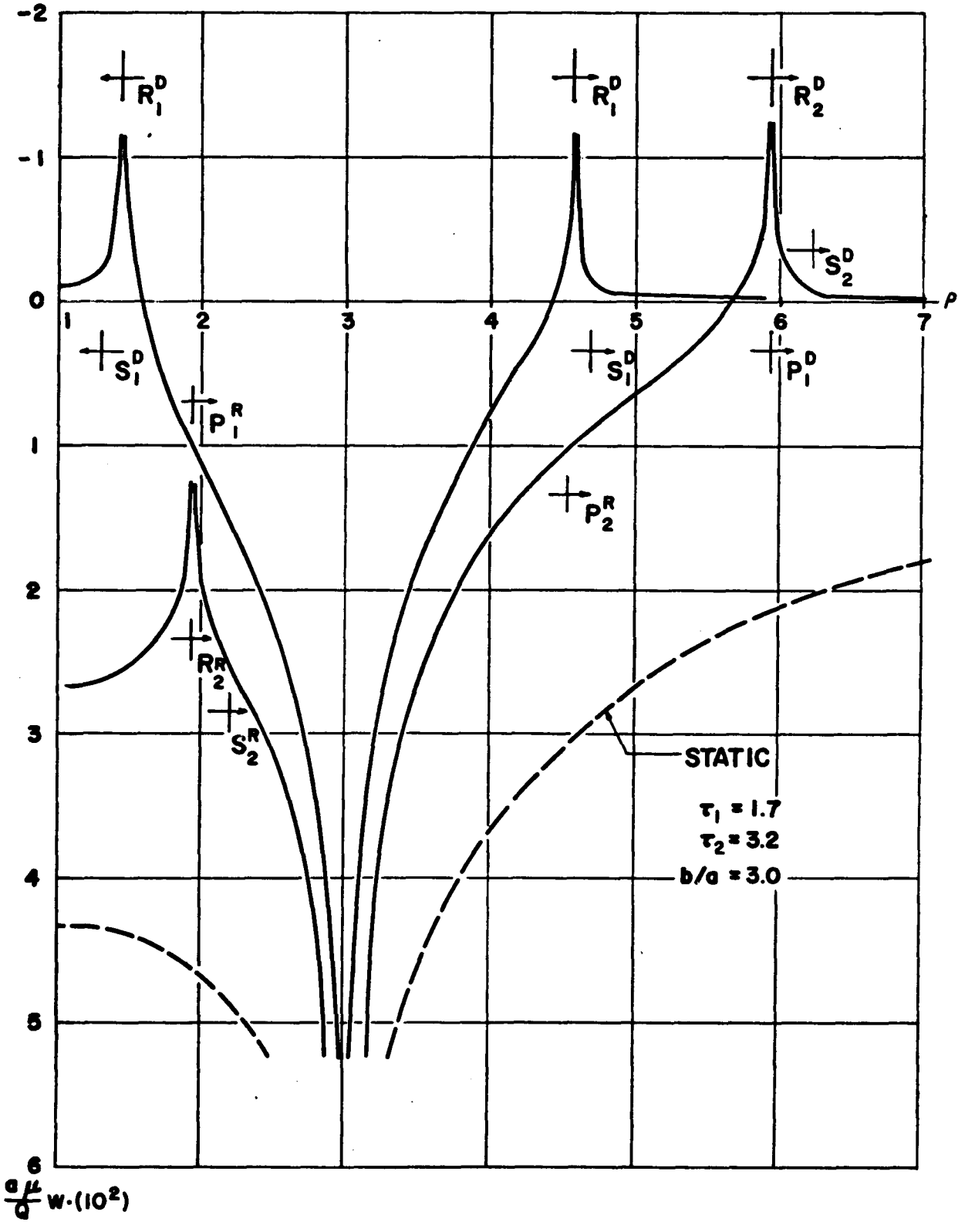

FIGURE 5. VERTICAL DISPLACEMENT PROFILES

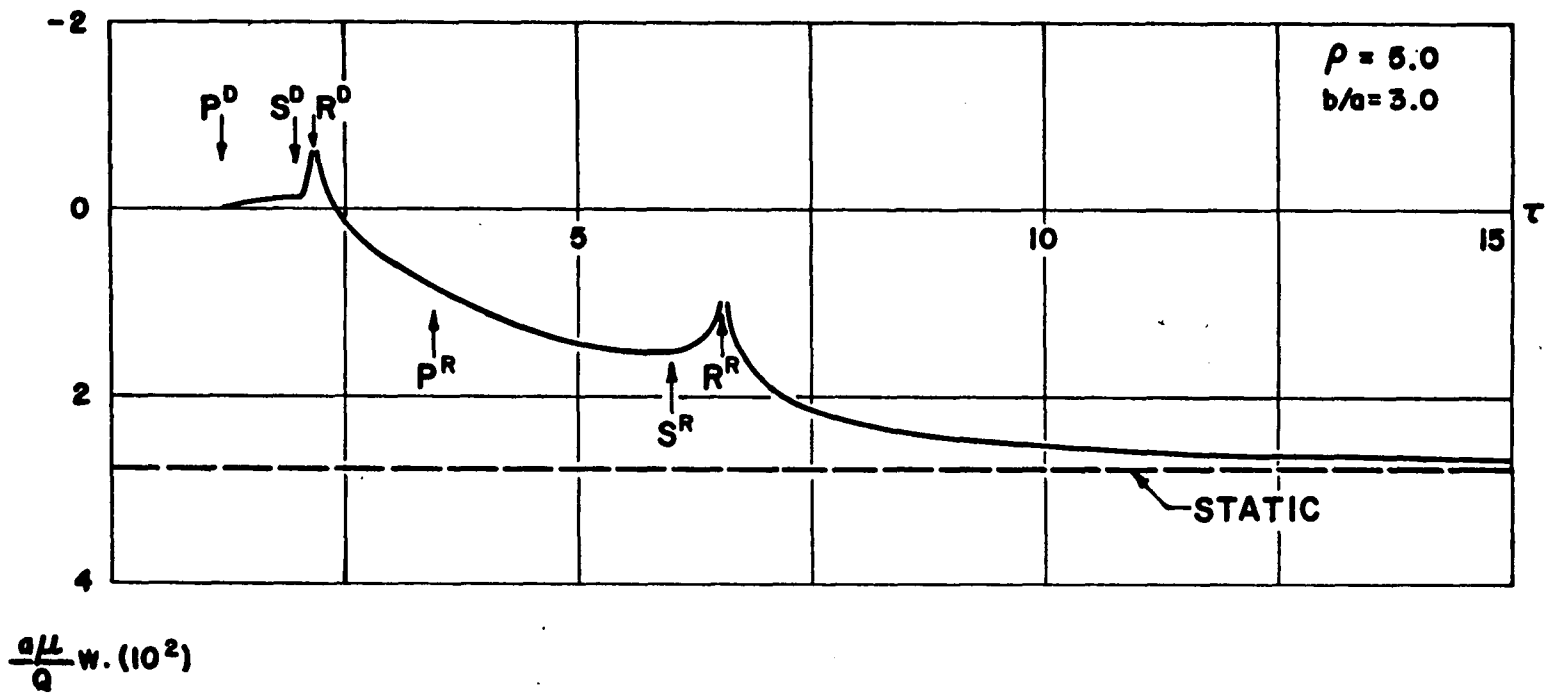

FIGURE 6. VERTICAL DISPLACEMENT VERSUS TIME τ

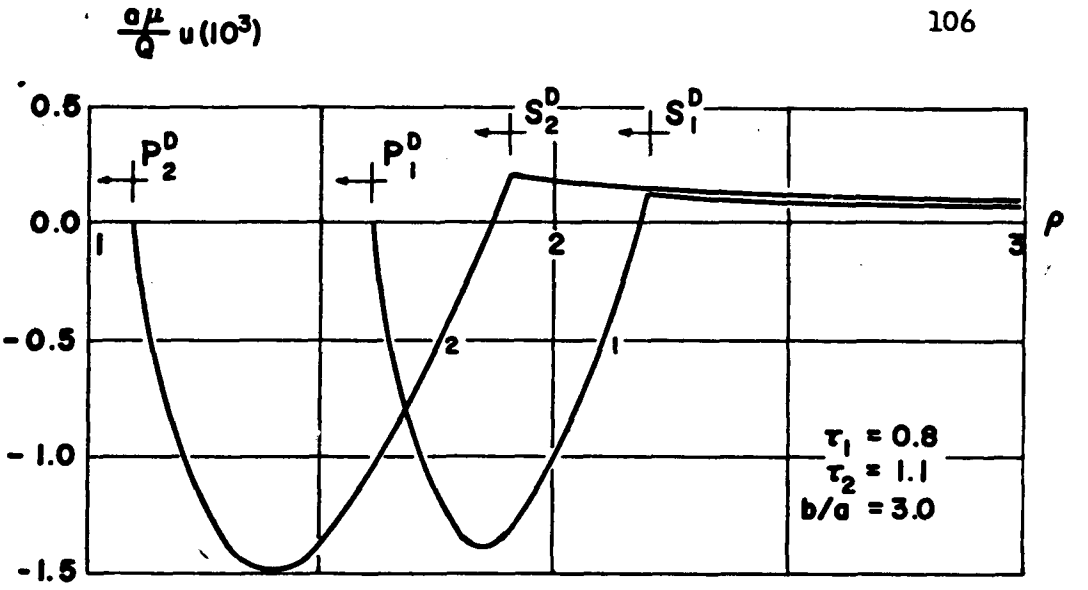

(a) INCIDENT BODY WAVES

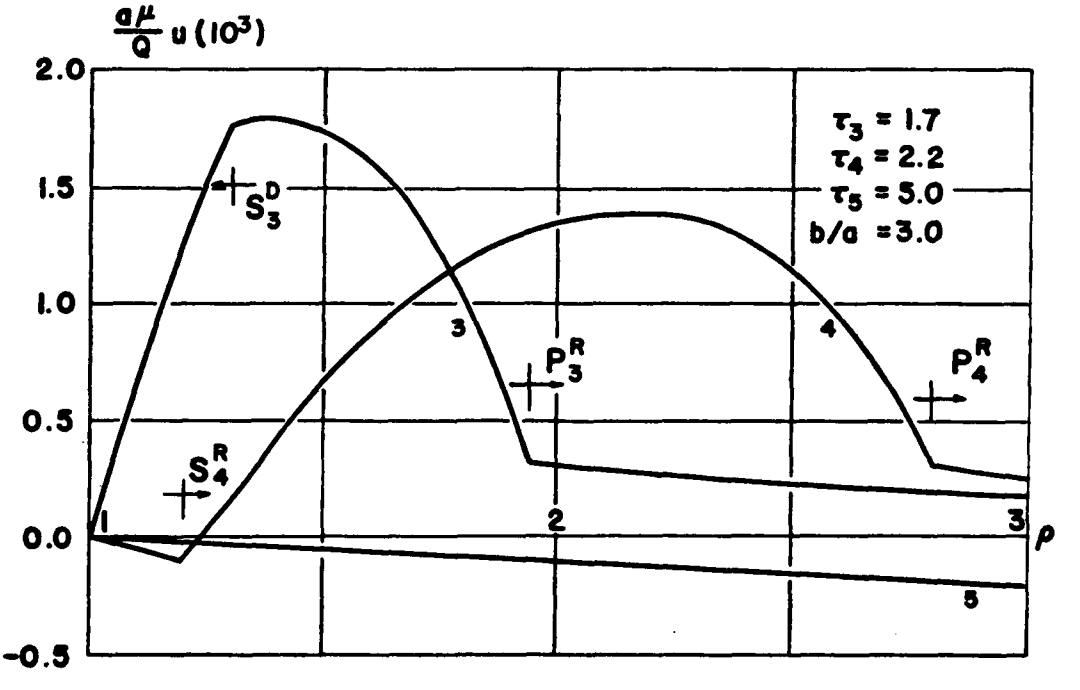

(b) REFLECTED BODY WAVES

FIGURE 7. RADIAL DISPLACEMENT PROFILES

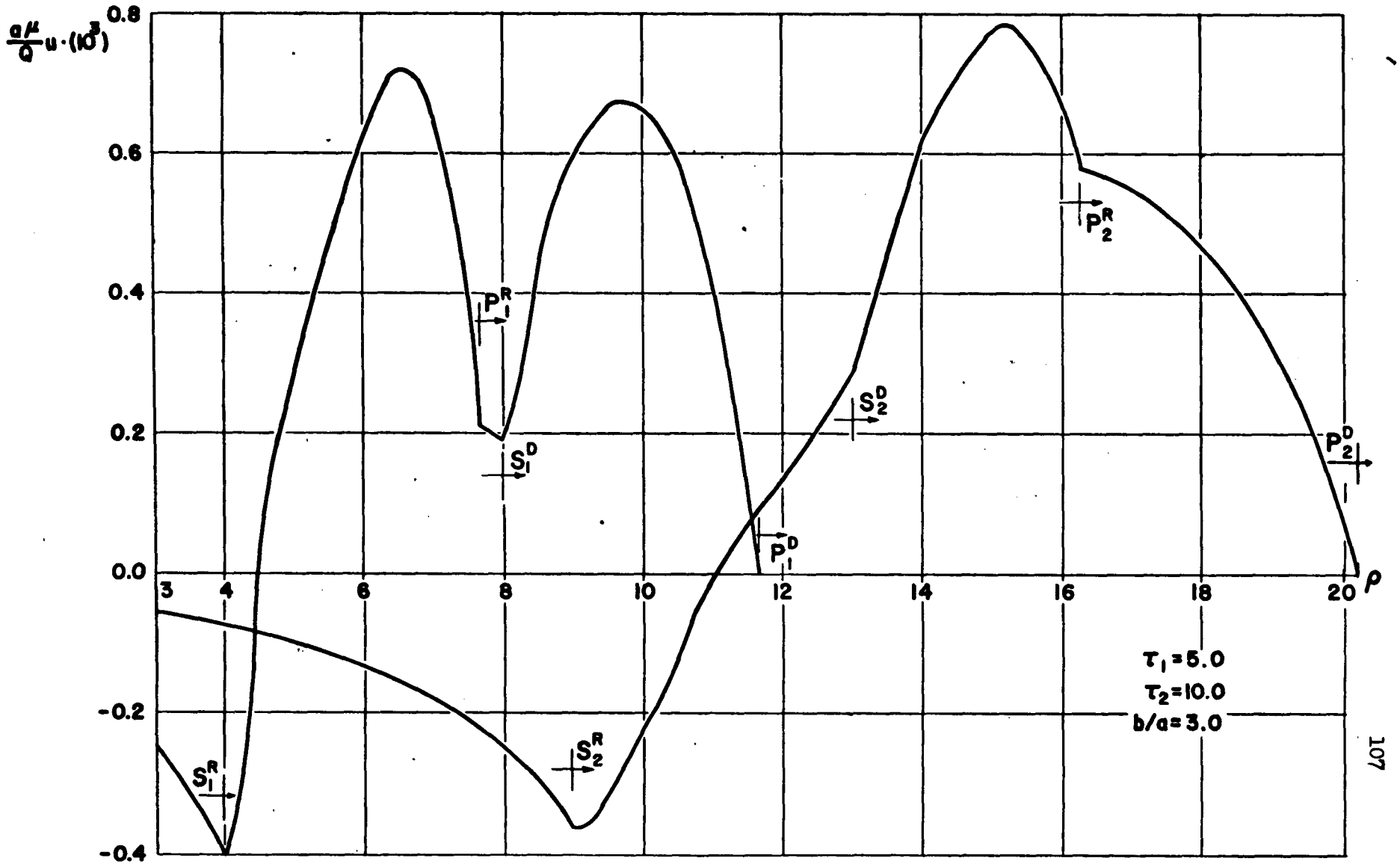

FIGURE 8. RADIAL DISPLACEMENT PROFILES: INTERACTION OF REFLECTED AND DIRECT OUTGOING BODY WAVES

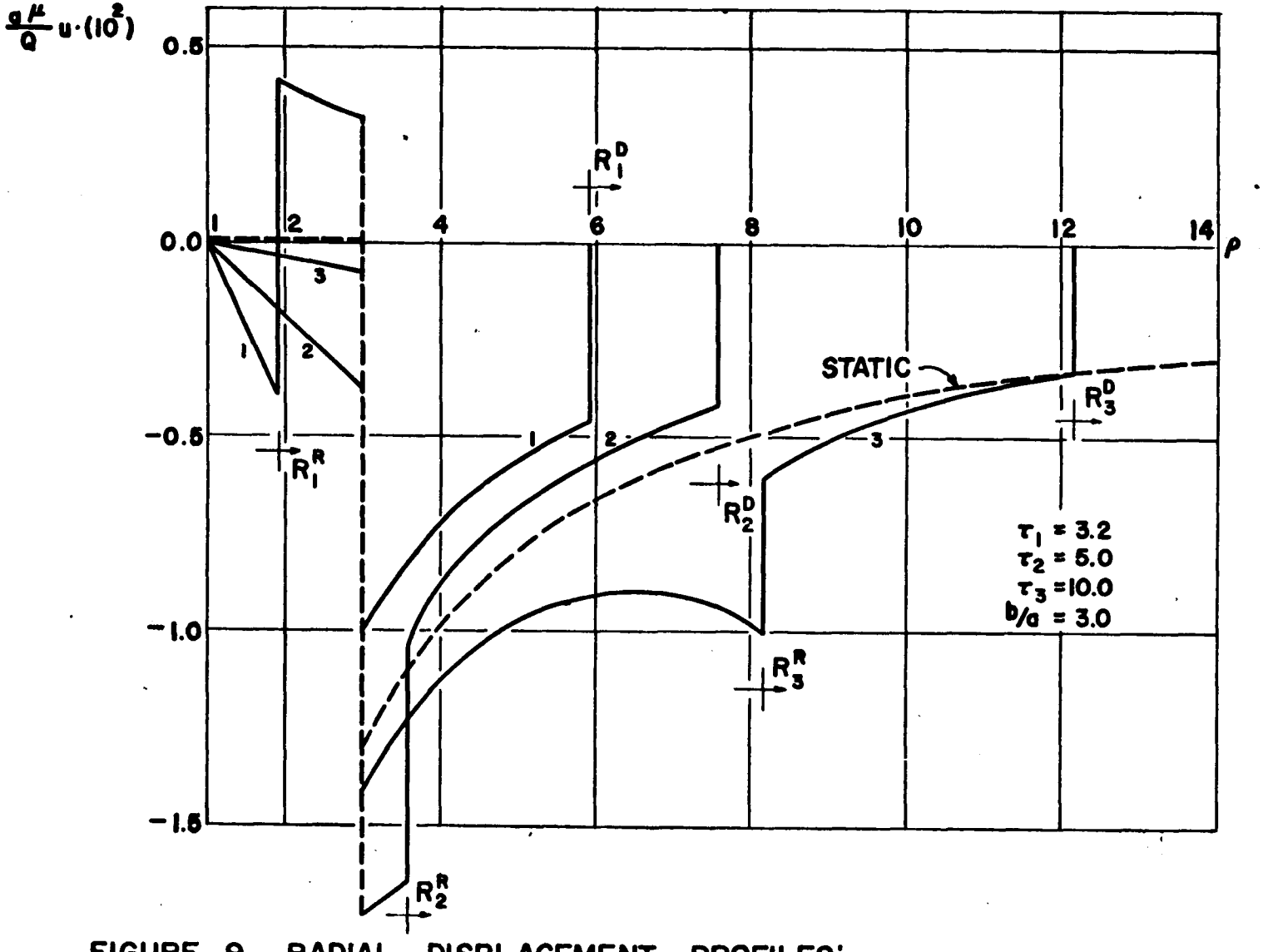

FIGURE 9. RADIAL DISPLACEMENT PROFILES:
REFLECTED AND DIRECT OUTGOING RAYLEIGH WAVES

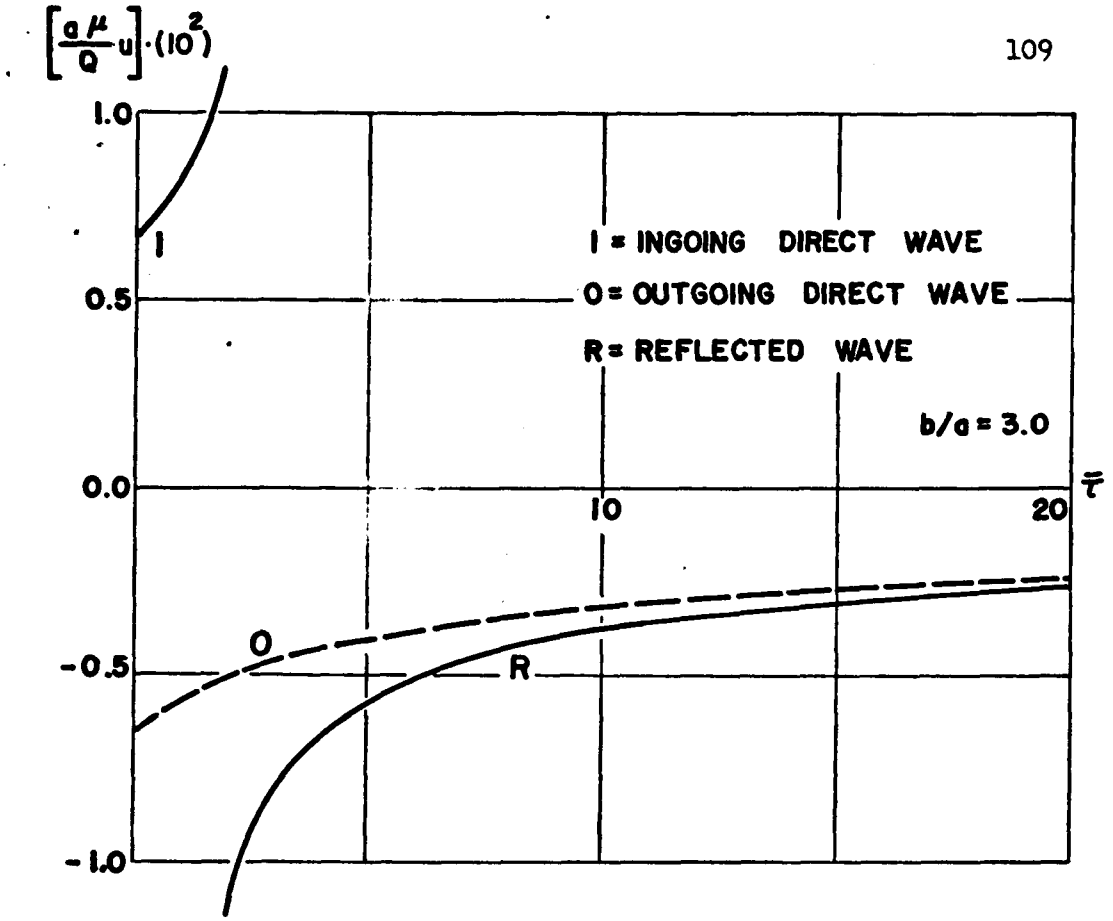

FIGURE 10-a. JUMP IN RADIAL DISPLACEMENT AT THE RAYLEIGH WAVE FRONTS VERSUS TIME $\bar{\tau}$

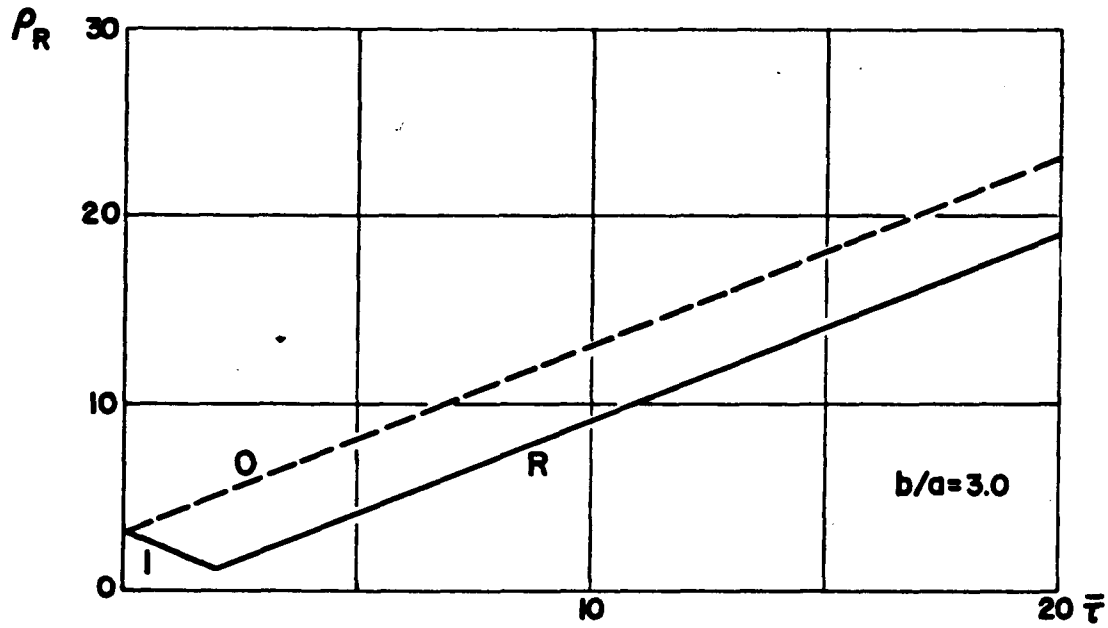

FIGURE 10-b. POSITION OF RAYLEIGH WAVE FRONTS VERSUS TIME $\bar{\tau}$

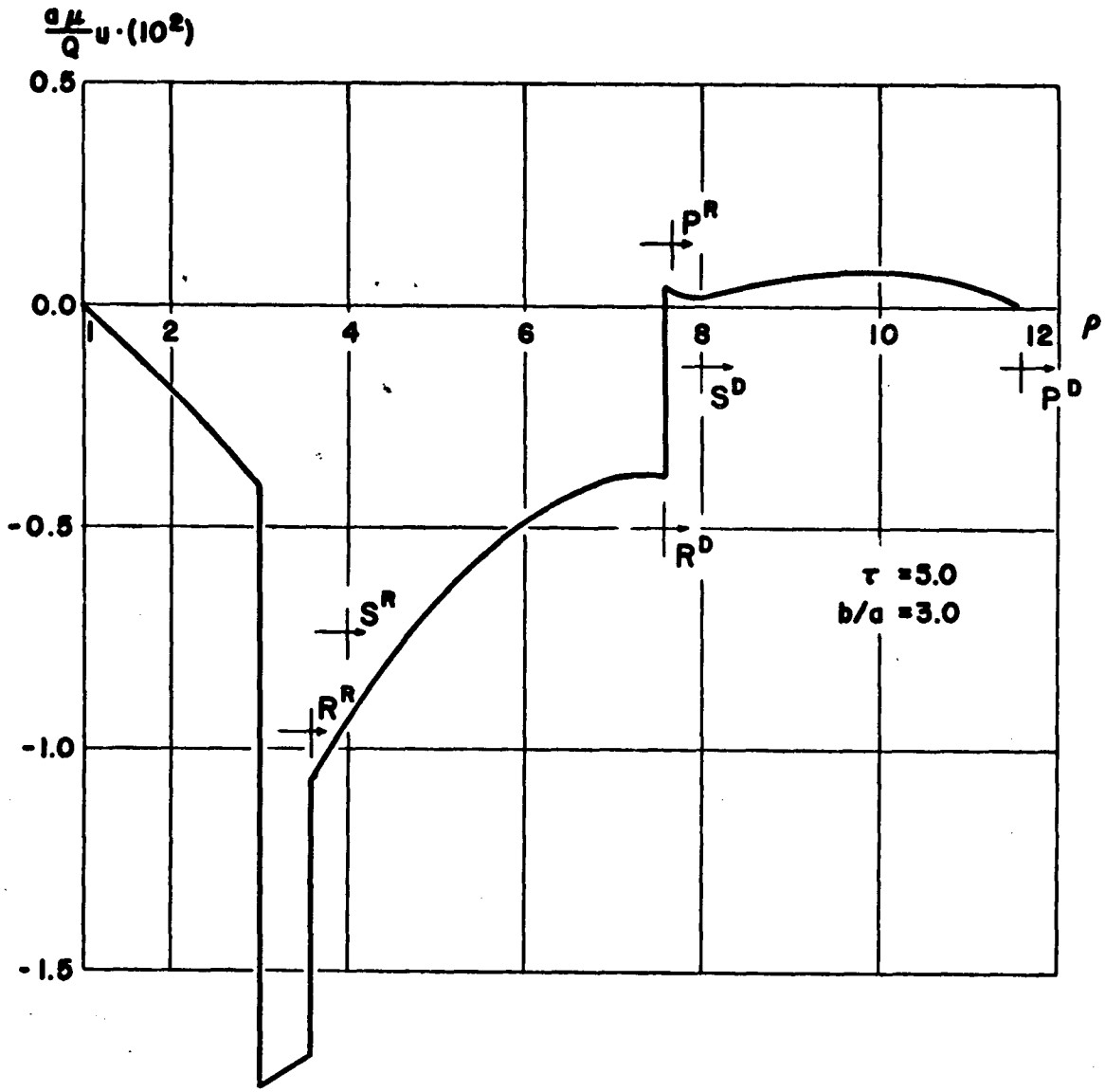

FIGURE 11 RADIAL DISPLACEMENT PROFILE: OUTGOING WAVES

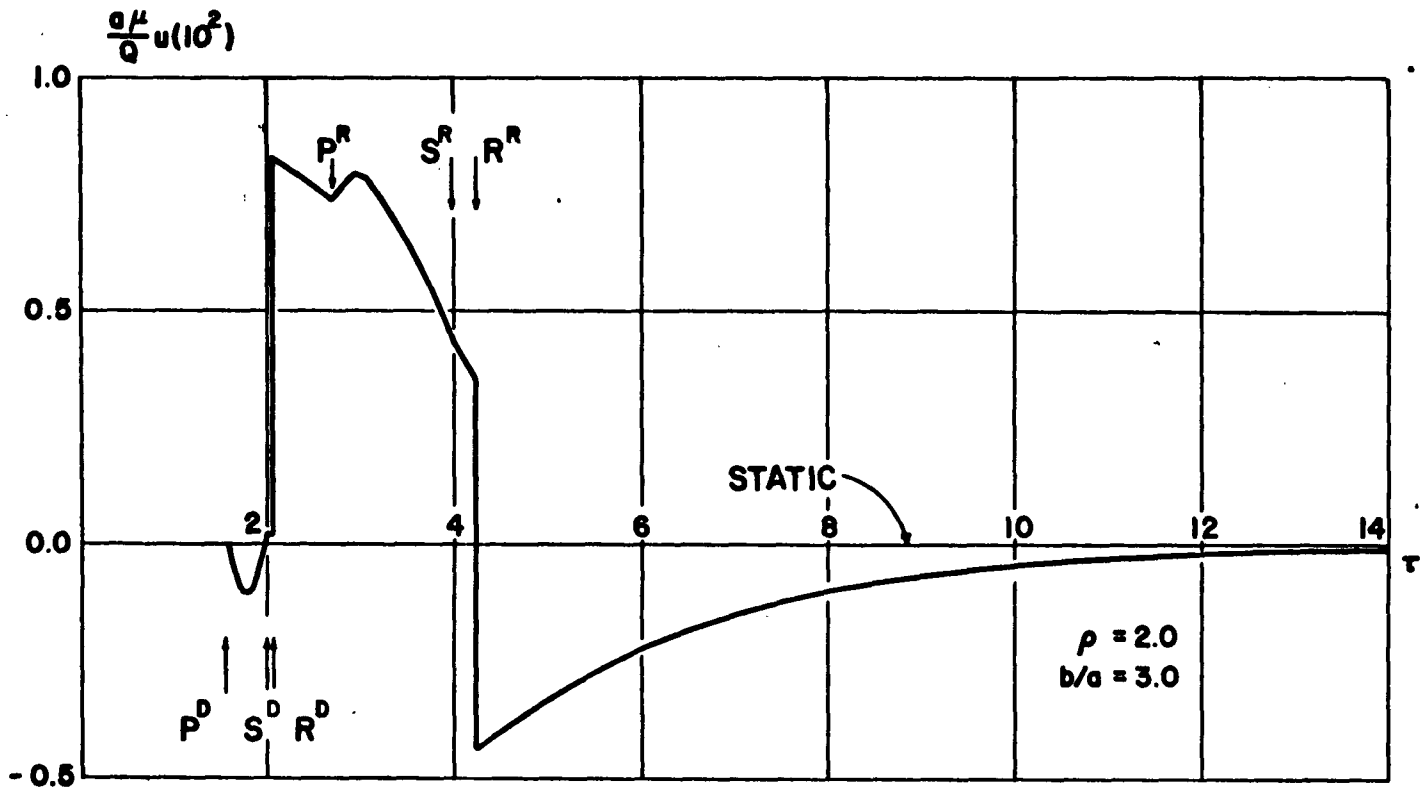

FIGURE 12. RADIAL DISPLACEMENT VERSUS TIME τ: INSIDE SOURCE

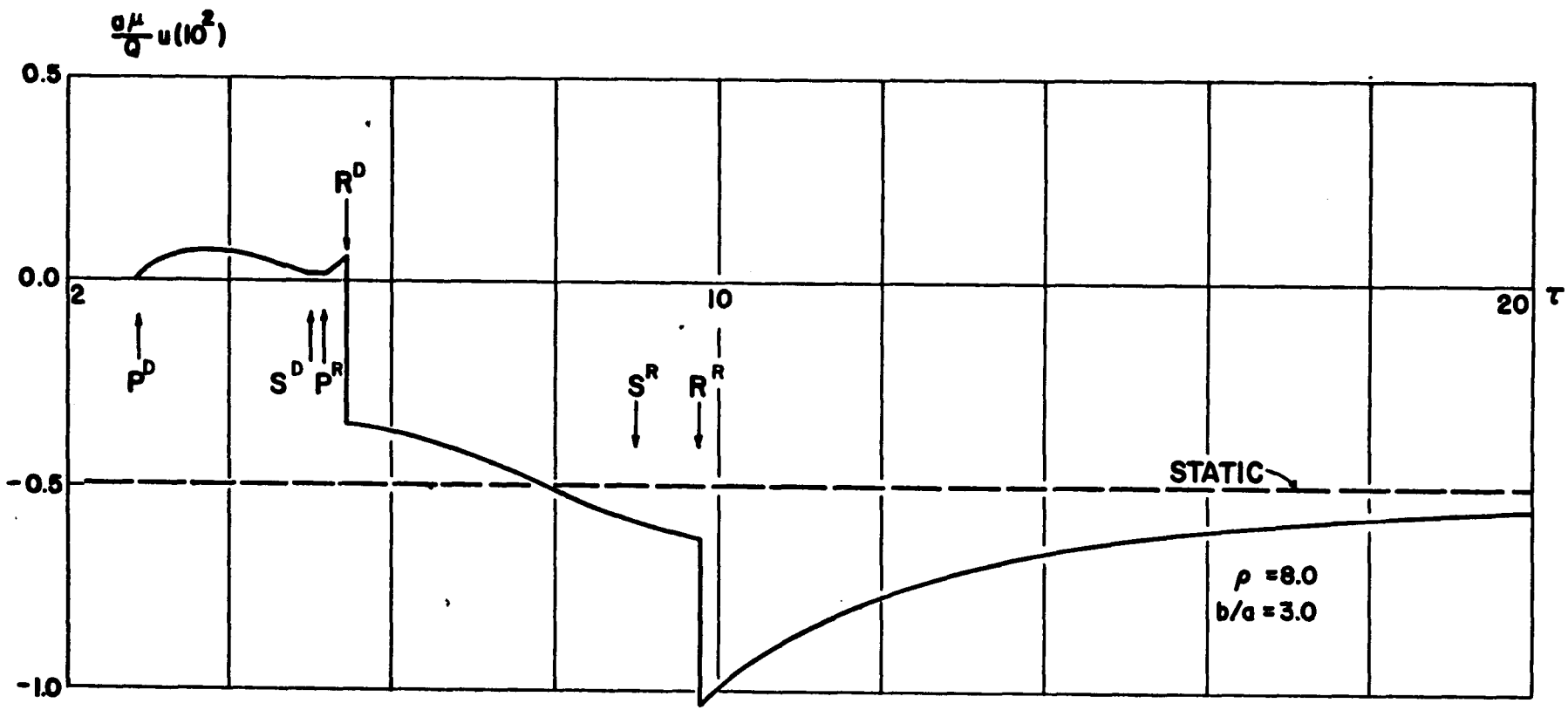

FIGURE 13. RADIAL DISPLACEMENT VERSUS TIME τ: OUTSIDE SOURCE

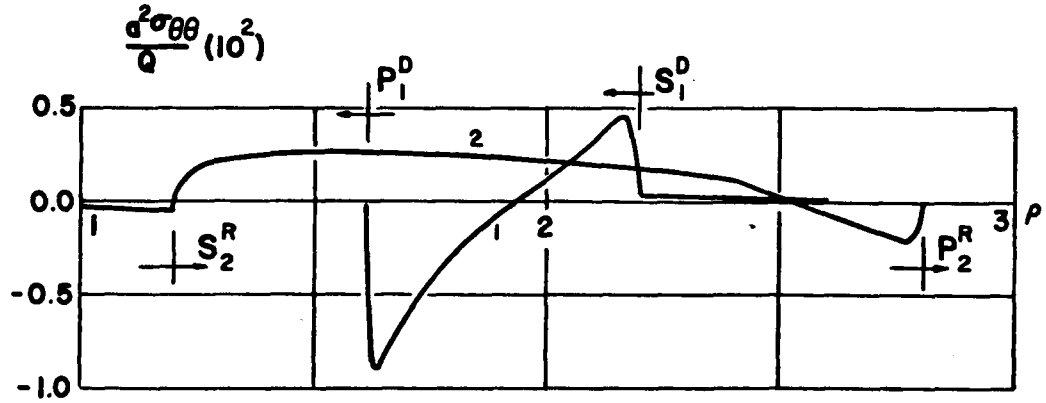

(a) CIRCUMFERENTIAL STRESS

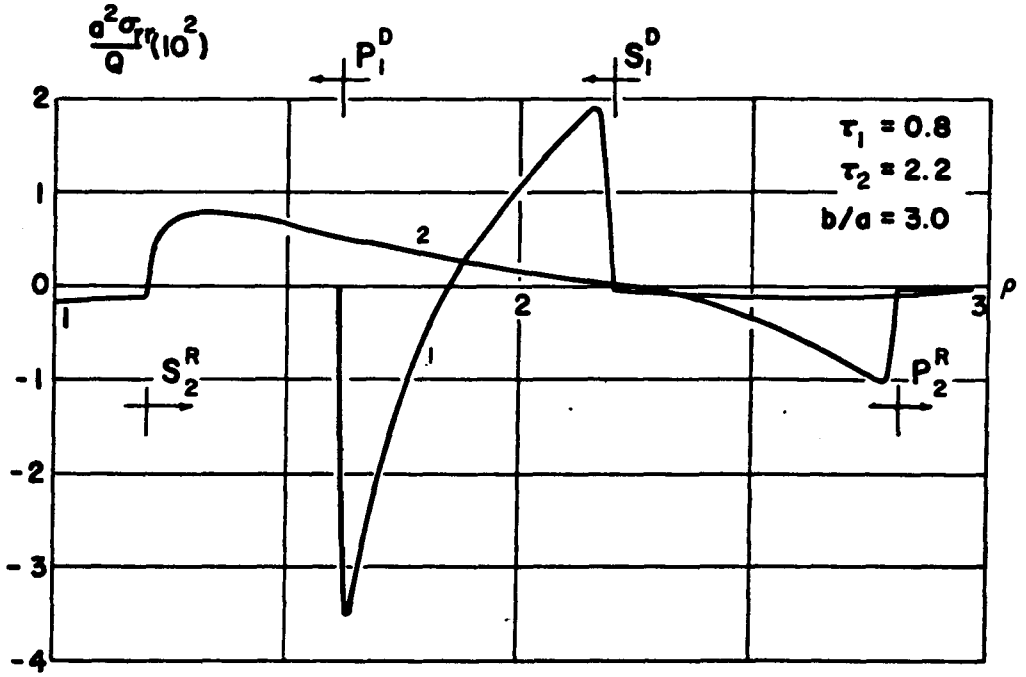

(b) RADIAL STRESS

FIGURE 14. BODY WAVE PROFILES INSIDE SOURCE

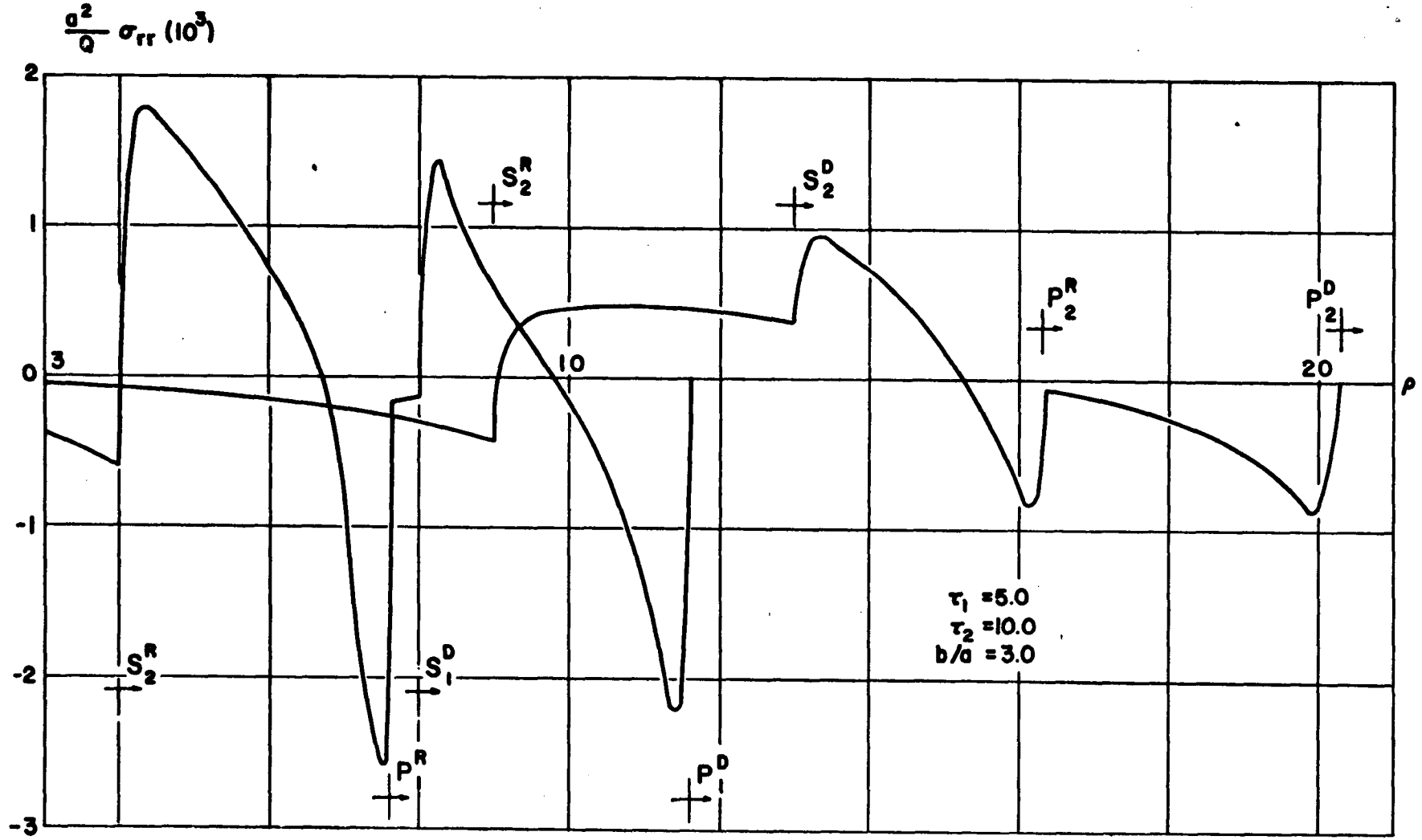

FIGURE 15. RADIAL STRESS PROFILES: INTERACTION OF REFLECTED AND DIRECT OUTGOING BODY WAVES

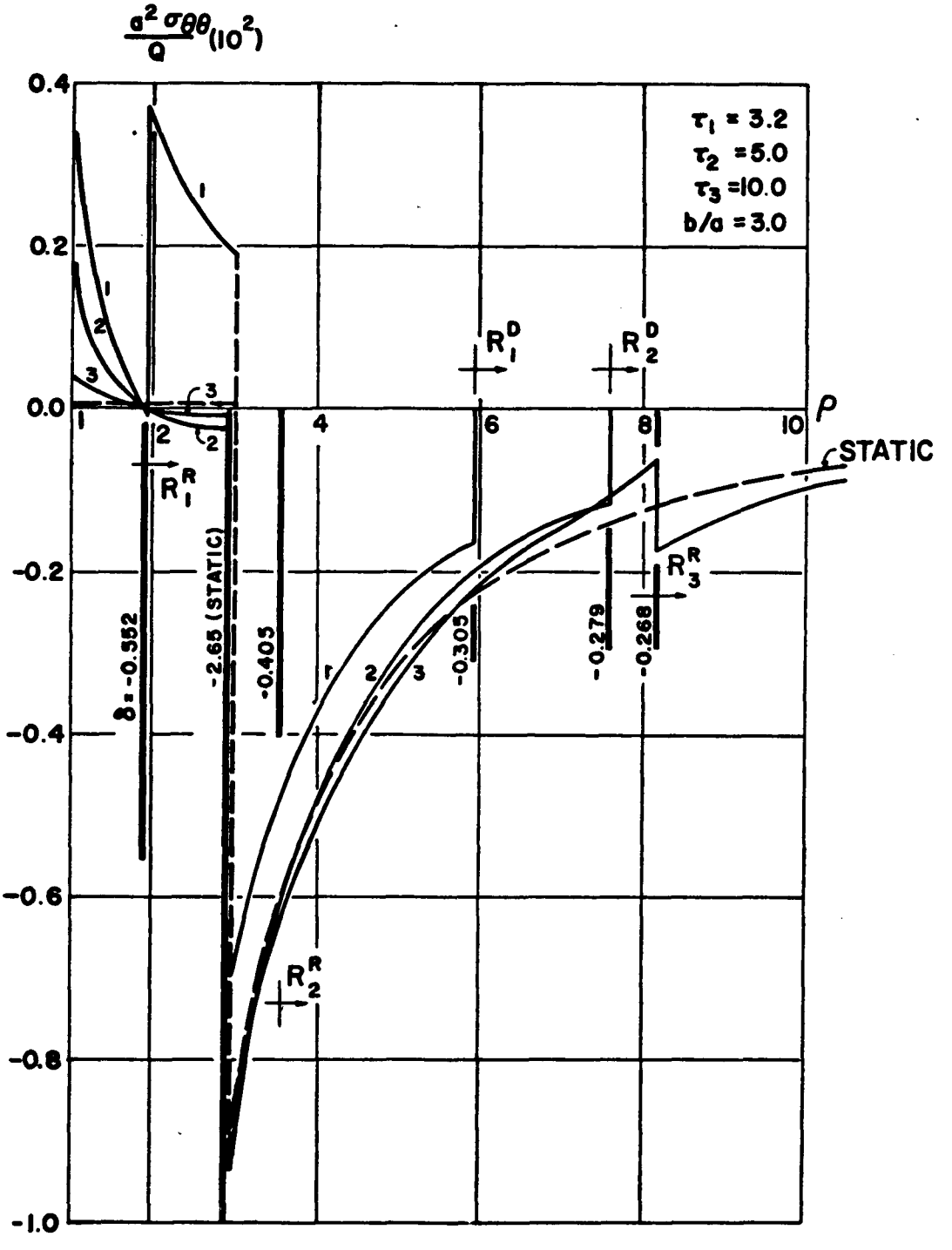

FIGURE 16. CIRCUMFERENTAL STRESS PROFILES: REFLECTED AND DIRECT OUTGOING RAYLEIGH WAVES

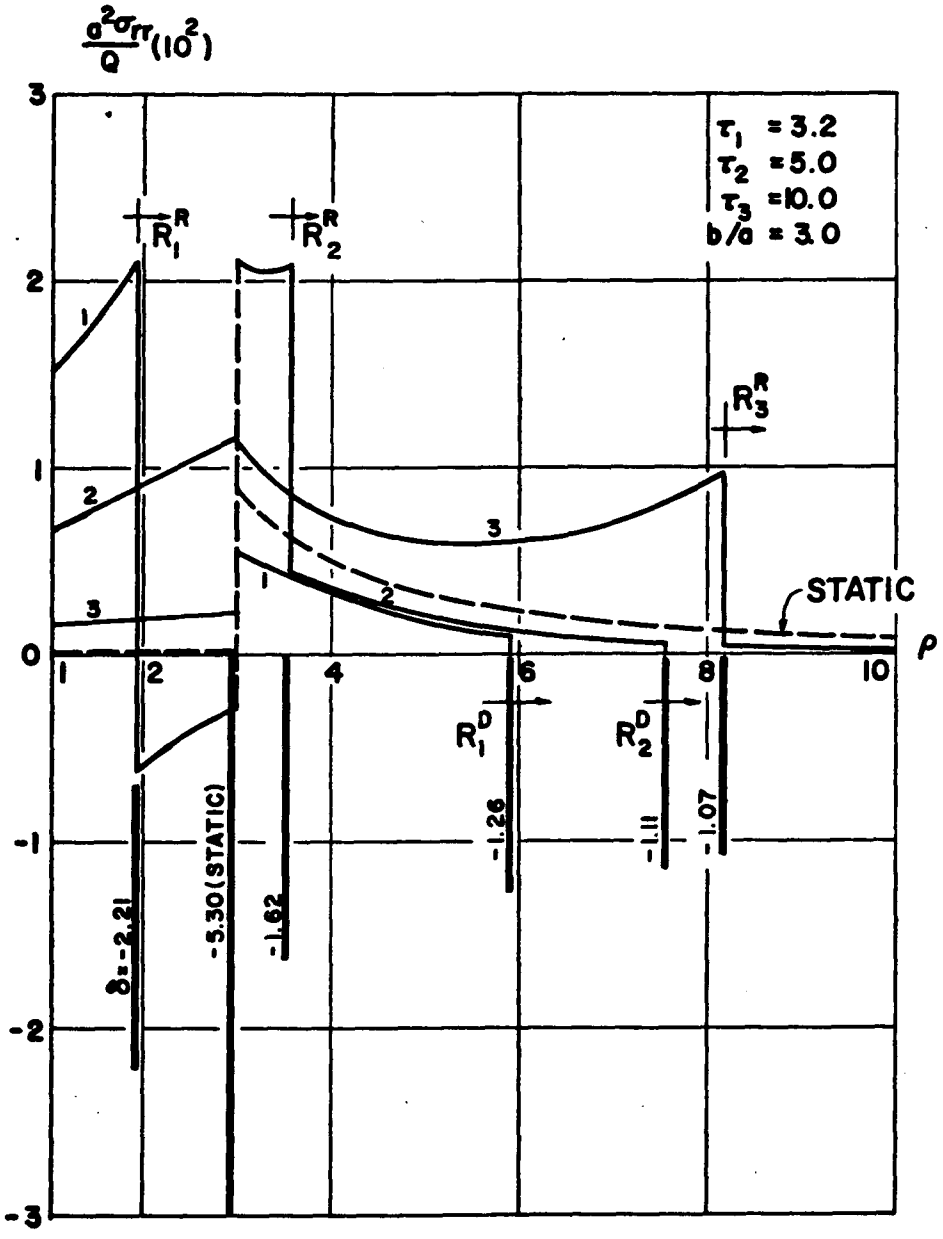

FIGURE 17. RADIAL STRESS PROFILES: REFLECTED AND DIRECT OUTGOING RAYLEIGH WAVES

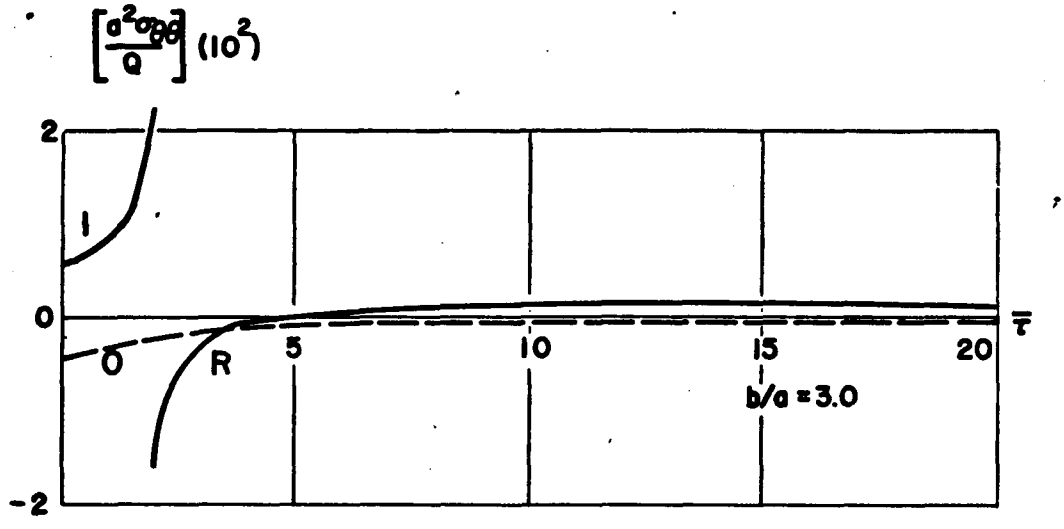

(a) CIRCUMFERENTIAL STRESS

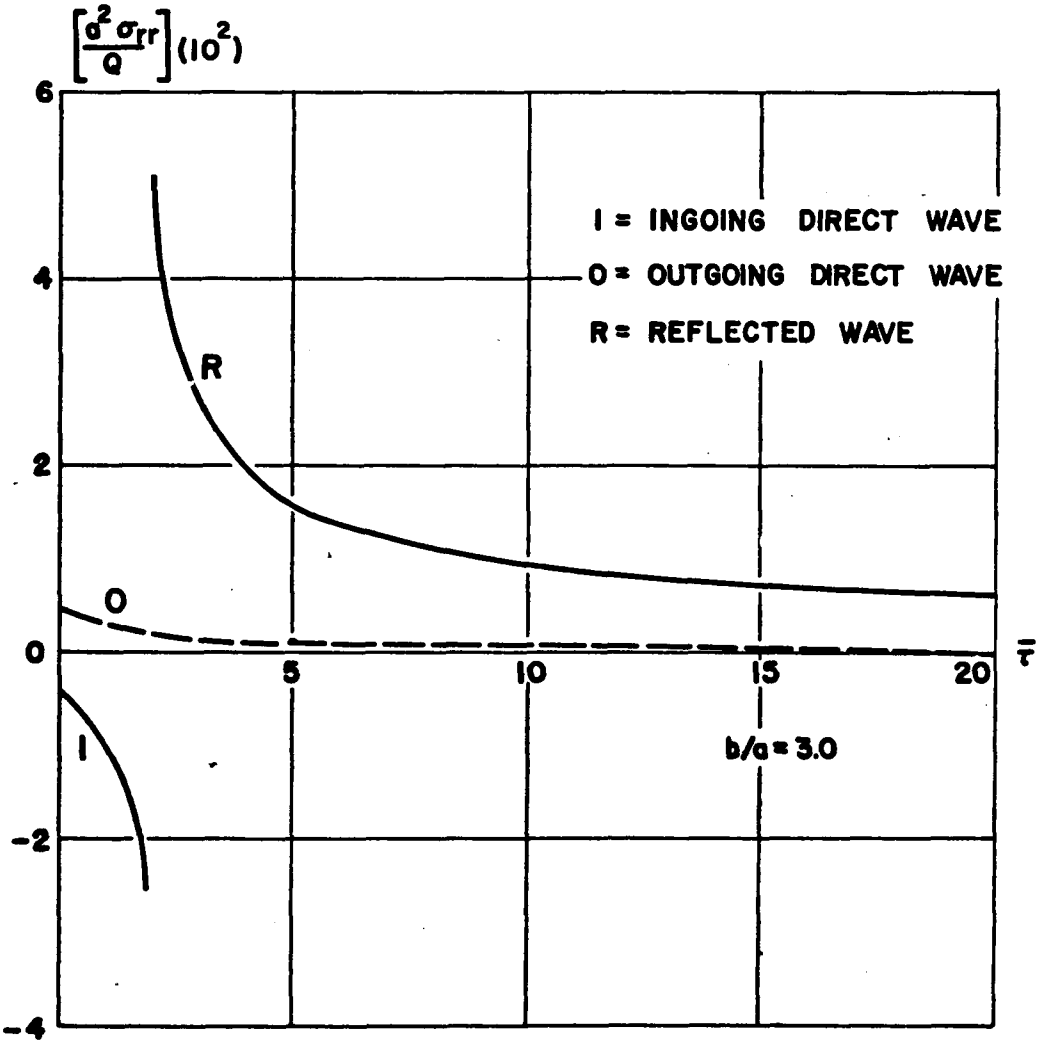

(b) RADIAL STRESS

FIGURE 18. JUMP AT THE RAYLEIGH WAVE FRONTS VERSUS TIME $\bar{\tau}$

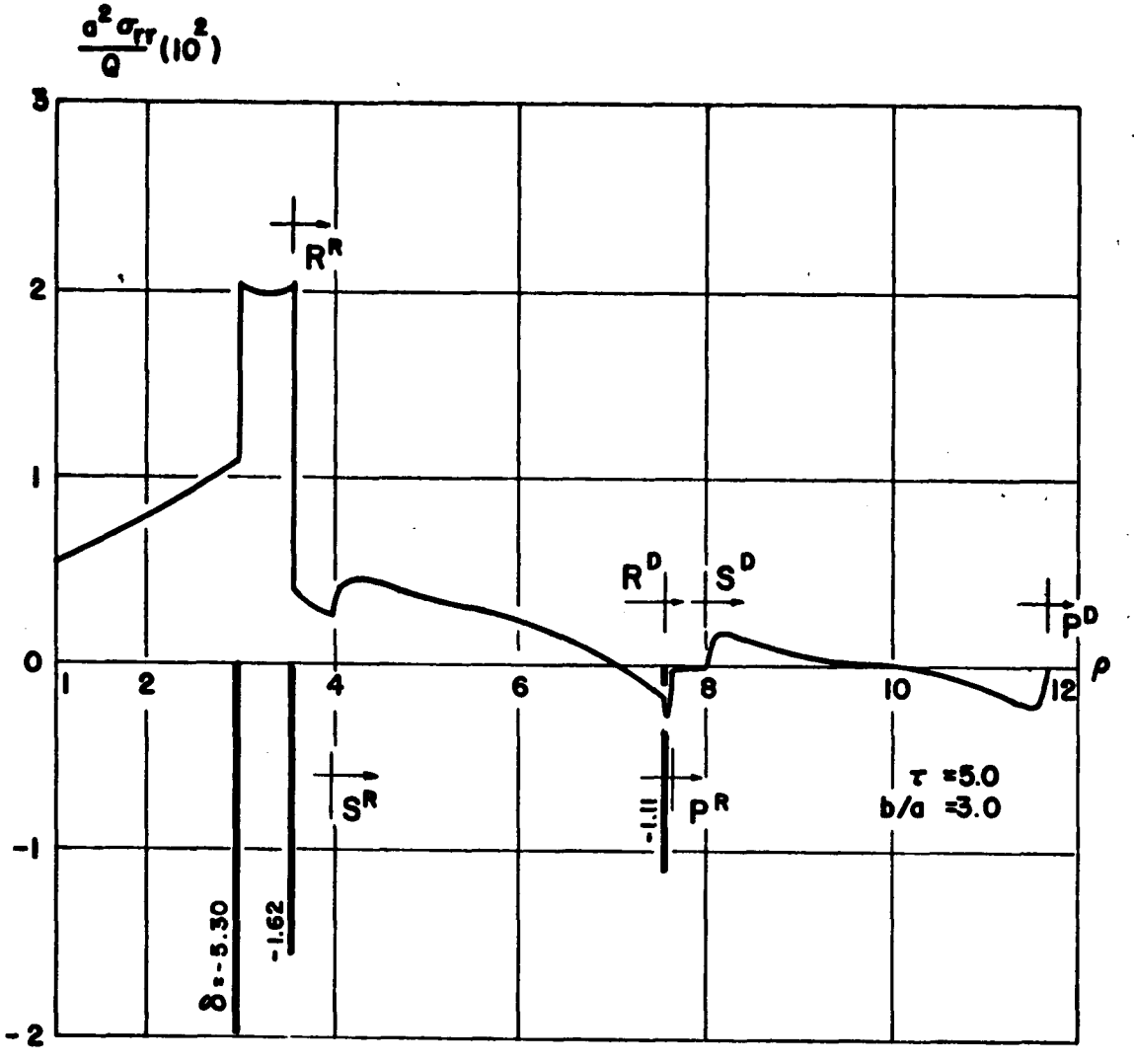

FIGURE 19. RADIAL STRESS PROFILE: OUTGOING WAVES

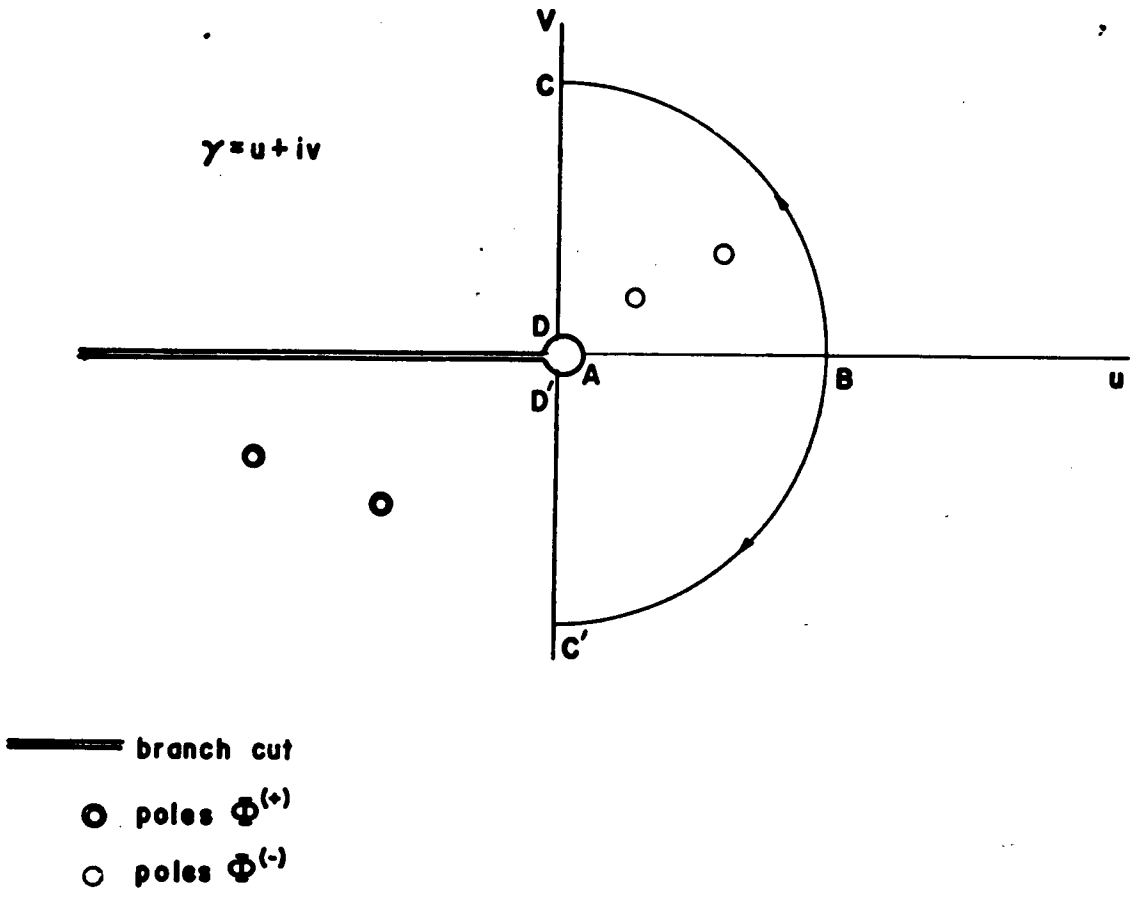

FIGURE 20. INTEGRATION PATHS IN COMPLEX γ-PLANE.

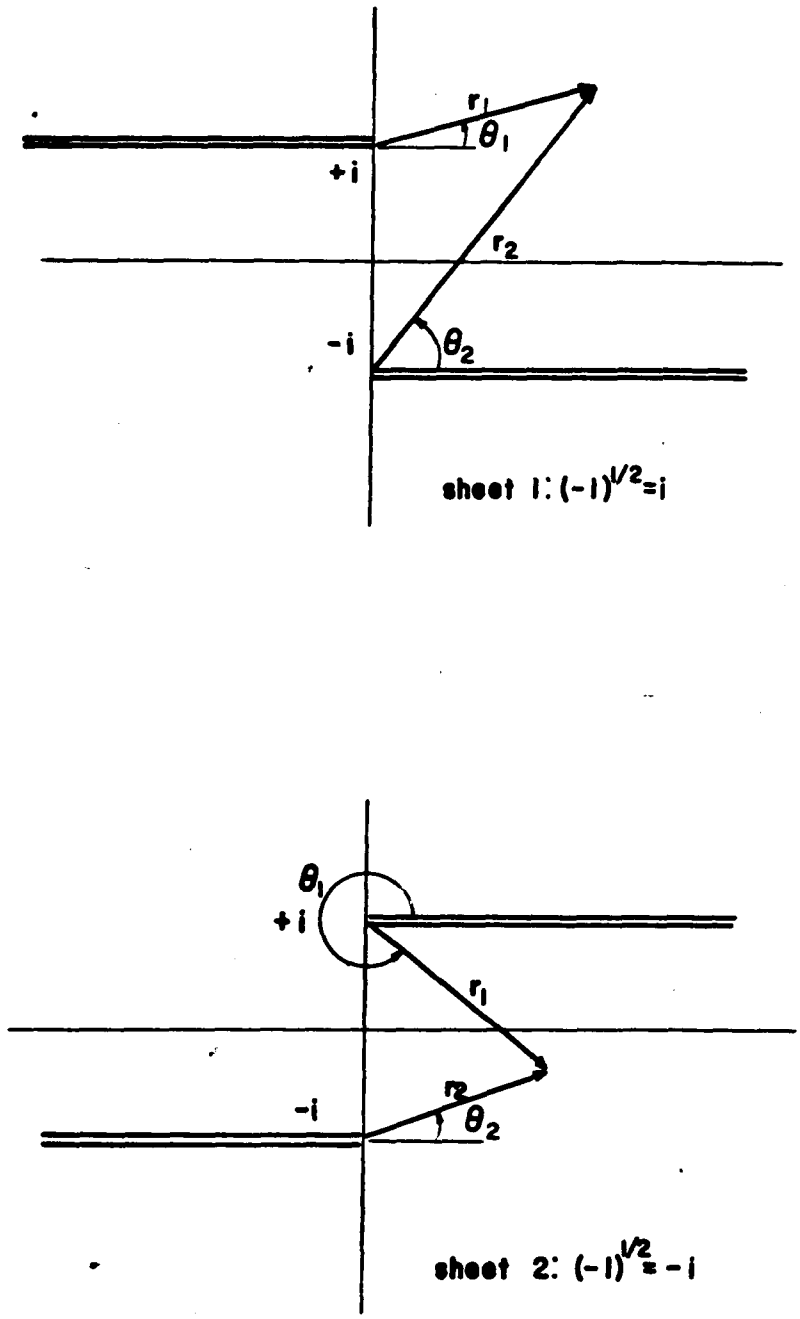

FIGURE 21. SHEETS AND BRANCH CUTS FOR THE MULTIVALUED FUNCTION $w=(\zeta^2+1)^{1/2}$

REFERENCES

1. M. Poisson, "Memoire sur l'equilibre et le mouvement des corps elastiques", Mem. Acad. Sci. Paris, 8, 1829 pp. 356-623
2. Lord Rayleigh, "On waves propagated along the plane surface of an elastic solid", Proc. Lond. Math. Soc. 17, 1887 pp. 4-11.
3. H. Lamb, "On the propagation of tremors over the surface on an elastic solid", Phil. Trans. Roy-Soc. Lond, (A), 203, 1904 pp. 1 - 42.
4. F. Sauter, "Der elastische Halbraum bei einer mechanischen beeinflussung seiner oberflache", ZAMM, 30, 1950, pp. 203-215.
5. K.B. Broberg, "Shock waves in elastic and elastic-plastic media", Kuhgl. Fortifikationsforvaltingen Betastningsbryans, Rep 109:12 Stockholmn, 1956.
6. C.L. Pekeris, "The seismic surface pulse", Proc Nat. Acad. Sci., 41, 1955, pp. 469-480.
7. C.C. Chao, "Dynamic response of an elastic half-space to tangential surface loadings", J. Appl. Mech., 27, 1960, pp. 559-567.
8. R.D. Gregory, "The propagation of waves in an elastic half-space containing a cylindrical cavity", Proc. Camb. Phil. Soc., 67, 1970, pp. 689-710.
9. W.M. Ewing, W.S. Jardetzky and F. Press, "Elastic Waves in Layered Media", McGraw Hill, New York, 1957.
10. J.H. Baltrukonis, W.G. Brottenberg and R.N. Schreiner, "Dynamics of a Hollow Elastic Cylinder Contained by an Infinitely Long Rigid Circular Cylindrical Tank", J. Acoust. Soc. Am., Vol. 32, No. 12, Dec. 1960.

11. A.R. Forsyth, "Theory of Functions of a Complex Variable", Third Edition, Vol. I, Dover, New York, 1965. p. 41 ff.

12. G.N. Watson,"A treatise on the Theory of Bessel Functions", University Press, Cambridge, 1966.

13. National Bureau of Standards Applied Mathematics Series, "Handbook of Mathematical Functions", U.S. Government Printing Office, Washington, D.C. 1968.

14. A. Cayley, "An Elementary Treatise on Elliptic Functions", 2nd Edition, Bell, London, 1895.

15. W. LePage, "Complex Variables and the Laplace Transform for Engineers", McGraw-Hill, New York 1961, p. 369.

16. F. Bowman, "Introduction to Elliptic Functions", Dover, New York, 1961, p. 21.

17. Shao, Chen, and Frank, "Tables of Zeroes and Gaussian Weights of Certain Associated Laguerre Polynomials and the Related Generalized Hermite Polynomials", IBM Technical Report TR oo.11000, (March 1964), pp. 24-25.

18. A.E.H. Love, "A Treatise on the Mathematical Theory of Elasticity", 4th Edition, Dover, New York, 1944, p. 274.

19. S. Timoshenko, "Theory of Elasticity", 3rd Edition, McGraw -Hill, New York 1970.

20. Bateman Manuscript Project, Cal. Inst. of Tech., "Higher Transcendental Functions", Vol.II, A. Erdelyi (Ed.), McGraw-Hill, New York, 1955, p. 93.

21. M. Lowengrub and I.N. Sneddon, "The distribution of stress in the vicinity of an external crack in an infinite elastic solid", Int. J. of Eng. Sci., Vol. 3, No. 4, Sept. 1965, pp. 459-460.

VITA

Edward R. Johnson was born in New York City on December 11, 1945.

He was graduated from James Monroe High School in June 1962. Attending Queens College and then the City College of New York, Mr. Johnson was a member of A.S.C.E. student chapter, elected to Tau Beta Pi, and received the Bachelor of Civil Engineering degree in February, 1967.

Continuing at the City College in the doctoral program, he received the Master of Science degree in February, 1968.

While employed as a Lecturer in the Department of Civil Engineering for the years 1968-70, Mr. Johnson was selected by the faculty of the City College as the recipient of the 1969 Jacob Feld Award for life membership in the New York Academy of Sciences.

Working towards the Ph.D. degree, he completed his dissertation in the early part of 1972.

. . .